Social insect genomes exhibit dramatic evolution in gene composition and regulation while preserving regulatory features linked to sociality

Daniel F. Simola, Lothar Wissler, Greg Donahue, et al.

Genome Res. 2013 23: 1235-1247 originally published online May 1, 2013
Access the most recent version at doi:10.1101/gr.155408.113

Social insect genomes exhibit dramatic evolution in gene composition and regulation while preserving regulatory features linked to sociality

Daniel F. Simola,[1,2,20] Lothar Wissler,[3,20] Greg Donahue,[1,2] Robert M. Waterhouse,[4] Martin Helmkampf,[5] Julien Roux,[6,21] Sanne Nygaard,[7] Karl M. Glastad,[8] Darren E. Hagen,[9,22] Lumi Viljakainen,[10] Justin T. Reese,[9,22] Brendan G. Hunt,[8] Dan Graur,[11] Eran Elhaik,[12] Evgenia V. Kriventseva,[4] Jiayu Wen,[13] Brian J. Parker,[13] Elizabeth Cash,[5] Eyal Privman,[6] Christopher P. Childers,[9,22] Monica C. Muñoz-Torres,[9] Jacobus J. Boomsma,[7] Erich Bornberg-Bauer,[3] Cameron R. Currie,[14] Christine G. Elsik,[9,22] Garret Suen,[14] Michael A.D. Goodisman,[8] Laurent Keller,[6] Jürgen Liebig,[5] Alan Rawls,[5] Danny Reinberg,[15] Chris D. Smith,[16] Chris R. Smith,[17] Neil Tsutsui,[18] Yannick Wurm,[6,23] Evgeny M. Zdobnov,[4] Shelley L. Berger,[1,2,19] and Jürgen Gadau[5,24]

[1–19]*[Author affiliations appear at the end of the paper.]*

Genomes of eusocial insects code for dramatic examples of phenotypic plasticity and social organization. We compared the genomes of seven ants, the honeybee, and various solitary insects to examine whether eusocial lineages share distinct features of genomic organization. Each ant lineage contains ~4000 novel genes, but only 64 of these genes are conserved among all seven ants. Many gene families have been expanded in ants, notably those involved in chemical communication (e.g., desaturases and odorant receptors). Alignment of the ant genomes revealed reduced purifying selection compared with *Drosophila* without significantly reduced synteny. Correspondingly, ant genomes exhibit dramatic divergence of noncoding regulatory elements; however, extant conserved regions are enriched for novel noncoding RNAs and transcription factor–binding sites. Comparison of orthologous gene promoters between eusocial and solitary species revealed significant regulatory evolution in both *cis* (e.g., *Creb*) and *trans* (e.g., *fork head*) for nearly 2000 genes, many of which exhibit phenotypic plasticity. Our results emphasize that genomic changes can occur remarkably fast in ants, because two recently diverged leaf-cutter ant species exhibit faster accumulation of species-specific genes and greater divergence in regulatory elements compared with other ants or *Drosophila*. Thus, while the "socio-genomes" of ants and the honeybee are broadly characterized by a pervasive pattern of divergence in gene composition and regulation, they preserve lineage-specific regulatory features linked to eusociality. We propose that changes in gene regulation played a key role in the origins of insect eusociality, whereas changes in gene composition were more relevant for lineage-specific eusocial adaptations.

[Supplemental material is available for this article.]

The insect order Hymenoptera encompasses several lineages, including ants, bees, and aculeate wasps, that independently evolved obligate eusociality. Such eusocial lineages are characterized by reproductive division of labor, cooperative brood care, and overlapping generations (Michener 1969). Ants (Formicidae) represent one of the oldest (~130 million years) and most successful exclusively eusocial lineages (Cardinal and Danforth 2011). They have colonized every terrestrial habitat except at the highest latitudes, and they have achieved substantial diversity in both individual and colonial traits. The ecological and evolutionary success of the more than 15,000 described extant ant species (http://www.antweb.org) is often attributed to their sociality and ability to engineer environments, e.g., by building elaborate nests, herding aphids for honeydew, or practicing sustainable agriculture (Crozier and Pamilo 1996; Hölldobler and Wilson 2009).

The genomes of seven ant species, representatives of four major lineages that comprise two-thirds of all ant species, have recently been sequenced and characterized independently (for review, see Gadau et al. 2012): Jerdon's jumping ant, *Harpegnathos saltator* (Ponerinae; n = 1033 extant species) (Bonasio et al. 2010); the globally invasive Argentine ant, *Linepithema humile* (Dolichoderinae; n = 692) (Smith et al. 2011a), the Florida carpenter ant, *Camponotus floridanus* (Formicinae; n = 2831) (Bonasio et al. 2010); and four ants within the hyperdiverse subfamily Myrmicinae

[20]These authors contributed equally to this work.
Present addresses: [21]Department of Human Genetics, University of Chicago, Chicago, IL 60637, USA; [22]Divisions of Animal and Plant Sciences, University of Missouri, Columbia, MO 65211, USA; [23]School of Biology & Chemistry, Queen Mary University of London, London E1 4NS, UK.
[24]Corresponding author
E-mail jgadau@asu.edu
Article published online before print. Article, supplemental material, and publication date are at http://www.genome.org/cgi/doi/10.1101/gr.155408.113.

($n = 6087$): the red harvester ant, *Pogonomyrmex barbatus* (Smith et al. 2011b), the invasive red imported fire ant, *Solenopsis invicta* (Wurm et al. 2011); and two agricultural leaf-cutter species, *Acromyrmex echinatior* and *Atta cephalotes* (Nygaard et al. 2011; Suen et al. 2011). Together with the honeybee, *Apis mellifera* (The Honeybee Genome Sequencing Consortium 2006), eight eusocial genomes are now available from two evolutionarily independent lineages. While ants and honeybees are both eusocial Hymenoptera, they differ significantly in many aspects. For instance, ants have wingless and often polymorphic worker castes, enjoy long life spans for insects, and are descendants of predatory wasps, whereas honeybees only have winged monomorphic workers with limited life spans and are derived from solitary bees.

Given the remarkable phenotypic diversity among eusocial insects, a key question is to what extent do derived and independent eusocial lineages harbor shared features of genomic organization that enable their eusocial lifestyles (Robinson et al. 2005; Gadau et al. 2012; Ferreira et al. 2013). To address this question, we performed a comprehensive characterization of the genomic basis for eusociality, using eight eusocial insect genomes in addition to 22 available solitary insect genomes. Our results reveal a variety of lineage-specific changes in both gene composition and gene expression regulation that have facilitated the evolution of eusociality.

Results

Ant genomes harbor thousands of taxonomically restricted genes

Comparison of existing gene annotations from the seven ant genomes showed that, while the number of protein-coding genes is only partially explained by genome assembly size ($R = 0.32$) (Fig. 1A), the number of orthologous genes shared among these ants varies considerably (3.1-fold) (Supplemental Fig. 1). This suggested that either existing annotations lack many valid genes, or ant genomes harbor an abundance of taxonomically restricted genes (TRGs), which have been associated with the evolution of novel functionalities in other systems (for review, see Khalturin et al. 2009). Previous analyses of individual ant genomes predicted up to 8000 species-specific TRGs (e.g., Smith et al. 2011b), in addition to 840 TRGs that are exclusively shared among ants (e.g., Bonasio et al. 2010).

To infer more accurately the origin and abundance of TRGs while minimizing annotation error, we applied two approaches to reannotate ant and honeybee genomes in terms of gene number and model quality. First, by comparing known protein sequences among species, we identified 3313 genes from 2635 orthologous groups that were missing from existing annotations (Supplemental Figs. 2–4; Supplemental Table 1). Second, we developed a broader approach involving 30 published arthropod

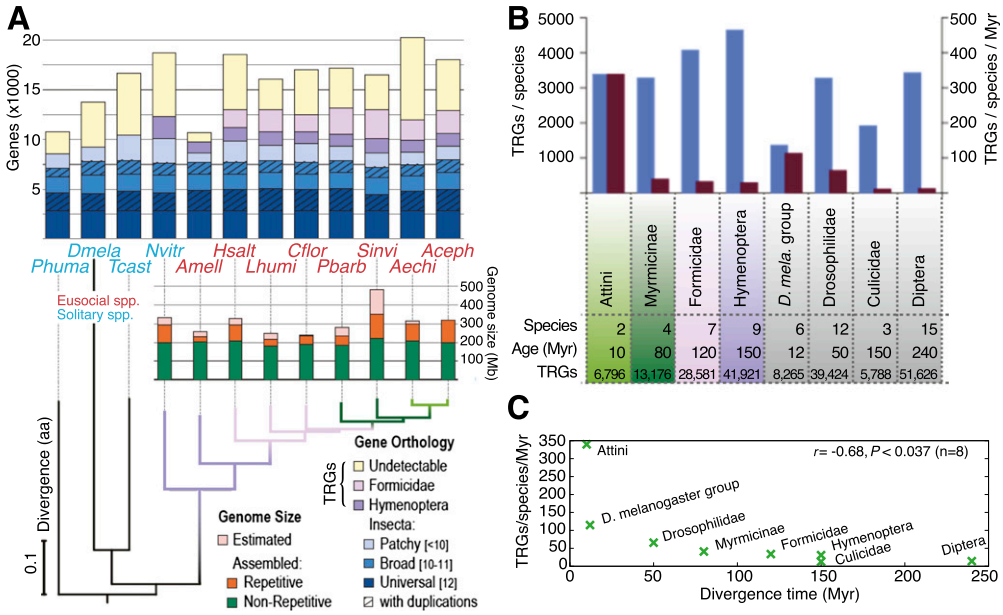

Figure 1. Overview of protein-coding gene composition and genome size in Hymenoptera. (*A*) Gene and genome content in seven ant species and honeybee (red), with representative solitary insects (blue) as outgroups. Orthology delineation among protein-coding genes from 12 insects identified orthologs present in all (Universal, $n = 12$) or almost all (Broad, $10 \leq n \leq 11$) species, conserved as single-copy genes or with paralogs (with duplications). Differential gene losses leave orthologs shared among fewer species across the phylogeny (Patchy, $n < 10$). Remaining ant genes exhibit orthology with honeybee ([*AMELL*] *Apis mellifera*) and/or jewel wasp ([*NVITR*] *Nasonia vitripennis*) (Hymenoptera), among ants (Formicidae), or lack orthology (Undetectable). Total estimated genome sizes vary among Hymenoptera, largely due to repetitive regions (orange bars); however, hymenopterans share a nonrepetitive core of ~200 Mb (green bars). A maximum-likelihood species tree computed from the concatenated alignment of all universal single-copy orthologs confirms the established ant phylogeny (Moreau et al. 2006). Rates of molecular evolution are comparable to the other hymenopterans, flour beetle ([*TCAST*] *Tribolium castaneum*; genome size ~200 Mb), and body louse ([*PHUMA*] *Pediculus humanus*; genome size ~108 Mb), but are much slower than the dipteran representative ([*DMELA*] *Drosophila melanogaster*; genome size 175 Mb). The ant species are (*HSALT*) *Harpegnathos saltator*; (*LHUMI*) *Linepithema humile*; (*CFLOR*) *Camponotus floridanus*; (*PBARB*) *Pogonomyrmex barbatus*; (*SINVI*) *Solenopsis invicta*; (*AECHI*) *Acromyrmex echinatior*; and (*ACEPH*) *Atta cephalotes*. (*B*) Occurrence (blue) and emergence rate (red) of taxonomically restricted genes (TRGs) in different taxonomic clades of Hymenoptera (colors) and Diptera (gray). The youngest clades of both Hymenoptera and Diptera exhibit the highest rates of TRG accumulation. Age is measured as the time between the most distant members of each group and hence does not reflect a clade's absolute age. (*C*) Rate of change of TRGs versus divergence time, for eight species groupings. Pearson's correlation coefficient is shown. *P*-value was computed using a two-tailed *t*-test.

genomes and conservative filtering steps and identified 5996 additional, previously missing genes (Supplemental Figs. 5–8; Supplemental Tables 2, 3). Thus, our significantly revised genome annotations include 9309 newly annotated genes for the eight eusocial species. These analyses corroborate that the honeybee has an exceptionally low gene number (Fig. 1A): We found only 223 previously missing genes in the honeybee versus 856 on average for ants (Supplemental Fig. 5) and relatively few TRGs compared with other insects. Whether this apparent gene loss is restricted to *Apis* honeybees or is shared with other corbiculate bees will soon be elucidated by ongoing efforts to sequence multiple bee and bumble bee genomes.

Having identified the missing genes from social insect genome annotations, we delineated TRGs for different clades within Hymenoptera and Diptera. Notably, we found 28,581 TRGs that are restricted to Formicidae (ant TRGs), and 42% of these genes appear to be species-specific, given our current taxon sampling (Fig. 1A,B). Thus, we estimate that each ant genome harbors an average of 4083 TRGs, of which 1715 appear to be species specific. Intriguingly, among the remaining, non-species-specific TRGs (i.e., TRGs present in multiple ant genomes), only 64 are present in all seven ant genomes (Supplemental Text 1). These 64 pan-ant TRGs have a median length of 97 amino acids (25th–75th percentile range of 72–149 amino acids), are well conserved and show strong expression support in two ant species (Fig. 2); however, they generally lack caste-specific expression ($n = 3$, FDR < 0.05) and do not encode any known protein domains. These results suggest that a broad "social toolkit" of conserved de novo protein-coding genes is not a requirement for eusociality.

Hymenoptera, especially the two leaf-cutter ants, exhibit a faster emergence rate for taxonomically restricted genes than Diptera

Having multiple genomes for two insect orders allowed us to compare rates of TRG emergence between Hymenoptera ($n = 9$)

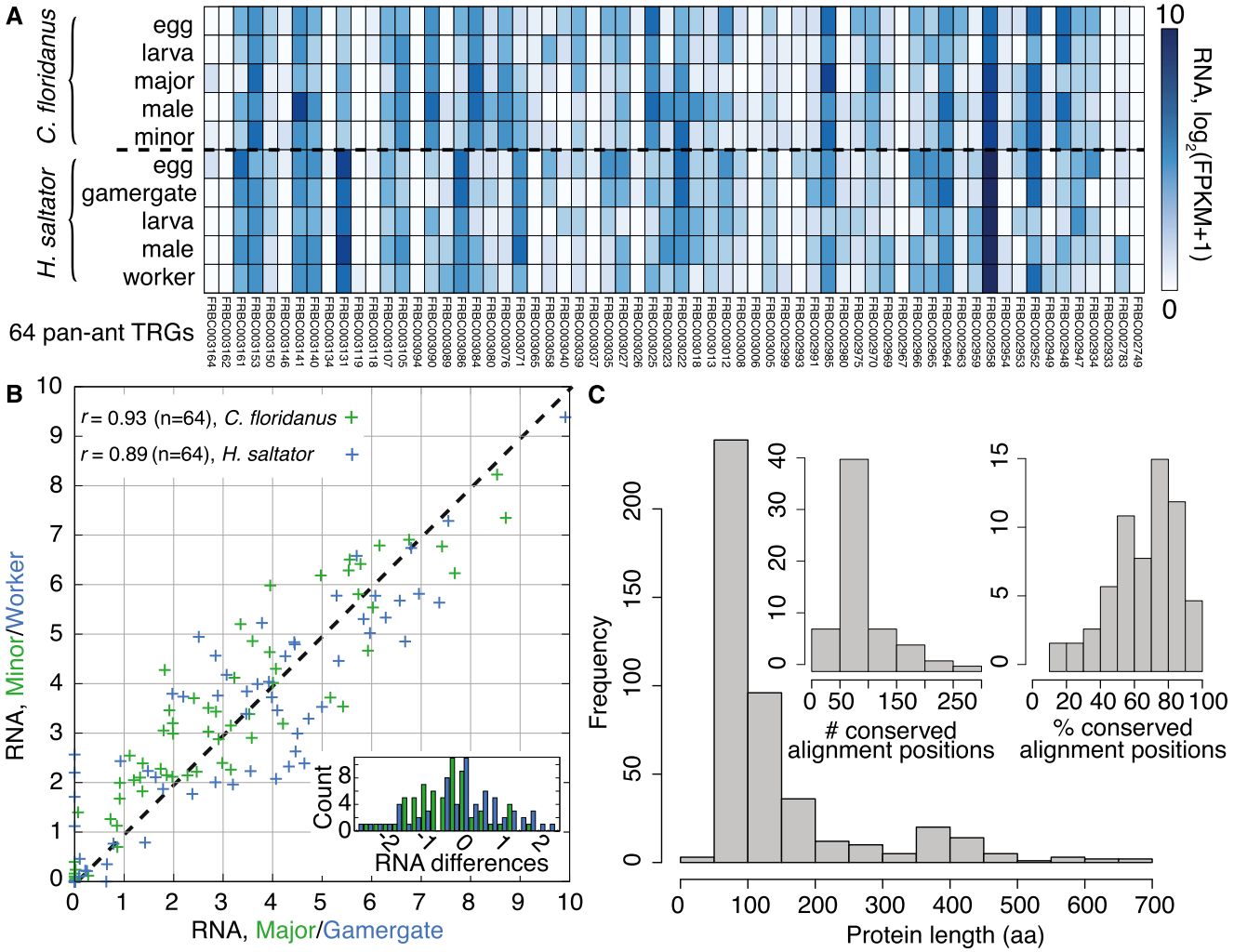

Figure 2. Analysis of 64 pan-ant taxonomically restricted genes (TRGs). (*A*) RNA expression support for 64 TRGs that are orthologous among all seven ant species but not found in other genomes. RNA expression levels, estimated as $\log_2$(FPKM + 1), are shown for various developmental stages and adult castes of *C. floridanus* and *H. saltator*. (*B*) Expression correlation between adult worker castes in *C. floridanus* (major vs. minor; green) and *H. saltator* (gamergate vs. worker; blue) for the 64 novel ant TRGs; Pearson's correlation coefficients are shown. (*Inset*) Histogram of differences in gene expression levels between castes (major − minor in green, gamergate − worker in blue) per gene. (*C*) Length distribution (in amino acids) of the 64 novel ant TRGs. (*Inset*) Distribution of the number (*left*) and percentage (*right*) of conserved alignment positions (see Supplemental Text 1).

and Diptera ($n = 15$). This comparison revealed that Hymenoptera have both a greater number of TRGs (4658 vs. 3442 average TRGs per species) and a faster TRG emergence rate (31 vs. 14 average TRGs per species per million years) than Diptera (Fig. 1B). Young insect lineages also tend to have a faster TRG emergence rate than older lineages ($R = -0.68$, $P < 0.04$) (Fig. 1C). Notably, the two leaf-cutter ant species, which diverged only 8–12 million years (Myr) ago (Schultz and Brady 2008), exhibit the highest number of TRGs ($n = 6796$) and the fastest TRG emergence rate of any sequenced insect lineage, gaining 340 TRGs per species per million years. In comparison, the *Drosophila melanogaster* subgroup ($n = 6$), also having diverged ~12 Myr ago, gains 115 TRGs per species/Myr. This pattern of rapid but transient expansions of gene content may coincide with dramatic life-history changes associated with early stages of lineage divergence. For example, *A. cephalotes* is distinguished from *A. echinatior* by loss of cuticular actinomycete cultures, physically distinct soldier castes, and claustral colony founding (Fernández-Marín et al. 2009; Villesen et al. 2009). In support of this, most leaf-cutter TRGs (68%) are species specific.

We hypothesize that these rapid TRG expansions observed for Hymenoptera may be due to differences in the rate of gene loss rather than gene gain. Natural selection is expected to be less efficient at removing superfluous genes from populations with small effective population sizes. Haplo-diploid sex determination and reproductive division of labor in eusocial Hymenoptera reduce effective population size relative to solitary and diploid Diptera (Crozier and Pamilo 1996; Gadau et al. 2012). The lack of a significant codon usage bias in ant genomes compared with *Drosophila* further supports the idea of relatively reduced selection efficiency in eusocial Hymenoptera (Supplemental Fig. 9; Supplemental Table 4; Supplemental Text 2).

Extensive gene family evolution in ants targets cytochromes, desaturases, olfactory receptors, and transcription factors

Gene families are sets of paralogs that often display functional similarity. Expansions or contractions in gene families may correspond to adaptive events coupled to life-history transitions (Ranson et al. 2002). To identify gene families in ants that have expanded or contracted due to natural selection, we examined changes in gene family size along branches of the phylogeny for 15 insects and estimated the rates of change, using a null model of gene family evolution that reflects the expected divergence due to neutral mutation and genetic drift (Supplemental Table 5; Supplemental Methods; Hahn et al. 2007). We found hundreds of gene family expansions and contractions along each of the terminal branches (Supplemental Fig. 10A) resulting in significant increases in variation for 281 families ($P < 0.01$). Along the branch leading to Formicidae, 11 significant expansions and nine significant contractions have occurred. Functional annotation of these 20 families showed that 55% possess DNA-binding capacity, generally characterized by zinc-finger or helix–loop–helix domains (Supplemental Fig. 11); of these 55% of the expanded and 22% of the contracted families may be involved in regulation of transcription. This suggests that changes in the transcription factor (TF) repertoire were important in the initial stages of ant evolution.

In addition, 96 gene families (34% of significant families) show significantly increased variation within Formicidae with several showing repeated expansions and contractions. This includes the P450 cytochrome superfamily, which has been linked to ecdysteroid metabolism and the detoxification of xenobiotics, and odorant receptor and desaturase genes, which are involved in chemical communication, e.g., caste and colony recognition (Nygaard et al. 2011; Smith et al. 2011b; Suen et al. 2011). Repeated changes in these families may reflect adaptations to novel ecological niches (e.g., tropics vs. desert or terrestrial vs. arboreal) and/or changes in social organization (e.g., colony size, mode of reproduction, division of labor). For instance, dietary specialization may conceivably demand novel genes to detoxify or metabolize novel compounds, while existing genes that help process undesirable food items could become unnecessary and therefore lost through genetic drift, e.g., P450 cytochrome pseudogenization in *P. barbatus* (Smith et al. 2011b) and loss of metabolic pathways in leaf-cutter ants (Nygaard et al. 2011; Suen et al. 2011). Analogously, the efficiency of chemical stimuli varies between environments and communication systems, necessitating tailored changes to groups of desaturases or olfactory receptors.

Desaturase proteins are central to the production of alkenes, a highly variable component of cuticular hydrocarbons reported to transmit complex signals like nest-mate recognition cues in ants (Martin and Drijfhout 2009; van Zweden et al. 2010). Manual annotation and phylogenetic analyses of the Δ9 and Δ11 desaturase gene families revealed that five ancestral subfamilies are present in all holometabolous insects (Supplemental Fig. 10B). Two of these subfamilies experienced multiple episodes of gene expansion at various times during hymenopteran evolution, resulting in 10–23 putatively functional genes in ants, compared with seven genes in *D. melanogaster*. Large numbers of related but nonfunctional gene fragments scattered throughout ant genomes also suggest that ants frequently altered their desaturase gene repertoire. For example, the invasive species *L. humile* and *S. invicta* possess 25 and 15 pseudogenes, respectively, suggesting that drastic changes in habitat and social organization following novel habitat invasion might have an immediate effect on genes implicated in social communication. Overall, the elevated number of desaturase genes and their variability in sequence and expression might reflect increased demand for chemical signal diversity used in ant social communication. Consistent with this, gene families presumably involved in the perception of these signals (e.g., olfactory receptors) (Smith et al. 2011b; Zhou et al. 2012) exhibit similar expansions.

Finally, we reanalyzed immune gene families of social and solitary insects, since the honeybee genome is reported to contain only one-third of the immune genes found in *Drosophila* (The Honeybee Genome Sequencing Consortium 2006), yet these families did not emerge from our gene family evolution analysis. The immune gene complements of eusocial insects did not differ from solitary insects as dramatically as previously proposed, because only three of 16 immune gene families showed significant changes in size between eusocial and solitary groups (FDR < 0.1) (Supplemental Table 6).

Ant genomes exhibit a strong degree of synteny

Comparative analysis of large-scale genome structure in the *Drosophila* clade (63 Myr) (Tamura et al. 2004) has revealed broad genome-scale similarity with 66% synteny, less than threefold change in total genome size, and little change in chromosome number (four to six chromosomes) (*Drosophila* 12 Genomes Consortium 2007). While genome size among the seven ants shows a similar threefold range, ant species cover twice the evolutionary distance, have more variable chromosome numbers (eight to 22 chromosomes) (Gadau et al. 2012), and exhibit extremely high recombination frequencies (e.g., 71 kb/cM for *Pogonomyrmex*

rugosus) (Sirviö et al. 2011). These differences between Formicidae and *Drosophila* should favor a rapid decline of synteny in ants. To examine this, we first assembled syntenic blocks of homologous sequences using pairwise alignment of single-copy exons among genomes (Supplemental Fig. 12A–C). While only 5.3% of assembled contigs exhibit significant homology among ants, they comprise 3639 syntenic blocks that cover 65% of each genome on average (minimum 57%, *H. saltator*; maximum 71%, *A. cephalotes*), largely consistent with estimates from *Drosophila* (66%) (*Drosophila* 12 Genomes Consortium 2007). Moreover, average synteny increases to 74% among the four Myrmicinae, which have comparable divergence time to the 12 sequenced *Drosophila* species, and to 86% between the two leaf-cutter ants (Supplemental Fig. 12A). Thus, despite fragmented genome assemblies and deep evolutionary history, ant genomes show moderate to strong genomic synteny, especially in gene-rich, euchromatic regions. Of course, given the variability in repetitive and total genome size in ants (see Fig. 1A), we do suspect that heterochromatic regions may harbor a greater degree of large-scale structural divergence.

Using a subset of 287 syntenic blocks showing strongest synteny in ants (Supplemental Fig. 13), we evaluated the extent of gene inversions and rearrangements in ants and other insects, using the *A. echinatior* genome as a common reference (the assembly of this species has the greatest N_{50} contig size) (Gadau et al. 2012). These highly syntenic blocks average 300 kb, include 10–15 genes per block, and harbor 8749 genes, including 5202 (91%) single-copy genes found in all seven ant genomes (Supplemental Fig. 1). As expected, both inversions and rearrangements increase with evolutionary distance from *A. echinatior*, although inversions appear to be more common overall (Supplemental Fig. 14). Notably, gene order in the *hox* cluster is identical among ants and is consistent with the ordering in *Drosophila* (Supplemental Fig. 15). Interestingly, all ant species display a lower percentage of gene rearrangements (<4%) compared with *D. melanogaster* or *A. mellifera* (~7%) and much lower compared with the parasitoid wasp *Nasonia vitripennis* (11%) (Supplemental Fig. 14B). In contrast, *D. melanogaster* shows 2.5-fold more gene inversions compared with *A. mellifera*, ants, and *N. vitripennis*, as expected phylogenetically. Thus, some lineages of Hymenoptera may have accumulated specific kinds of structural divergence, including rearrangements, at a faster rate than *Drosophila* and independent of eusociality.

Ant conserved regions harbor an abundance of regulatory elements and are enriched near neuronal genes

Leveraging the high structural homology among ant genomes, we generated global multiple sequence alignments of all 3639 syntenic blocks (Supplemental Fig. 12D) and identified more than 1.7 million conserved elements (CEs), including 424 CEs that span at least 1 kb (Supplemental Fig. 16). After conservatively comparing CEs against all annotated exonic sequences, including those from TRGs, and masking likely untranslated regions (UTRs), nearly half (49%) of the CEs appear to be intergenic (Supplemental Fig. 16D). By counting nucleotides delimited by CEs, we estimated that, on average, 18.6% of each ant genome undergoes purifying selection; similar analysis restricted to Myrmicinae (using 74% of the four genome sequences, compared with 65% for seven ants) yielded approximately the same estimate of 20.7%. Purifying selection is greatest for exons (59%), microRNAs (miRNAs) (92%), and tRNAs (28%), i.e., explicitly functional DNA sequences (Supplemental Fig. 16D,E). These estimates may be overestimated, because syntenic blocks are generally depleted for repetitive DNA, a major source of evolutionary variation. Thus, ants appear to exhibit 1.8-fold to 2.8-fold less purifying selection than *D. melanogaster* (37%–53%) (Siepel et al. 2005; Sella et al. 2009) and threefold more than *Homo sapiens* (5.5%) (Lindblad-Toh et al. 2011), consistent with the hypothesis that eusocial insects have reduced selection efficiency (see above).

When grouping genes by the location of proximal CEs, we recovered several significant functional categories. For example, 2883 genes harboring promoter CEs are enriched for 35 categories pertaining to system, organ, and anatomical structure development, signal transduction, and cell differentiation (FDR < 0.05). Also, the 2721 genes associated with the top 5% of CEs (ultraconserved elements) (Supplemental Fig. 16F) are enriched for 113 categories that are not represented among all CEs (FDR < 0.05) (Supplemental Table 7), 24 (21%) of which identify nervous system regulation as a key process associated with strongest conservation in ants. This is consistent with the significant differences in brain structure seen in many ants between workers and queens, worker subcastes, and age-dependent worker task groups (Gronenberg et al. 1996).

To examine whether CEs exhibit conservation beyond primary sequence, we predicted their secondary structures and identified 3318 significant structural CEs (Supplemental Methods). Most of these structures are short (91% <15 nt), likely forming hairpins, and the majority are located near protein-coding genes (61% ≤5 kb, 37% ≤1 kb) (Supplemental Table 8). While structural CEs are enriched in likely 3′ UTRs ($P < 10^{-15}$), similar to vertebrate genomes (Parker et al. 2011), 60% are intergenic, suggestive of functional small noncoding RNAs (see below). Genes near structural CEs are enriched for functional categories related to development (e.g., imaginal disc–derived wing morphogenesis, specification of segmental identity and head) and cellular dynamics (cell motility, cell migration) (Supplemental Table 9). These results indicate that DNA sequences conserved among ants identify genes and regulatory processes known to be involved in the transition to and elaboration of eusociality.

Given the abundance of conserved regulatory elements in ant genomes, we examined three mechanisms previously implicated in the regulation of social traits or phenotypic plasticity: direct modification of DNA by methylation (Kucharski et al. 2008; Bonasio et al. 2012; Smith et al. 2012), transcriptional and translational regulation by small RNAs (Pauli et al. 2011), and transcriptional regulation by transcription factors (TFs) (Rebeiz et al. 2011).

Ant genomes exhibit distinct signatures of DNA methylation

DNA methylation has been implicated in regulating gene function in social insects (Glastad et al. 2011). For example, relative depletion of CpG dinucleotides (CpG O/E, a sequence-based signature of DNA methylation) correlates negatively with DNA methylation and distinguishes classes of genes that are differentially expressed between honeybee queens and workers (Elango et al. 2009). We found that all seven ants are distinct from the honeybee in exhibiting unimodal CpG O/E distributions and significantly less CpG depletion over exons genome-wide (i.e., higher mean CpG O/E) (Fig. 3A). Interestingly however, *H. saltator* (a basal ant in our analysis) exhibits moderately greater exonic CpG depletion than the six other ants (Fig. 3A). In contrast, CpG O/E patterns over introns and promoters are broadly similar across Hymenoptera with little CpG depletion. Moreover, ant CEs do not differ substantially from genomic background in terms of CpG depletion

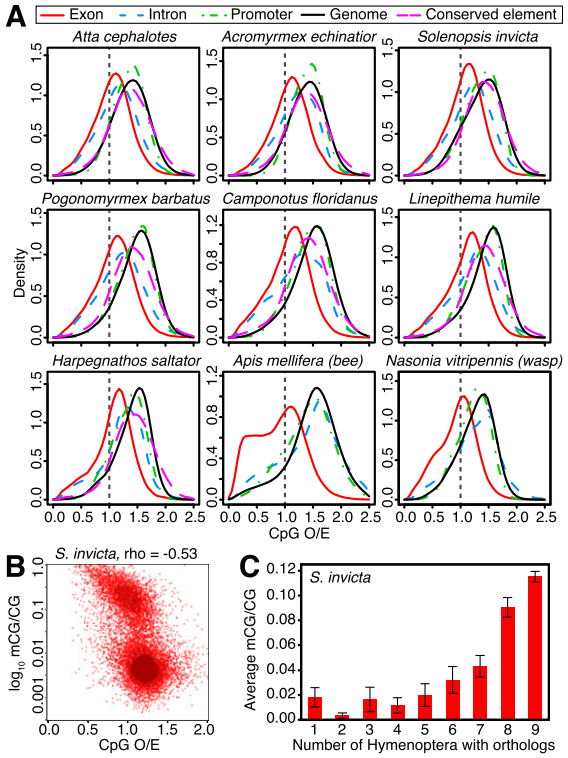

Figure 3. DNA methylation profiles in ant genomes. (*A*) Normalized CpG content (CpG O/E) of different genomic elements, including exons, introns, and promoter regions (1.5 kb upstream of coding sequence start sites) for protein-coding genes, nongenic conserved elements, and genome-wide background (1-kb fragments). Exons show the strongest evidence of CpG depletion in ants, indicating that they are the most highly methylated regions of the genome in all taxa (confirmed by Bisulfite-seq; *below*). Introns also show slight depletion of CpGs in ants, suggesting some intron methylation. (*B*) Scatterplot of $\log_{10}$(mCG/CG) methylation levels estimated by Bisulfite-seq versus CpG O/E for coding sequences in *S. invicta* reveals a bimodal distribution of gene body methylation. (*C*) Average methylation levels (mCG/CG) for protein-coding genes in *S. invicta* males, grouped according to the number of taxa in Hymenoptera with orthologs for each gene; indicating that conserved genes tend to be highly methylated. Error bars indicate 95% confidence intervals for the mean.

(Fig. 3A). These observations are consistent with a coarser, domain-scale analysis of GC bias (Supplemental Figs. 17–21; Supplemental Table 10; Supplemental Text 3), in which eusocial insects, especially ants, show a negative relationship between genome-wide GC content and exonic bias toward GC-rich domains ($R = -0.93$, $P < 0.0007$) (Supplemental Fig. 21). These analyses confirm that the honeybee is an outlier among hymenopterans in terms of sequence-based patterns of DNA methylation.

To confirm statistical patterns of DNA methylation experimentally, we generated a complete bisulfite-sequence map for *S. invicta*. We found that high levels of DNA methylation (mCG/CG) correspond well with CpG depletion in exons (Spearman's $R = -0.53$) (Fig. 3B; Supplemental Tables 11,12), indicating that some genes in ants are distinguished by DNA methylation, similar to the honeybee (see also Bonasio et al. 2012; Smith et al. 2012). Functional analysis of genes putatively methylated in all seven ant genomes (low CpG O/E) revealed enrichment for housekeeping functions, including transcription, translation, and cellular metabolic function (FDR < 0.05) (Supplemental Tables 13–15), as reported for the honeybee (Elango et al. 2009). Next, we computed the average methylation level of genes, grouped by the number of hymenopteran species with orthologs. Interestingly, levels of DNA methylation (mCG/CG and CpG O/E) increase with evolutionary conservation of protein-coding genes, especially when genes have orthologs in more distant Hymenoptera (Fig. 3C). Thus, highly conserved genes are preferentially targeted by DNA methylation. We also note that CpG O/E is a poor predictor of methylation for genes with paralogs (i.e., multicopy genes), regardless of orthology (Supplemental Figs. 22–24; Supplemental Tables 11, 12). Thus, while ants and the honeybee exhibit significantly distinct statistical patterns predictive of DNA methylation, all insects that possess DNA methyltransferases likely methylate exons of highly conserved genes, indicating a common role for DNA methylation independent of eusociality.

Conserved miRNAs and small noncoding RNAs exhibit caste differential expression

Recent investigations have uncovered novel regulatory roles for various classes of noncoding RNAs (e.g., Loewer et al. 2011). We first evaluated known miRNA genes (Bonasio et al. 2010) and found that 63 are highly conserved among ants (average ~80% conservation) (Supplemental Fig. 16D). We then reannotated the seven ant genomes for miRNAs and uncovered 24 novel loci, 18 of which are specific to ants (Supplemental Table 16). Using RNA-seq gene expression data, we confirmed that a total of 115 miRNAs are expressed in *C. floridanus*, including 20 of the novel miRNAs. Several miRNAs show stage- and caste-specific expression (Supplemental Fig. 25), and many, including 12 of the novel ant-specific miRNAs, are predicted to share orthologous gene targets among ant species, typically located in 3′ UTRs (data not shown).

We also used several small and poly(A)$^+$ RNA-seq data sets (Bonasio et al. 2010) to identify more than 70,000 CEs that overlap transcribed sequences in *C. floridanus* and *H. saltator*. Most transcribed CEs (~64%) are intergenic, including 23,000 CEs located more than 2 kb upstream of protein-coding genes (Supplemental Table 17); these CEs comprise a class of predominantly small, conserved noncoding RNAs. Many conserved noncoding RNAs show moderate differences in expression level between adult worker castes, notably a group of 2290 RNAs that overlap CpG islands and show the highest median expression difference between *C. floridanus* worker castes (Supplemental Fig. 26A,C). Interestingly, CpG islands are also the only nonexonic regions significantly enriched for CEs ($P < 0.01$) (Supplemental Fig. 16D, top), and CpG island RNA expression levels correlate positively with expression levels of the nearest downstream protein-coding genes ($0.1 \leq R \leq 0.5$), with stronger correlations generally found for CpG islands closer to genes (Supplemental Fig. 26B). Functional analysis of these downstream genes revealed a striking enrichment for regulatory processes targeting neuron differentiation and neurogenesis, steroid hormone signaling, cell differentiation, and gene expression (FDR < 0.1) (Supplemental Table 18). These results support the notion that ant CpG islands, which are broadly hypomethylated in ants (Bonasio et al. 2012; this study), may serve a regulatory role, perhaps by harboring enhancer binding sequences or by being preferentially targeted by regulators of chromatin structure (Ramirez-Carrozzi et al. 2009), where small RNAs may be directly or indirectly involved (Kim et al. 2010; Pauli et al. 2011).

Genome-wide evolution of TF-binding sites is more divergent within ants than between eusocial and solitary insects

The genomic organization of sequence-specific TF-binding sites (TFBSs) represents a profound source for transcriptional regulatory

variation potentially used during the evolution of insect sociality (Gadau et al. 2012). We evaluated the extent of TF-mediated regulatory evolution by analyzing the genome-wide occurrence and distribution of 59 TFBSs (Supplemental Fig. 27), corresponding to developmentally expressed TFs that exhibit broad conservation in their genomic copy number (i.e., they do not belong to evolutionarily variable gene families) (Supplemental Table 19) and nonadaptive coding sequence evolution (93% of branch tests for positive selection in TF loci were not significant) among insects (Supplemental Fig. 28; Supplemental Table 20). Indeed, 26% of all CEs and 48% of ultraconserved CEs harbor at least one TFBS (Supplemental Fig. 29A), confirming that conserved regions are broadly enriched for regulatory elements in ants. In fact, most of these CEs harbor multiple TFBSs (average 4.3 TFBSs/CE) (Supplemental Fig. 29B), suggesting that preservation of TF coregulation is also important.

We proceeded to examine whether ant genes that harbor conserved TFBSs in their promoters (0–2 kb upstream of ORFs) exhibit evolutionary changes in TF regulation among insects, including the eight eusocial species and 20 solitary species. For most TFs, the average number of promoter binding sites remains similar across insects, although a few TFs do show overall gains in Hymenoptera (e.g., Antennapedia, Giant) (Fig. 4A). To evaluate the extent of divergence of TF regulation, we compared genome-wide TFBS profiles by computing Euclidean distances between species using the number of TFBSs per gene per TF (Fig. 4A, right; Supplemental Fig. 30). Eusocial species (especially ants) exhibit striking divergence in promoter TFBSs that is greater than their divergence from solitary species. Moreover, the two leaf-cutter ants differ more from each other than the two most divergent flies, and the honeybee shows greater divergence from ants than from flies. This suggests that while many TFBSs remain conserved in ants, the overall architecture of TF-mediated gene regulation is highly variable across insects, especially between convergently evolved eusocial lineages in Hymenoptera.

Ant genomes exhibit similar patterns of *cis*-regulatory evolution associated with evolutionary increased gene expression plasticity between worker castes

To evaluate whether gains or losses of TFBSs are specifically maintained in eusocial insects but not solitary insects, we examined whether individual gene promoters exhibit changes in TFBS abundance between eusocial ($n = 8$) and solitary ($n = 20$) species. Indeed, we identified nearly 2000 significant genes (FDR < 0.25) (Supplemental Fig. 29C; Supplemental Tables 21, 22), which represent potential drivers of the genome-wide divergence pattern (see above). This analysis implicates 30 TFs, 16 of which are associated with more than 100 significant genes each (Fig. 4B). Most of the significant TFs show either predominant gains ($n = 7$) or losses ($n = 8$) of TFBSs in the eusocial genomes (e.g., SHN and EMS), although a few TFs show more complex patterns of gains and losses (e.g., CREB) (Fig. 4C). We also identified 292 genes that exhibit significant changes in TFBS abundance for multiple TFs, i.e., apparent targets of concentrated *cis*-regulatory rewiring (Fig. 4D). These 292 genes are enriched for 41 functional categories involved in hormone regulation and transcription factor activity (FDR < 0.05) (Supplemental Table 23) and include *nervous wreck*, which regulates synaptic growth and neurotransmission (Coyle et al. 2004), and *choline O-acetyltransferase*, a key enzyme for synthesizing the neurotransmitter acetylcholine (Fig. 4D). This suggests that the insect neuroendocrine system has been targeted for regulatory changes during eusocial evolution. Thus, specific TF regulatory proteins conserved among insects exhibit significant divergence in their targets of regulation between eusocial and solitary lineages.

We next assessed whether any genes exhibit regulatory changes specifically in ants, and we found 141 genes with significant TFBS gains in ants but zero predicted binding sites for the majority (≥80%) of other species (Supplemental Fig. 31), including the honeybee (Supplemental Fig. 32). Intriguingly, evolution of binding sites for CREB, a TF regulator of long-term memory (CREBB, Ishimoto et al. 2009) and secretory activity (CREBA, Abrams and Andrew 2005) in insects, affects the most genes in this analysis ($n = 31$). This suggests that ants may have preferentially altered the binding distribution of CREB as a possible means to achieve gene expression plasticity between specialized castes (see below). Indeed, evolutionary gains/losses of CREB-binding sites perfectly discriminate eusocial from solitary species (and ants from the honeybee) in a Principle Components Analysis (Supplemental Fig. 33). Moreover, one of CREB's cofactors, the transcriptional coactivator and histone acetyltransferase CBP, was recently reported to play a role in maintaining caste-specific gene expression patterns in *C. floridanus* (Simola et al. 2013). These results suggest that while many genes show significant *cis*-regulatory changes specific to ants, the majority (>90%) of genes with significant eusocial-associated regulatory evolution tend to exhibit similar changes in both ants and the honeybee, broadly suggestive of the importance of *cis*-regulatory changes in the evolutionary origins of or convergence on eusociality.

Since TF-binding events regulate gene expression levels, we proceeded to examine whether changes in TFBS abundance between ant species may be indicative of evolutionary increases in gene expression plasticity between castes within a species. Interestingly, genes with the most significant changes in TFBS abundance between eusocial and solitary insects show elevated levels of plasticity in a socially sophisticated ant, *C. floridanus,* compared to *H. saltator,* whose colonies are smaller and exhibit less reproductive division of labor (average 0.39 vs. 0.27, $P < 10^{-8}$) (Fig. 4B, bottom). Furthermore, different TFs show significantly different levels of plasticity in *C. floridanus* ($P < 0.05$) but not *H. saltator* ($P < 0.13$) (Fig. 4B, bottom), as well as correlations in plasticity between species when grouped by TF ($R = 0.65$, $P = 0.002$) or for individual genes ($R = 0.30$, $P = 0.003$) (Supplemental Fig. 34). Gene targets of nine TFs show greater plasticity compared with all ant orthologs ($P < 0.05$) (Fig. 4B, asterisks), notably for Empty spiracles (EMS), which regulates brain morphogenesis and antennae development in *Drosophila* (Cohen and Jürgens 1990), and CREB (see above), which shows the second largest effect (albeit not significant in this analysis). These results suggest that caste-associated gene expression plasticity is a continuously evolving trait in eusocial insects that is partly determined by TFBS abundance (see also Supplemental Fig. 33).

Known eusocial pathways exhibit *cis* and *trans* regulatory evolution for several TFs

Finally, we analyzed patterns of regulatory evolution in the salivary gland and wing development regulatory networks, which are known to exhibit phenotypic plasticity between workers and queens and between different worker castes and task groups (Abouheif and Wray 2002; Li and White 2003). We were struck by the over-representation of TFs associated with eusocial regulatory evolution (see above) among key regulators of these networks

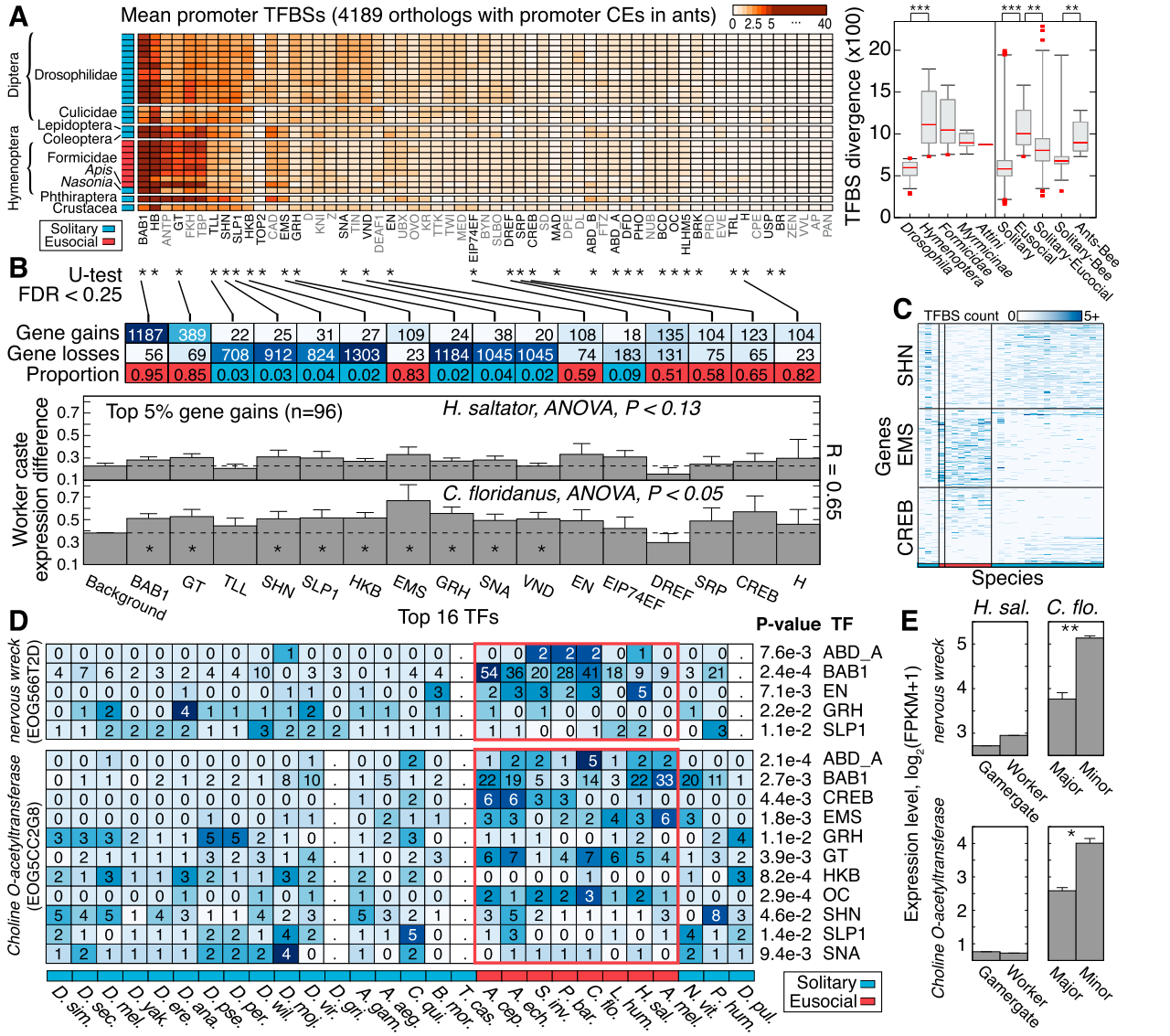

Figure 4. Evolution of transcription factor binding sites (TFBS) in insects. (*A*) Heatmap showing number of promoter TFBSs per gene for 59 TFs in 28 insect species ($n = 4189$ genes associated with 2-kb promoter CEs in ants). Species (rows), ordered by phylogenetic grouping, are denoted as solitary (blue) or eusocial (red). TFs were clustered hierarchically using average linkage by computing Euclidean distance between TFBS profiles over all queried genes. (*Right*) Boxplots show distributions of Euclidean distance values for pairs of species, computed using genome-wide TFBS abundance profiles over genes and TFs (see Supplemental Fig. 30). Each boxplot reflects a group of paired comparisons. *P*-values estimated by two-tailed Mann–Whitney *U*-test. (**) $P < 10^{-5}$; (***) $P < 10^{-10}$. (*B*) Genes and TFs exhibiting significant TFBS evolution between solitary and eusocial groups. Three thousand two hundred and thirty-one of 4189 genes had sufficient data for significance testing. (*)TF with significant promoter TFBS evolution (two-tail Mann–Whitney *U*-test; FDR < 0.25). *Top* two rows indicate numbers of genes showing significant gain or loss of binding sites for the specified TF. *Bottom* row indicates proportion of significant genes showing more TFBSs in eusocial compared with solitary insects. More than 93% of tested genes are single-copy in the ant genomes. *Bottom* panels show the mean and standard error of the standard deviation in RNA expression levels (*y*-axis) for 96 genes with greatest significance in multiple TFs (top 5%), grouped by TF. Expression levels estimated by $\log_2(\text{FPKM} + 1)$. (FPKM) Fragments per kilobase per million reads. (*) Significantly increased caste variation in RNA expression (compared with all ant orthologs, Background, $P < 0.05$). (*C*) TFBS abundance profiles for significant genes, shown for three TFs. Species order (*x*-axis) as in *A*. (*D*) TFBS abundance profiles for two neuronal genes with significance in multiple TFs. Cell colors are row-normalized. Periods (.) Missing data. *P*-values were computed by a Mann–Whitney *U*-test. (*E*) mRNA expression level estimates for the genes in *D*, shown for different worker castes in *H. saltator* (reproductive/nonreproductive) and *C. floridanus* (major/minor). Error bars indicate standard error over three biological replicates. (**) FDR < 0.01; (*) FDR < 0.25.

(Fig. 5A,B; Supplemental Text 4). In particular, *fork head* (FKH), an essential regulator of insect salivary glands and labial silk gland development in *Bombyx mori* (Mach et al. 1995), has undergone considerable loss of TFBSs in its own promoter in the eusocial genomes (Fig. 5C)—an example of *trans*-regulatory evolution that may confer pleiotropic effects. Furthermore, the regulatory network for wing development in ants harbors three TFs—*abdominal A* (*abdA*), *snail* (*sna*), and *engrailed* (*en*)—for which we found significant changes in TFBS abundance; *engrailed* was previously shown to be down-regulated in wing discs of workers compared with queens during larval development in two ant species (Abouheif and Wray 2002). These observations support the hypothesis that

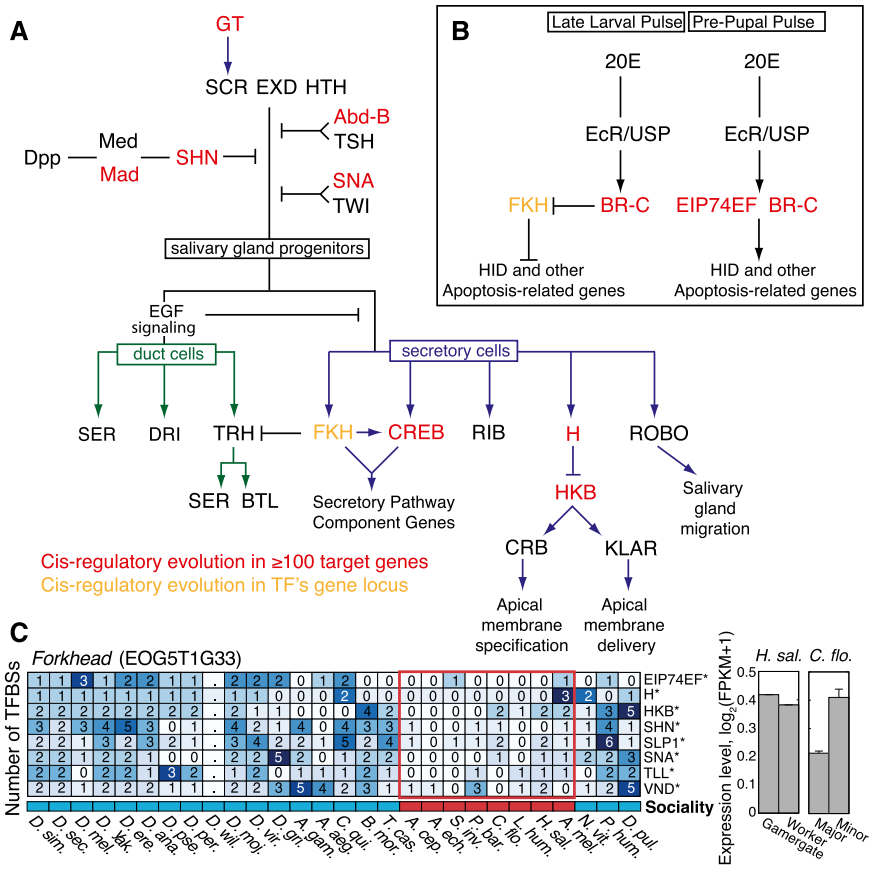

Figure 5. Transcription-factor-mediated signaling pathways controlling salivary gland development. (*A*) *Sex combs reduced* (SCR) in combination with *extradenticle* (EXD) and *homothorax* (HTH) direct the specification of cells to the salivary gland fate in PS2 of the *Drosophila* embryo; these TFs are essential for the downstream regulation of genes required for gland cell differentiation and morphogenesis. Boundaries of salivary gland development are restricted along the anterior/posterior axis by *abdominal B* (Abd-B) and *teashirt* (TSH), along the dorsal axis by *decapentaplegic* (DPP) signaling, and along underlying mesoderm by *twist* (TWI) and *snail* (SNA). *Epidermal growth factor* (EGF) signaling determines the decision to differentiate into duct or secretory cells. (*B*) Regulation of programmed cell death of embryonic salivary gland by 20-hydroxyecdysone (20E). Cell death is inhibited by *fork head* (FKH) expression in embryonic salivary gland cells. A pulse of 20E at the late larval stage triggers *broad* (BR-C)–mediated FKH inhibition. A second pulse of 20E at the prepupal stage leads to BR-C and *ecdysone-induced protein 74EF* (EIP74EF) directed transcription of apoptotic genes, including *wrinkled* (HID). TFs associated with TFBS evolution in more than 100 target genes (*cis*-regulatory evolution) (see Fig. 4) (red). The promoter of the *fork head* locus (yellow), which encodes a TF involved in the regulation of secretory cells, shows significant changes in the gain or loss of promoter TFBSs in ants (*trans*-regulatory evolution), as detailed in *C*. (*Right*) mRNA expression level estimates for *fork head*, shown for different worker castes in *H. saltator* (reproductive/non-reproductive) and *C. floridanus* (major/minor). Error bars indicate standard error over three biological replicates.

regulatory rewiring both in promoters of loci encoding TF regulators (*trans*-regulatory evolution) and in promoters of target loci (*cis*-regulatory evolution) may serve as an evolutionary driving force enabling morphological and behavioral plasticity in eusocial insects.

Discussion

Given the remarkable phenotypic diversity among eusocial insects, a key question is to what extent do derived and independent eusocial lineages harbor shared features of genomic organization that enable a eusocial lifestyle. Our analysis of eight "socio-genomes" (Robinson et al. 2005), together with several solitary insect genomes, suggests that despite a pattern of broad sequence divergence expected by deep evolutionary history, key changes in gene regulation (both in *cis* and in *trans*) may have convergently evolved in the early stages of eusocial evolution, whereas changes in gene composition may have been more important for lineage-specific social and ecological adaptations. Ant intergenic sequences are enriched for regulatory elements, including miRNAs, noncoding RNAs, and TF-binding sites that are conserved in both DNA sequence and homologous genomic position. Nearly 2000 genes share similar *cis*-regulatory changes in eusocial compared with solitary insects, and most of these changes are similar in both eusocial lineages of ants and honeybees. These genes are enriched for neuronal and hormonal functions and implicate a few specific TFs in eusocial evolution, notably EMS and CREB. Changes in TFBS abundance are linked to evolutionary increases in phenotypic plasticity from ants with a simpler social organization to those with more complex social organization. The locus encoding one key TF, *fork head*, also shows significant regulatory evolution in ants, which has potentially facilitated pleiotropic effects in *trans* for regulatory networks relevant to eusociality, e.g., exocrine gland and wing development. Finally, six gene families with putative transcription regulatory activity experienced significant gains in family size during early ant evolution.

Our analysis of evolutionary changes in gene composition in ants contextualizes these results. We found an abundance of taxonomically restricted genes (TRGs) in ants as well as a higher rate in the emergence of TRGs in ants compared with flies, suggesting functional ties to eusocial adaptations. In other systems, TRGs can comprise 10%–33% of a species' protein-coding gene complement and have been linked both to morphological adaptations (Khalturin et al. 2009; Tautz and Domazet-Lošo 2011) and to eusocial traits, including caste differentiation (Kamakura 2011) and complex behavioral repertoires (Johnson and Tsutsui 2011). Importantly, while TRGs likely play important roles involved in the elaboration of social adaptations in individual lineages, TRGs that are critical for early eusocial evolution or the maintenance of eusociality should be conserved in multiple ant genomes. We found 64 ant-specific TRGs that are conserved in all seven ant genomes; however, these genes show limited differential expression between adult worker castes in two different species, at least using pooled tissue data. These novel genes may be relevant for the evolution of eusociality in ants, but their specific functional significance remains unclear.

In conclusion, evolutionary changes in gene regulation seem to dominate our view of the shared genomic features associated

with the origins of eusociality. However, the broad spectrum of changes observed in eusocial insect genomes suggests that the origin, maintenance, and elaboration of insect eusociality was not necessarily restricted to a small set of genes or regulatory elements. Instead, the organization of eusocial insect genomes appears to harbor sufficient degrees of freedom to allow convergence of higher-order complex traits, such as eusociality, from unique, lineage-specific evolutionary trajectories that involve distinct genes and modes of regulation. Such genomic complexity may be especially engendered by ants, where extreme reproductive divisions of labor resulting from a eusocial lifestyle may effectively reduce the strength of natural selection, thereby facilitating rapid sequence divergence among lineages.

Methods

In addition to the Methods described below, the Supplemental Material includes information for the following: quality assessment of annotated genes (see also Supplemental Figs. 3, 4; Supplemental Table 1), identification of paralogous genes (see also Supplemental Figs. 7, 8), codon usage bias (see also Supplemental Fig. 9; Supplemental Text 2; Supplemental Table 4), gene family evolution (see also Supplemental Fig. 10), multiple genome alignment (see also Supplemental Fig. 12), synteny analysis (see also Supplemental Figs. 13, 14), conserved structural RNA analysis (see also Supplemental Table 8), GC compositional analysis (see also Supplemental Figs. 17–21; Supplemental Text 3), and testing positive selection of single-copy orthologs (see also Supplemental Fig. 28).

Assessing homology of known genes among insect species (AntOrthoDB)

The OrthoDB orthology delineation procedure (Waterhouse et al. 2011) was used to delineate orthologous genes at each radiation along the insect species phylogeny, which includes seven sequenced ant and five outgroup insect species (Supplemental Table 1). OrthoDB has been updated to include these results, along with protein descriptors, Gene Ontology, and InterPro attributes (http://cegg.unige.ch/orthodbants) (Supplemental Fig. 2). See Quality Assessment of Annotated Gene Sets in AntOrthoDB in the Supplemental Material for additional information.

Identification of taxonomically restricted genes

Taxonomically restricted genes (TRGs) were identified as protein-coding genes that lack sequence similarity to annotated proteins outside of a focal taxonomic group (e.g., Formicidae) (Fig. 1B), using the official gene sets for 30 arthropod species. Ortholog identification was based on all versus all BLASTP searches among all annotated proteins ($E < 1 \times 10^{-3}$). For Formicidae TRGs, BLAST hits within ant genomes were ignored. Among TRGs, subsets of genes that only occur within an individual species were identified and denoted as lineage-specific genes (LSGs), given our taxon sampling. Among LSGs, genes were conservatively filtered if the gene (1) matched in other proteomes when low complexity filtering was deactivated, (2) matched proteins in SwissProt taxonomic divisions (except invertebrates) as potential contaminations, or (3) appear not to be lineage specific if a similar sequence with matching gene model was found in the genome. To control for false LSGs, putative homologs of genes that were predicted in only one of the ant species were screened against the genomes of the other eight Hymenoptera using a custom-built pipeline. True missing genes had to (1) yield a significant BLAST hit in another genome using its predicted peptide sequence as query for TBLASTN ($E \leq 1 \times 10^{-5}$, low-complexity filtering activated), and (2) yield a seemingly functional gene model based on the alignment of the protein query against the genomic sequence. GeneWise v2.4.1 was used to align the protein query against the scaffold in a strand- and position-specific manner. Strandedness and position (±50 kb) were derived from the TBLASTN hit. Only GeneWise models with a score >35, coverage of the query sequence >75%, and zero indels (ORF-disrupting frameshift mutations) were accepted as valid gene models. Applying this procedure yielded a total of 2936 (previously lineage-specific) genes, along with 6369 newly identified genes that produced valid gene models in multiple Hymenoptera species (Supplemental Fig. 5). This yields a total of 12,054 LSGs within Formicidae (42.2% of all 28,581 Formicidae TRGs).

Insect phylogeny

The phylogeny shown in Figure 1 was estimated by maximum likelihood from the concatenated alignment of conserved protein sequences of 2756 single-copy orthologs across 12 insect species, comprising 792,477 well-aligned amino acids. Sequence alignments were performed with MAFFT (Katoh et al. 2002), conserved cores were selected with Gblocks (Castresana 2000), and the phylogeny was built with PhyML (Guindon et al. 2010). Using 4346 single-copy orthologs defined across the seven ant species, *A. mellifera* and *N. vitripennis*, protein lengths were compared to examine the agreement of ant genes with those of their bee and wasp orthologs (Supplemental Fig. 6; Supplemental Table 2).

Conserved elements

Conserved elements were identified from whole-genome sequence alignments using phastCons (Siepel et al. 2005). Conserved and nonconserved HMMs were estimated with parameters (-target -coverage 0.25 -expected -length 12 -estimate-trees), given a phylogenetic tree (described above) for initialization. Resulting conserved elements (CEs) were filtered to remove any regions whose consensus sequence consisted of gaps only. A subset of ultra-conserved elements (UCEs) were identified as those CEs having length ≥5 nt and LOD/length scores in the top fifth percentile of all CEs, where LOD denotes the log-odds ratio of the posterior probability of conservation to that of nonconservation across the nucleotides delimited by the CE. Noncoding conserved RNAs are defined as transcribed ant CEs and do not overlap annotated ant exonic sequences. Specifically, for each CE, associated DNA sequences from each of seven ant genomes as well as their consensus sequences were locally aligned to all annotated exon sequences from each of the genomes using nucleotide BLAST (*E*-value of 10). A CE was considered to be exonic if any one associated DNA sequence showed significant alignment to any one exon from any ant genome. CEs were annotated as transcribed if at least 25% of the element overlaps an annotated transcript whose expression level is greater than the fifth percentile of genome-wide expression levels in at least two independent biological samples, for each species (see RNA Expression Analysis, below).

DNA methylation

Normalized CpG dinucleotide content (CpG O/E) was calculated using the equation:

$$CpG\frac{O}{E} = \frac{length^2}{length} \times \frac{CpG\ count}{C\ count \times G\ count}.$$

Bisulfite-seq data were obtained using genomic DNA from six pooled whole-body haploid males of *S. invicta* from a single

colony (NCBI GEO accessions GSE39959). Bisulfite conversion and sequencing were performed by the Beijing Genomics Institute (Shenzhen, China). Bisulfite treatment was performed using the EZ DNA Methylation-Gold Kit (Zymo Research Corporation). Sequencing was performed using the Illumina HiSeq2000. Reads passing quality control were mapped using Bowtie and Bismark (Langmead et al. 2009; Krueger and Andrews 2011). Aligned reads were processed using SAMtools to remove PCR duplicated reads (rmdup) and parsed using custom Perl scripts to obtain methylated and unmethylated read counts on a per-nucleotide basis. Fractional methylation was calculated for each CpG site with three or more reads as mCG/CG, where mCG is the number of reads with methylated cytosine at a CpG site (according to bisulfite conversion), and CG is the total number of reads with either unmethylated or methylated (converted and unconverted) cytosine at the same CpG site. Fractional methylation values were averaged across each annotated element with data for three or more sites (otherwise the element was discarded). Functional enrichment was performed using Gene Ontology annotation of single-copy *D. melanogaster* orthologs of *H. saltator* genes belonging to single-copy seven-ant orthologs, as analyzed by the DAVID (Huang et al. 2009a; Huang et al. 2009b) functional annotation tool.

MicroRNA identification

Hymenoptera small RNA sequences were downloaded from the NCBI Sequence Read Archive (SRA) database (Accession numbers: SRX018737, SRX023147–SRX023156) and searched against the ant genome assemblies using BLASTN. Alignments having ≤2-nt mismatches were retained and analyzed using MIREAP with a minimum folding energy of −18 kcal/mol (http://sourceforge.net/projects/mireap/). An miRNA was considered ant specific when the precursor hairpin and subsequent mature miRNA were present in ≥4/7 ant genomes. This conservative strategy ignores other likely ant-specific miRNAs absent in the current assemblies. Novel miRNA coordinates are listed in Supplemental Table 16.

Target analysis was performed after aligning novel, ant-specific miRNAs to the annotated ant genes. As a proxy for 3′ UTRs, 750 bp of sequence downstream from each stop codon was extracted. miRNA:mRNA target analysis was performed using miRanda (Enright et al. 2003) with parameters: -sc 140 -en 20. Target predictions were considered conserved if at least four ant orthologous ant genes were targeted by the respective miRNA using OrthoDB.

Identification and analysis of transcription factor–binding sites

Identification of TFBS in insects

Position weight matrices (PWMs) for 56 transcription factors (TFs) were taken from DMMPMM (Bigfoot) and iDMMPMM (Kulakovskiy et al. 2009). PWMs for CREB (CREBA and CREBB) and the promoter elements CPE and DPE were obtained from Transfac (http://www.gene-regulation.com). Sequence motifs showing significant similarity to each PWM were predicted using pwm_scan (Levy and Hannenhalli 2002). For each of 28 insect species (as described in text), each PWM was scanned across the 2-kb promoters of protein-coding genes whose orthology among species was established by OrthoDB. To obtain stringent TFBS predictions, an empirical score distribution was estimated for each PWM for each species' genome as the set of all nominally significant ($P < 0.05$) motif scores identified within the target set of promoter sequences [pwm_scan -s 1 -p ln(0.05)]. Candidate binding sites were then selected for each genome as those scoring in the top 0.02% among this set of nominally significant sites [pwm_scan -s 2 -p ln(1/5000)], where 1/5000 is the recommended *P*-value roughly estimating expected frequency (Levy and Hannenhalli 2002). (See also Supplemental Figs. 27, 29.)

Between species comparison of number of TFBSs

Each gene of interest was tested for showing a difference in the number of proximal promoter-binding sites for each TF in eight eusocial species compared with 20 solitary species using a two-tailed Mann–Whitney (rank-sum) *U*-test. To control for potential bias due to variation in nucleotide frequency, GC bias was estimated from the promoter sequences of each genome and used to scale the number of binding sites for each motif x: GC(x)/avg(GC). Only genes having TFBS estimates for at least three eusocial and five solitary (or vice versa) species were used for evaluation. Significant genes were identified using a Benjamini–Hochberg false discovery rate (FDR) of 25%.

Genes with TFBS changes for multiple TFs

Each gene showing a significant change in TFBS abundance between eusocial and solitary genomes was also tested for significant change for multiple TFs by summing the number of 2-kb promoter TFBSs for all TFs and testing for significant difference in total TFBS abundance between eusocial and solitary genomes using a *t*-test. Genes with $|T|$ values in the top 15% overall were retained.

RNA expression analysis

Raw RNA-seq expression data for *C. floridanus* and *H. saltator* were downloaded from NCBI GEO using accession number GSE22680 (Bonasio et al. 2010) or GSE37523 (Simola et al. 2013). Raw sequence reads were mapped using Bowtie + TopHat (Langmead et al. 2009) allowing one mismatch and up to 50 alignments per read (-v 1 -k 50 -best) and default parameter values otherwise. Expression levels for previously annotated gene models were quantified with these maps using Cufflinks (Trapnell et al. 2010), correcting for fragment bias (-frag -bias -correct) and uncertain alignment location (-multi-read -correct) and default parameter values otherwise. Expression levels are reported as $\log_2(FPKM+1)$ unless otherwise stated.

Data access

Sequencing data for DNA methylation in *S. invicta* have been deposited in the NCBI Gene Expression Omnibus (GEO; http://www.ncbi.nlm.nih.gov/geo/) under accession number GSE39959. Additional supplemental files are freely available for download from the Hymenoptera Genome Database (http://hymenopteragenome.org/ant_genomes/?q=consortium_datasets) (Munoz-Torres et al. 2011).

List of affiliations

[1]Department of Cell and Developmental Biology, University of Pennsylvania, Philadelphia, Pennsylvania 19104, USA; [2]University of Pennsylvania Epigenetics Program, Philadelphia, Pennsylvania 19104, USA; [3]Institute for Evolution and Biodiversity, University of Münster, 48149 Münster, Germany; [4]Department of Genetic Medicine and Development, University of Geneva and Swiss Institute of Bioinformatics, 1211 Geneva, Switzerland; [5]School of Life Sciences, Arizona State University, Tempe, Arizona 85287, USA; [6]Department of Ecology and Evolution, University of

Lausanne, 1015 Lausanne, Switzerland; [7]Centre for Social Evolution, University of Copenhagen, 2100 Copenhagen, Denmark; [8]School of Biology, Georgia Institute of Technology, Atlanta, Georgia 30332, USA; [9]Department of Biology, Georgetown University, Washington, DC 20057, USA; [10]Department of Biology, University of Oulu, 3000 Oulu, Finland; [11]Department of Biology and Biochemistry, University of Houston, Houston, Texas 77204, USA; [12]The Johns Hopkins University, Bloomberg School of Public Health, Baltimore, Maryland 21205, USA; The Johns Hopkins University, School of Medicine, Baltimore, Maryland 21205, USA; [13]The Bioinformatics Centre, University of Copenhagen, 2100 Copenhagen, Denmark; [14]Department of Bacteriology, University of Wisconsin–Madison, Madison, Wisconsin 53706, USA; [15]Department of Biochemistry, New York University, New York, New York 10003, USA; Howard Hughes Medical Institute, New York University, New York, New York 10003, USA; [16]Center for Computing for Life Science, San Francisco State University, San Francisco, California 94117, USA; [17]Department of Biology, Earlham College, Richmond, Indiana 47374, USA; [18]Department of Environmental Science, Policy, and Management, University of California, Berkeley, California 94720, USA; [19]Department of Biology and Department of Genetics, University of Pennsylvania, Philadelphia, Pennsylvania 19104, USA.

Acknowledgments

This work was supported by grants from NSF to J.G. and C.R.S. (IOS-0920732) and a Howard Hughes Medical Institute Collaborative Innovation Award #2009005 to D.R., S.L.B., and J.L. D.F.S. was supported in part by an NRSA post-doctoral fellowship from the University of Pennsylvania Department of Cell and Developmental Biology. L.V. was supported in part by Academy of Finland grant #130290. B.H., K.G., and M.G. were supported by the U.S. National Science Foundation (grant numbers DEB-1011349, DEB-0640690, and IOS-0821130) and the Georgia Tech-Elizabeth Smithgall Watts endowment. Y.W. was supported in part by the BBSRC (grant BB/K004204/1). S.N. and J.J.B. were supported by the Danish National Research Foundation. R.M.W. was supported by SNSF 125350 and 143936 to E.M.Z. J.R., E.P., L.K., and Y.W. were supported by grants from the Swiss NSF and En ERC advanced grant. We thank Mira Han for help with running and interpreting the gene family evolution analyses.

References

Abouheif E, Wray GA. 2002. Evolution of the gene network underlying the wing polyphenism in ants. *Science* **297:** 249–252.
Abrams EW, Andrew DJ. 2005. CrebA regulates secretory activity in the *Drosophila* salivary gland and epidermis. *Development* **132:** 2743–2758.
Bonasio R, Zhang G, Ye C, Mutti NS, Fang X, Qin N, Donahue G, Yang P, Li Q, Li C, et al. 2010. Genomic comparison of the ants *Camponotus floridanus* and *Harpegnathos saltator*. *Science* **329:** 1068–1071.
Bonasio R, Li Q, Lian J, Mutti NS, Jin L, Zhao H, Zhang P, Wen P, Xiang H, Ding Y, et al. 2012. Genome-wide and caste-specific DNA methylomes of the ants *Camponotus floridanus* and *Harpegnathos saltator*. *Curr Biol* **22:** 1755–1764.
Cardinal S, Danforth BN. 2011. The antiquity and evolutionary history of social behavior in bees. *PLoS ONE* **66:** e21086.
Castresana J. 2000. Selection of conserved blocks from multiple alignments for their use in phylogenetic analysis. *Mol Biol Evol* **17:** 540–552.
Cohen SM, Jürgens G. 1990. Mediation of *Drosophila* head development by gap-like segmentation genes. *Nature* **346:** 482–485.
Coyle IP, Koh YH, Lee WCM, Slind J, Fergestad T, Littleton JT, Ganetzky B. 2004. Nervous wreck, an SH3 adaptor protein that interacts with Wsp, regulates synaptic growth in *Drosophila*. *Neuron* **41:** 521–534.
Crozier RH, Pamilo P. 1996. *Evolution of social insect colonies: Sex allocation and kin selection*. Oxford University Press, New York.
Drosophila 12 Genomes Consortium. 2007. Evolution of genes and genomes on the *Drosophila* phylogeny. *Nature* **450:** 203–218.
Elango B, Hunt BG, Goodisman MAD, Yi SV. 2009. DNA methylation is widespread and associated with differential gene expression in castes of the honeybee, *Apis mellifera*. *Proc Natl Acad Sci* **106:** 11206–11211.
Enright AJ, John B, Gaul U, Tuschl T, Sander C, Marks DS. 2003. MicroRNA targets in *Drosophila*. *Genome Biol* **5:** R1.
Fernández-Marín H, Zimmerman JK, Nash DR, Boomsma JJ, Wcislo WT. 2009. Reduced biological control and enhanced chemical pest management in the evolution of fungus farming in ants. *Proc Biol Sci* **276:** 2263–2269.
Ferreira PG, Patalano S, Chauhan R, Ffrench-Constant R, Gabaldon T, Guigo R, Sumner S. 2013. Transcriptome analyses of primitively eusocial wasps reveal novel insights into the evolution of sociality and the origin of alternative phenotypes. *Genome Biol* **14:** R20.
Gadau J, Helmkampf M, Nygaard S, Roux J, Simola DF, Smith CR, Suen G, Wurm Y, Smith CD. 2012. The genomic impact of 100 million years of social evolution in seven ant species. *Trends Genet* **28:** 14–21.
Glastad KM, Hunt BG, Yi SV, Goodisman MAD. 2011. DNA methylation in insects: On the brink of the epigenomic era. *Insect Mol Biol* **20:** 553–565.
Gronenberg W, Heeren S, Hölldobler B. 1996. Age-dependent and task-related morphological changes in the brain and the mushroom bodies of the ant *Camponotus floridanus*. *J Exp Biol* **199:** 2011–2019.
Guindon S, Dufayard JF, Lefort V, Anisimova M, Hordijk W, Gascuel O. 2010. New algorithms and methods to estimate maximum-likelihood phylogenies: Assessing the performance of PhyML 3.0. *Syst Biol* **59:** 307–321.
Hahn MW, Han MV, Han SG. 2007. Gene family evolution across 12 *Drosophila* genomes. *PLoS Genet* **3:** e197.
Hölldobler B, Wilson EO. 2009. *The superorganism*. W.W. Norton, New York.
The Honeybee Genome Sequencing Consortium. 2006. Insights into social insects from the genome of the honeybee *Apis mellifera*. *Nature* **443:** 931–949.
Huang DW, Sherman BT, Lempicki RA. 2009a. Bioinformatics enrichment tools: Paths toward the comprehensive functional analysis of large gene lists. *Nucleic Acids Res* **37:** 1–13.
Huang DW, Sherman BT, Lempicki RA. 2009b. Systematic and integrative analysis of large gene lists using DAVID Bioinformatics Resources. *Nature Protoc* **4:** 44–57.
Ishimoto H, Sakai T, Kitamoto T. 2009. Ecdysone signaling regulates the formation of long-term courtship memory in adult *Drosophila melanogaster*. *Proc Natl Acad Sci* **106:** 6381–6386.
Johnson BR, Tsutsui ND. 2011. Taxonomically restricted genes are associated with the evolution of sociality in the honey bee. *BMC Genomics* **12:** 164.
Kamakura M. 2011. Royalactin induces queen differentiation in honeybees. *Nature* **473:** 478–483.
Katoh K, Misawa K, Kuma K, Miyata T. 2002. MAFFT: A novel method for rapid multiple sequence alignment based on fast Fourier transform. *Nucleic Acids Res* **30:** 3059–3066.
Khalturin K, Hemmrich G, Fraune S, Augustin R, Bosch TC. 2009. More than just orphans: Are taxonomically-restricted genes important in evolution? *Trends Genet* **25:** 404–413.
Kim TK, Hemberg M, Gray JM, Costa AM, Bear DM, Wu J, Harmin DA, Laptewicz M, Barbara-Haley K, Kuersten S, et al. 2010. Widespread transcription at neuronal activity-regulated enhancers. *Nature* **465:** 182–187.
Krueger F, Andrews SR. 2011. Bismark: A flexible aligner and methylation caller for Bisulfite-Seq applications. *Bioinformatics* **27:** 1571–1572.
Kucharski R, Maleszka J, Foret S, Maleszka R. 2008. Nutritional control of reproductive status in honeybees via DNA methylation. *Science* **319:** 1827–1830.
Kulakovskiy IV, Favorov AF, Makeev VJ. 2009. Motif discovery and motif finding from genome-mapped DNase footprint data. *Bioinformatics* **25:** 2318–2325.
Langmead B, Trapnell C, Pop M, Salzberg SL. 2009. Ultrafast and memory-efficient alignment of short DNA sequences to the human genome. *Genome Biol* **10:** R25.
Levy S, Hannenhalli S. 2002. Identification of transcription factor binding sites in the human genome. *Mamm Genome* **13:** 510–514.
Li T-R, White KP. 2003. Tissue-specific gene expression and ecdysone-regulated genomic networks in *Drosophila*. *Dev Cell* **5:** 59–72.
Lindblad-Toh K, Garber M, Zuk O, Lin MF, Parker BJ, Washietl S, Kheradpour P, Ernst J, Jordan G, Mauceli E, et al. 2011. A high-resolution map of human evolutionary constraint using 29 mammals. *Nature* **478:** 476–482.
Loewer S, Cabili MN, Guttman M, Loh Y-H, Thomas K, Park IH, Garber M, Curran M, Onder T, Agarwal S, et al. 2011. Large intergenic non-coding RNA-RoR modulates reprogramming of human induced pluripotent stem cells. *Nat Genet* **42:** 1113–1117.
Mach V, Takiya S, Ohno K, Handa H, Imai T, Suzuki Y. 1995. Silk Gland Factor-1 involved in the regulation of Bombyx Sericin-1 gene contains Fork Head motif. *J Biol Chem* **270:** 9340–9346.

Martin S, Drijfhout F. 2009. A review of ant cuticular hydrocarbons. *J Chem Ecol* **35:** 1151–1161.
Michener CD. 1969. Comparative social behavior of bees. *Annu Rev Entomol* **14:** 299–342.
Moreau CS, Bell CD, Vila R, Archibald SB, Pierce NE. 2006. Phylogeny of the ants: Diversification in the age of angiosperms. *Science* **312:** 101–104.
Munoz-Torres MC, Reese JT, Childers CP, Bennett AK, Sundaram JP, Childs KL, Anzola JM, Milshina N, Elsik CG. 2011. Hymenoptera genome database: Integrated community resources for insect species of the order Hymenoptera. *Nucleic Acids Res* **39:** D658–D662.
Nygaard S, Zhang G, Schiott M, Li C, Wurm Y, Hu H, Zhou J, Ji L, Qiu F, Rasmussen M, et al. 2011. The genome of the leaf-cutting ant *Acromyrmex echinatior* suggests key adaptations to advanced social life and fungus farming. *Genome Res* **21:** 1339–1348.
Parker BJ, Moltke I, Roth A, Washietl S, Wen J, Kellis M, Breaker R, Pedersen JS. 2011. New families of human regulatory RNA structures identified by comparative analysis of vertebrate genomes. *Genome Res* **21:** 1929–1943.
Pauli A, Rinn JL, Schier AF. 2011. Non-coding RNAs as regulators of embryogenesis. *Nat Rev Genet* **12:** 136–149.
Ramirez-Carrozzi VR, Braas D, Bhatt DM, Cheng CS, Hong C, Doty KR, Black JC, Hoffmann A, Carey M, Smale ST. 2009. A unifying model for the selective regulation of inducible transcription by CpG islands and nucleosome remodeling. *Cell* **138:** 114–128.
Ranson H, Claudianos C, Ortelli F, Abrall C, Hemingway J, Sharakhova MV, Unger MF, Collins FH, Feyereisen R. 2002. Evolution of supergene families associated with insecticide resistance. *Science* **298:** 179–181.
Rebeiz M, Jikomes N, Kassner VA, Carroll SB. 2011. Evolutionary origin of novel gene expression pattern through co-option of the latent activities of existing regulatory sequences. *Proc Natl Acad Sci* **108:** 10036–10043.
Robinson GE, Grozinger CM, Whitfield CW. 2005. Sociogenomics: Social life in molecular terms. *Nat Rev Genet* **6:** 257–270.
Schultz TR, Brady SG. 2008. Major evolutionary transitions in ant agriculture. *Proc Natl Acad Sci* **105:** 5435–5440.
Sella G, Petrov DA, Przeworski M, Andolfatto P. 2009. Pervasive natural selection in the *Drosophila* genome? *PLoS Genet* **56:** e1000495.
Siepel A, Bejerano G, Pedersen JS, Hinrichs AS, Hou M, Rosenbloom K, Clawson H, Spieth J, Hillier LW, Richards S, et al. 2005. Evolutionarily conserved elements in vertebrate, insect, worm, and yeast genomes. *Genome Res* **15:** 1034–1050.
Simola DF, Ye C, Mutti NS, Dolezal K, Bonasio R, Liebig J, Reinberg D, Berger S. 2013. A chromatin link to caste identity in the carpenter ant *Camponotus floridanus*. *Genome Res* **23:** 486–496.
Sirviö A, Pamilo P, Johnson RA, Page RE Jr, Gadau J. 2011. Origin and evolution of the dependent lineages in the genetic caste determination system of *Pogonomyrmex* spp. *Evolution* **65:** 869–884.
Smith CD, Zimin A, Holt C, Abouheif E, Benton R, Cash E, Croset V, Currie CR, Elhaik E, Elsik CG, et al. 2011a. Draft genome of the globally widespread and invasive Argentine ant (*Linepithema humile*). *Proc Natl Acad Sci* **108:** 5673–5678.
Smith CR, Smith CD, Robertson HM, Helmkampf M, Zimin A, Yandell M, Holt C, Hu H, Abouheif E, Benton R, et al. 2011b. Draft genome of the red harvester ant *Pogonomyrmex barbatus*. *Proc Natl Acad Sci* **108:** 5667–5672.
Smith CR, Mutti NS, Jasper WC, Naidu A, Smith CD, Gadau J. 2012. Patterns of DNA methylation in development, division of labor and hybridization in an ant with genetic caste determination. *PLoS ONE* **78:** e42433.
Suen G, Teiling C, Li L, Holt C, Abouheif E, Bornberg-Bauer E, Bouffard P, Caldera EJ, Cash E, Cavanaugh A, et al. 2011. The genome sequence of the leaf-cutter ant *Atta cephalotes* reveals insights into its obligate symbiotic lifestyle. *PLoS Genet* **7:** e1002007.
Tamura K, Subramanian S, Kumar S. 2004. Temporal patterns of fruit fly *Drosophila* evolution revealed by mutation clocks. *Mol Biol Evol* **21:** 36–44.
Tautz D, Domazet-Lošo T. 2011. The evolutionary origin of orphan genes. *Nat Rev Genet* **12:** 692–702.
Trapnell C, Williams BA, Pertea G, Mortazavi A, Kwan G, van Baren MJ, Salzberg SL, Wold BJ, Pachter L. 2010. Transcript assembly and quantification by RNA-seq reveals unannotated transcripts and isoform switching during cell differentiation. *Nat Biotechnol* **28:** 511–515.
van Zweden JS, Brask JB, Christensen JH, Boomsma JJ, Linksvayer TA, d'Ettorre P. 2010. Blending of heritable recognition cues among ant nestmates creates distinct colony gestalt odours but prevents within-colony nepotism. *J Evol Biol* **23:** 1498–1508.
Villesen P, Murakami T, Schultz TR, Boomsma JJ. 2009. Identifying the transition between single and multiple mating of queens in fungus-growing ants. *Proc Biol Sci* **269:** 1541–1548.
Waterhouse RM, Zdobnov EM, Tegenfeldt F, Li J, Kriventseva EV. 2011. OrthoDB: The hierarchical catalog of eukaryotic orthologs in 2011. *Nucleic Acids Res* **39:** D283–D288.
Wurm Y, Wang J, Riba-Grognuz O, Corona M, Nygaard S, Hunt BG, Ingram KK, Falquet L, Nipitwattanaphon M, Gotzek D, et al. 2011. The genome of the fire ant *Solenopsis invicta*. *Proc Natl Acad Sci* **108:** 5679–5684.
Zhou X, Slone JD, Rokas A, Berger SL, Liebig J, Ray A, Reinberg D, Zwiebel L. 2012. Phylogenetic and transcriptomic analysis of chemosensory receptors in a pair of divergent ant species reveals sex-specific signatures of odor coding. *PLoS Genet* **8:** e1002930.

Received January 24, 2013; accepted in revised form April 24, 2013.

Supplemental Materials

Social insect genomes exhibit dramatic evolution in gene composition and regulation while preserving regulatory features linked to sociality

Daniel F. Simola, Lothar Wissler, Greg Donahue, Robert M. Waterhouse, Martin Helmkampf, Julien Roux, Sanne Nygaard, Karl M. Glastad, Darren E. Hagen, Lumi Viljakainen, Justin T. Reese, Brendan G. Hunt, Dan Graur, Eran Elhaik, Evgenia V. Kriventseva, Jiayu Wen, Brian J. Parker, Elizabeth Cash, Eyal Privman, Christopher P. Childers, Monica C. Muñoz-Torres, Jacobus J. Boomsma, Erich Bornberg-Bauer, Cameron Currie, Christine G. Elsik, Garret Suen, Michael A. D. Goodisman, Laurent Keller, Jürgen Liebig, Alan Rawls, Danny Reinberg, Chris D. Smith, Chris R. Smith, Neil Tsutsui, Yannick Wurm, Evgeny M. Zdobnov, Shelley L. Berger, and Jürgen Gadau

Table of contents

List of Contributions

Project Coordination: Jürgen Gadau, **GC Composition Analysis:** Eran Elhaik, Justin T. Reese, Dan Graur, Christine G. Elsik, **Gene Homology (AntOrthoDB), Phylogeny, Gene Set Quality Assessment:** Robert M. Waterhouse, Evgenia V. Krisventseva, Evgeny M. Zdobnov, Lothar Wissler, **Taxonomically Restricted Genes, Genes With Paralogs:** Lothar Wissler, Erich Bornberg-Bauer, **Codon Usage Bias:** Julien Roux, **Gene Family Evolution:** Martin Helmkampf, Lothar Wissler, **Desaturases:** Martin Helmkampf, Elizabeth Cash, **Immune Genes:** Lumi Viljakainen, **Multiple Genome Alignment:** Daniel F. Simola, **Synteny:** Greg Donahue, **Conserved Elements:** Daniel F. Simola, **DNA Methylation:** Karl M. Glastad, Brendan G. Hunt, Michael A. D. Goodisman, **Conserved Structural RNAs:** Sanne Nygaard, Jiayu Wen, Brian J. Parker, **Micro RNA:** Darren E. Hagen, Christine G. Elsik, **Transcription Factor Binding Sites, RNA Expression Analysis:** Daniel F. Simola, Alan Rawls, Jürgen Gadau, **Positive Selection:** Julien Roux, Eyal Privman, **Hymenoptera Genome Database:** Christopher P. Childers, Monica C. Muñoz-Torres, Justin T. Reese, Christine G. Elsik, **Additional Manuscript Preparation:** Chris R. Smith, Christopher D. Smith, Neil Tsutsui, Garret Suen, Cameron Currie, Yannick Wurm, Laurent Keller, Jürgen Liebig, Danny Reinberg, Shelley L. Berger

Materials and Methods

Quality Assessment of Annotated Gene Sets in AntOrthoDB

Orthologs 'present-in-all-but-one' species

AntOrthoDB (Supplemental Fig. 2, Supplemental Table 1) orthologous groups were examined to identify groups with genes from 11 out of the 12 species which contain (i) strictly one gene in each species (single-copy) and (ii) at least one species with more than one gene (multi-copy). Orthologous genes that are present in all but one of the 12 insects indicate true gene losses or genes that are missing from the genome annotation or assembly. This analysis revealed that amongst the seven ant species, there are generally few lost or missing genes, apart from *S. invicta* (~500 genes) and *A. echinatior* (~200 genes) (Supplemental Fig. 3).

Potentially missing or missed orthologs

AntOrthoDB orthologous groups delineated across the seven ant species plus *A. mellifera* and *N. vitripennis* were examined to identify those with gene members in honeybee and/or wasp but without gene members in one or two ant species. For each potentially missing or missed ant gene, a seed gene was identified from a closely-related ant species and three TBLASTN searches were performed: the seed protein sequence against the genome of the species where the ortholog appears to be missing, its own genome, and the genome of the bee or wasp (outgroup species). The results were analyzed to distinguish cases where the ortholog is indeed likely to be missing from the assembled genome – either no significant BLAST hits were found, the hits were less significant than those to the outgroup genome, or the ortholog may have been missed by the annotation procedure (or was poorly annotated and hence failed the orthology delineation procedure); otherwise the BLAST hits were more significant than those to the outgroup genome. This

analysis identified 3,313 potentially missing or missed ant orthologs from 2,635 orthologous groups (Supplemental Fig. 4): ~200 cases from *LHUMI*, *PBARB*, and *ACEPH*, ~450 cases from *HSALT* and *CFLOR*, ~650 cases from *AECHI*, and ~1,100 cases from *SINVI*. Cases with 'No Hits' or 'Probably Missing' may be true gene losses, which occur relatively frequently in insect evolution, and which may relate to certain specific biological traits of each species. Cases with 'Probably Present' may highlight potential errors with the automatic gene annotation procedures, resulting in incomplete or missed gene annotations. Hence, 'Probably Present' genes should be targeted for manual curation efforts to improve future releases of the official gene sets.

Protein length concordance among orthologs

Employing 4,346 single-copy orthologs defined across the seven ant species, *A. mellifera* (*AMELL*) and *N. vitripennis* (*NVITR*), protein lengths were compared to examine the agreement of predicted ant genes with those from honeybee and wasp (Supplemental Fig. 6 and Supplemental Table 2). This analysis compared some of the most accurately predicted proteins in each species, as conserved single-copy orthologs are often the simplest genes to predict using homology-based approaches. As a baseline, the honey bee – *Nasonia* wasp comparison shows a concordance of 0.91 with more bee proteins that are shorter than wasp their orthologs. Compared to the honey bee, ant protein length concordance values range from 0.91 for *HSALT* to 0.83 for *SINVI*, and *HSALT*, *LHUMI*, *CFLOR*, and *AECHI*, tend towards longer coding-sequence predictions while *PBARB*, *SINVI*, and *ACEPH* tend towards shorter predictions. Compared to the *Nasonia* wasp, ant protein length concordance values range from 0.90 for *HSALT* to 0.81 for *SINVI*, and all the ant species tend towards shorter predictions.

Codon Usage Bias

Complete coding sequences (CDS) corresponding to all annotated genes in the 7 ant genomes were downloaded from *http://antlab.sfsu.edu/~antdata/* (Supplemental Table 4). CDS sequences of the 5 outgroups were downloaded from their respective genome project homepages. Sequences quality was controlled as in (Hambuch and Parsch 2005): CDS sequences whose length was not a multiple of three, did not correspond to the length of the predicted protein or contained an internal stop codon were eliminated; the longest CDS of genes showing multiple isoforms was retained; CDS shorter than 100 nt were eliminated as short sequences can affect the measure of codon usage bias.

The analysis was performed both on the full dataset and on the subset of genes having only single-copy orthologs in the 12 species, based on the AntOrthoDB analyses (above). This guarantees that the results are not due to patterns of species-specific genes or species-specific duplicate genes. Only the results from this dataset are described here but the results were virtually unchanged when the complete dataset was used.

Codon usage bias was estimated using the "effective number of codons" measure (ENC or N_C) (Wright 1990). ENC values range from 20 in the case of extreme bias where one codon is exclusively used for each amino-acid, to 61 when the use of alternative synonymous codons is equally likely. ENC is thus a simple measure that can be used to quantify how far the codon usage of genes from different species departs from equal usage of synonymous codons (Drosophila 12 Genomes Consortium 2007, Vicario et al. 2007, Heger and Ponting 2007, Gingold et al. 2011). ENC measures were calculated for

all genes of the 12 species using the CodonW program (*http://codonw.sourceforge.net/*) (Supplemental Fig. 9). CodonW reports for %GC and %GC at 3rd positions of synonymous codons (GC3s) in CDS sequences were also used in the analysis.

Cytoplasmic ribosomal proteins for 10 of the 12 genomes were obtained from M. Helmkampf (7 ants + *D. melanogaster*, *A. mellifera* and *N. vitripennis*; see CD Smith et al 2011, CR Smith et al. 2011, Suen et al. 2011). To retrieve ribosomal proteins from the genomes of *P. humanus* and *T. castaneum*, a similar methodology was applied: all ribosomal proteins of *D. melanogaster* were blasted (BLASTP) against the proteomes and all hits with an e-value smaller than 1e–10 were retained (Supplemental Table 4).

The dataset of randomized CDS sequences was created to reproduce the properties of the real dataset regarding CDS lengths and nucleotide compositions: for each protein of the real dataset, a new CDS sequence was created by randomly choosing at each position a new codon among all of the synonymous codons displaying the same %GC content.

Genes With Paralogs

Across the 30 arthropod genomes, the number of genes with paralogs (GWPs), which may serve as a rough approximation for genetic redundancy, was determined. GWP counts were derived from BLASTP-based inference of homology and single-linkage clustered gene families (see section on Gene Family Evolution below). A total of four different sets of criteria were used to define homology, i.e. when two protein sequences are considered homologs based in the BLASTP hit, to prevent misinterpretation due to threshold effects. These sets define when two protein sequences are considered to be homologs which affects the E-value cutoff, the minimum alignment coverage of the local alignment constructed by BLAST, and the minimum percent identity within the local alignment:

	Set 1	*Set 2*	*Set 3*	*Set 4*
Min. E-value	1e–10	1e–20	1e–5	1e–10
Min. alignment coverage	70%	0	30%	50%
Min. sequence identity	30%	0	30%	0

Overall, the number of GWPs is relatively homogeneous among different groups of insects, and the distributions of GWPs seem independent from the exact homolog definition as all sets show comparable trends (Supplemental Fig. 8, Supplemental Table 3). The three mosquitoes (Culicidae) seem to be a slight outlier, showing higher GWP counts than the other tested groups, although it is currently unclear how much this trend might be influenced by the low taxon sampling. GWP counts in ants (Formicidae) are comparable to the other two Hymenoptera and to those in Drosophilidae. Among ants, the highest redundancy was found in the *H. saltator* genome (Supplemental Fig. 8).

Gene Family Evolution

Gene families were identified by a relaxed reciprocal BLAST method (Drosophila 12 Genomes Consortium 2007) and subsequent single-linkage clustering. Clustering of genes into gene families was done using their encoded protein sequences and performing

all vs. all BLASTP searches. Gene models were obtained from official gene sets available from 30 arthropod species with fully sequenced genomes. All protein-coding genes were added to a graph as nodes. If a homologous relationship between query and subject proteins was determined with BLAST, a directed edge was added from query to subject. A query gene was considered a homolog to a subject gene if the BLAST E-value was smaller or equal to 1e–10, and the local alignment covered at least 70% of the longer of the two sequences with at least 30% sequence identity. After all BLAST hits were evaluated, non-reciprocal edges were removed from the graph. Finally, gene families were obtained from the graph as subgraphs using single linkage clustering.

For the evolutionary analysis of gene families, only 15 of the 30 arthropod species were retained for the final dataset, including five drosophilids and six ant species. The remaining species were discarded due to large evolutionary distances to the focal ant species (e.g., *Ixodes scapularis*, *Daphnia pulex*), or due to concerns that differences in sequencing depth (e.g., drosophilids sequenced to low coverage) or annotation quality (e.g., *S. invicta*, see below for a detailed explanation) might bias the analyses.

In total, 33,891 gene families were identified, of which 5,681 remained after filtering out families which were inferred to lack members in the most recent common ancestor of the 15 species using the `-filter` option provided by CAFE v2.2 (Hahn et al. 2007), the software used for all subsequent analyses of gene family evolution (Supplemental Fig. 10). This step removed all gene families with members in only hymenopteran or non-hymenopteran insect taxa (which represents the basal split in our species tree), including all lineage-specific gene families. An additional six gene families, predicted to be made up mostly of transposable elements, were discarded due to their exceptionally strong influence on parameter estimates during preliminary analyses, leaving a total of 5,675 families containing 111,420 genes in the final dataset. The largest of these gene families contained 1,822 members across all 15 species. The topology of the species phylogeny required by CAFE were taken from this study and the literature (Drosophila 12 Genomes Consortium 2007, Wiegmann et al. 2009). Divergence times were obtained from timetree.org (Hedges et al. 2006), a public resource reporting consensus estimates of divergence times, resulting in the following ultrametric tree:

```
((tcas:300,((dvir:47,(((dmel:13,dere:13):22,dana:35):2,dpse:37):1
0):228,aaeg:275):25):50,(((((pbar:110,(aech:8,acep:8):102):13,cf
lo:123):3,lhum:126):6,hsal:132):32,amel:164):27,nvit:190):160)
```

To assess the rate and direction of gene family size change along the phylogeny and to identify families which are characterized by significant size changes, we applied five models of gene gain and loss with varying numbers of parameters estimated within CAFE's maximum likelihood framework. Unless noted otherwise, probabilities for gene gain and loss were assumed to be equal, and did not vary between gene families:

– model 1: one parameter for one global rate of gene gain and loss (λ) on all branches of the phylogeny
– model 2: two parameters for two global rates, one for gene gain (λ) and one for gene loss (μ)
– model 3: three parameters, one each for ants, drosophilids, and other taxa
– model 4: three parameters for three rate categories

– model 5: four parameters for four rate categories
– model 6: five parameters for five rate categories

To assign branches to one of the rate categories in model 4–6, a two-parameter analysis was run for each branch, estimating a rate specific to the focal (foreground) branch and a background rate for the remaining branches. The branch-specific rates were then categorized by *k*-means clustering with $k = 3$, $k = 4$ and $k = 5$, respectively. This approach served as an approximation for the fully parameterized model with independent rates for each branch, which did not converge to a single maximum due to its complexity. We employed the likelihood ratio test to find the model which best fit the data.

Gene families with an overall size distribution that differed from the null distribution expected under random birth and death at a significance level of $p \leq 0.01$ were considered as having potentially evolved under the influence of natural selection. By calculating exact *p*-values for all transitions between parent and child nodes of these families (the "Viterbi" method; Hedges et al. 2006), we identified the branches characterized by the most unlikely amount of change. Transitions with a likelihood of $p \leq 0.01$ were considered significant, indicating lineage-specific adaptation. Gene families of interest were functionally annotated using BLAST against the Swiss-Prot (De Bie et al. 2006) and Pfam databases (The UniProt Consortium 2012), and Blast2GO (Punta et al. 2002) and the Gene Ontology database (Conesa et al. 2005). To test whether gene families with significant size changes in ants (i.e., along one or several internal or terminal ant branches) are significantly enriched in certain Gene Ontology terms in comparison to all gene families, we employed the topGO package implementing the elim algorithm which accounts for the tree-like, non-independent structure of GO categories (*p*-value ≤ 0.005) (The Gene Ontology Consortium 2000). All datasets are available from the authors upon request.

Why *S. invicta* was excluded from the gene family evolution analyses

In various analyses on annotated genes, we found hints that the gene annotation of the *S. invicta* genome (version 2.2.3) may not be exhaustive. As reported in the Gene Set Quality Assessment section above, *S. invicta* stands out among the seven ants displaying the highest number of missing genes and the shortest gene models. Similar patterns were found in KEGG pathway annotation (Alexa et al. 2006) obtained from KAAS (Kaneshina et al. 2012) with full proteomes and the BBH method (Supplemental Fig. 14). Despite our efforts to identify missing genes, we therefore excluded *S. invicta* from the gene family analysis to prevent potentially inflated estimates of gene turnover and incorrect ancestral gene counts in the statistical analysis of gene family size variation without a significant loss in phylogenetic resolution.

Desaturases

Desaturase genes were identified by reciprocal blastp using the *D. melanogaster* desat1 gene (CG5887) as query against the official gene sets of all seven ant species and *Acyrthosiphon pisum*, *Anopheles gambiae*, *A. mellifera*, *B. mori*, *D. melanogaster*, *N. vitripennis* and *T. castaneum*. Manual annotation was carried out for the ant species as described elsewhere (CR Smith et al. 2011), and functional gene copies were distinguished from pseudogenes by ORF length and number of premature stop codons.

A total of 179 putatively functional, homologous genes were aligned using the L-INS-i algorithm implemented in MAFFT v6 (Katoh et al. 2002). Ambiguously aligned positions were eliminated by ALISCORE (Moriya et al. 2007). Based on the LG+G substitution model (Misof et al. 2009), a maximum likelihood tree was then constructed using RAxML v.7.2.6 (Le, Gascuel 2008). Nodal confidence values were computed by performing a rapid bootstrap analysis with 500 replicates.

Immune Genes

In the comparison of immune gene contents across insects manually annotated immune genes of *P. barbatus*, *L. humile,* and *A. cephalotes* were used. In addition, immune genes were identified in the genomes of *A. echinatior*, *S. invicta*, *C. floridanus* and *H. saltator* using honeybee immune proteins as a query and the reciprocal best hit approach in the similarity searches as described in (CD Smith et al. 2011, CR Smith et al. 2011, Suen et al. 2011). For gene family characterization hidden Markov model (HMM) profiles (Stamatakis 2006) were made in HMMER3 (Eddy 1998) for the following immune gene families: lysozymes, thioester-containing proteins (TEPs), Gram-negative-bacteria-binding proteins (GNBPs), peptidoglycan-recognition proteins (PGRPs), fibrinogen-related proteins (FREPs), galectins, class B and class C scavenger receptors (SCR-B and SCR-C), clip-domain serine proteases (CLIPs), serine protease inhibitors (serpins) and C-type lectins (CTLs). The profiles were based on alignments of immune gene sequences retrieved from ImmunoDB (*http://cegg.unige.ch/Insecta/immunodb*) and corresponding honeybee sequences. These profiles were used in a HMMER3 search against each ant genome in order to find homologs for each gene family. Detailed immune gene identification based on the same approaches was also made for *N. vitripennis*. For *A. mellifera*, *T. castaneum*, *B. mori* and *Drosophila* data for immune gene family sizes were obtained from published analyses (Durbin et al 1998, Sackton and Clark 2009, Sackton et al. 2007, Zou et al. 2007, Tanaka et al. 2008). The HMM profiles were tested against honeybee, *Drosophila* and *T. castaneum* genomes, and the same number of paralogs for each immune gene family was found as reported in the published analyses except for cSPs, for which a smaller number of paralogs was found in all three species (see Supplemental Table 6).

Multiple Genome Alignment

Whole-genome multiple alignments of ant genome sequences were generated for three taxonomic groups: Formicidae (n=7), Myrmicinae (n=4), and Attini (n=2). These alignments were generated in two stages: (1) identification and (2) alignment of homologous contigs among species. First, homologous DNA sequence contigs from each assembled genome in the taxonomic group of interest were identified using Mercator (Lall et al. 2006), given softmasked versions of each genome sequence and a set of constraints defined as the significant nucleotide alignments between exons of 9,975 single-copy orthologs among the seven ant species. OrthoMCL (Chen et al. 2006) was used to identify these single-copy orthologs, and Blat (Kent 2002) was used to align all pairs of exons for these genes, retaining high scoring pairs (HSPs) with at least 90% sequence identity over at least 22 nt. On average, this yielded 81,811 significant alignments (or 8.2 HSPs per gene) between pairs of species. Mavid (Bray and Pachter 2004) was then used for multiple alignment of the resulting set of homologous contigs,

given the phylogenetic tree estimated for the ant species by PAML (Yang 2007) using the single-copy orthologous gene sequences (4-fold degenerate sites codon-based model). Recursive optimization (`--r`) was used during alignment. Gene annotations were ported to the multiple alignments using custom software, removing any annotations with imperfect sequence identity between an individual genome and its alignment (due to spurious homology assessment).

Synteny

AntOrthoDB (above) discovered 244,281 relationships among all possible gene pairs from different ant species. A relationship is supported by synteny if the two genes (i) fall within 20 kb of each other on the seven-species alignment; (ii) share, among their thirty nearest neighbors on the seven-species alignment, at least three one-to-one orthologs; or (iii) share, among their thirty nearest neighbors or all other genes on the same scaffold, at least three confirmed one-to-one orthologs.

Large regions of pairwise conservation (synteny blocks) were assessed in the following way. For every pair of scaffolds from two different species sharing at least one pair of genes related by synteny, a syntenic block was defined as a pair of regions, one on each scaffold, from the most upstream to the most downstream genes involved in syntenic relationships with genes on the opposite scaffold. Blocks are not sub-divided over inversions, rearrangements, or internal syntenic relationships to other scaffolds.

Synteny plots were created in the following way. For a given scaffold in *A. echinatior* (the "pivot species") and a given comparison species, the rank-order of genes on the *A. echinatior* scaffold was used to construct a composite scaffold in the comparison species which minimizes rank disruption (in other words, the composite scaffold is a sequence of scaffolds from the comparison species placed in an order which produces the least departure from the *A. echinatior* rank-order). Orthology relationships are then plotted by their size in *A. echinatior* and their rank in *A. echinatior* (abscissa) and on the composite scaffold (ordinate) and colored by whether there is an inversion.

Conserved Structural RNAs

The EvoFold (Pedersen et al. 2006) RNA structure screen was based on the 7 ant species multiple alignment, which was used for structure prediction by utilizing comparative genomics features of conserved structure, such as compensatory double substitutions and compatible single substitutions. The screen was restricted to a set of conserved alignment segments based on the PhastCons predicted elements, as paired regions of structural RNAs evolve slowly. PhastCons regions were extended by 20 bases and combined when overlapping to also include fast-evolving single-stranded regions. Since EvoFold is sensitive to misaligned sequences, we applied a conservative sequence filter to the extracted alignment segments, which discards sequences with a significant excess number of mismatches given the branch-lengths of the relating phylogenetic tree (Parker et al. 2011). *C. floridanus* was used as reference species and gaps in it removed from the alignments. EvoFold (v.2.0) (Pedersen et al. 2006) was then applied to these filtered alignments in both their forward and reverse directions, in overlapping windows of length 150 bp with an offset of 50 bp. Low-confidence predictions that are short (< 7 base-pairs); with excessive amount of bulges (>50% bulges in stem); based on shallow or low quality alignments (removal of low confidence base pairs with posterior probability <

50%; removal of dangling base pairs; sequences > 25% bp cannot form structure; sequences > 7.5% positions are gapped; sequences > 10% contradictory substitution; entries with sequence counts < 3); or overlapping repeats were eliminated from the prediction set. P-values for double substitutions evidence were computed using a Monte Carlo test as in (Parker et al. 2011), though due to the small number of species in the alignments, an independent test set could not be held out. We defined a high confidence set with P-value < 0.05.

Genomic regions were defined as follows: coding sequences (CDS) annotation from *C. floridanus* was used, 3'UTR and 5'UTR were defined by the 3rd quartile of the UTR sizes in the well-annotated *D. melanogaster* genome (3' UTR length: 600 bp and 5' UTR length: 250 bp). Each prediction was assigned to the genomic region it had the greatest overlap with. GO enrichments for the structures were defined with the overall homologous gene GO annotations (blast2GO results) as a background, to reveal the additional enrichment of GO terms of structures above background. The TopGO package (The Gene Ontology Consortium 2000) in R bioconductor was used for the GO analysis, calculating P values with the "elim" method. Intronic, CDS, and UTR structures were assigned the GO of their enclosing gene (defined by >=1 bp overlap); intergenic regions were excluded. The structures were tested for homology against the structures of RFAM v. 10.1. Hits above the defined RFAM noise cutoff (NC), which are likely homologues, are considered to be significant. All structure predictions are available for viewing and download at *http://people.binf.ku.dk/jeanwen/data/ants*.

Positive Selection

We applied the branch-site test of the program Codeml from the PAML package (Yang 2007, Zhang et al. 2005) to 4,261 gene families which did not experience duplications (single-orthologs families). A model allowing for positive selection at some sites of a protein, on a selected branch of the tree (ratio of number of non-synonymous substitutions per non-synonymous site, d_N/d_S or $\omega > 1$) is compared through a Likelihood Ratio Test (LRT) to a model where elevated rates of evolution on this branch are due to relaxed selective constraints ($d_N/d_S \sim 1$) (Zhang et al. 2005, Yang and dos Reis 2011). We successively changed the branch of interest to test for positive selection on 15 branches of the insect phylogeny (Supplemental Fig. 26) and FDR-corrected the ensemble of p-values (Yang and dos Reis 2011, Anisimova and Yang 2007, Kosiol and Anisimova 2012, Benjamini and Hochberg 1995).

Given their impact on the rate of false positives of the positive selection tests (Markova-Raina and Petrov 2011, Fletcher and Yang 2010, Schneider et al. 2009), we took great care at filtering out potential gene predictions and alignments errors. We filtered CDS sequences as described above (see section on codon usage bias). The quality filtering pipeline used for multiple alignments is adapted from the pipeline of the Selectome database (*http://selectome.unil.ch*) (Proux et al. 2008): multiple alignments of protein sequences of gene families were first computed by M-Coffee (Wallace et al. 2006) from the T-Coffee package v8.93 (Notredame et al. 2000), which combines the output of different aligners (mafftgins_msa, muscle_msa, kalign_msa, t_coffee_msa). We kept only amino acid positions where the M-Coffee score was 7 or above, eliminating residues not consistently aligned by different aligners. We then used MaxAlign v1.1

(Gouveia-Oliveira et al. 2007) to remove badly aligned sequences. Finally we used a stringent Gblocks filtering (v0.91b; type = codons; minimum length of a block = 4; no gaps allowed) (Castresana 2000), to remove gap-rich regions from the alignments. The results from this analysis are available for download at the Ant Genomes Portal (*http:hymenopteragenome.org/ant_genomes/*).

To test for functional categories enrichment (Supplemental Table 20) we used the Gene Ontology functional annotation (Ashburner et al. 2000) transferred from the *D. melanogaster* member of each family and extracted from Flybase (*http://flybase.org/static_pages/downloads/FB2011_02/go/gene_association.fb.gz*). We applied a SUMSTAT test (Tintle et al. 2009) and used the LRT value from the positive selection analysis (transformed using the fourth square root to stabilize variance) as score for each gene family. We implemented an algorithm similar to the Elim algorithm of the topGO software (The Gene Ontology Consortium 2000) to decorrelate the graph structure of the Gene Ontology. The false discovery rate was assessed using 100 permutations of scores of gene families.

To check that the dependence of our results to the methodology used, we constructed another dataset including all gene families that could pass CDS quality filters (6,186 families, including families with gene duplications). Sequences were aligned using PRANK (v100701), one of the most realistic aligner currently available (Markova-Raina and Petrov 2011, Fletcher and Yang 2010, Löytynoja and Goldman 2008, Löytynoja and Goldman 2005, Jordan and Goldman 2012). We then filtered alignments based on the confidence score attributed by Guidance (v1.1) (Penn et al. 2010, Privman et al. 2012). Gene family phylogenies were built using RAxML (v7.2.9) (Le and Gascuel 2008). Finally, the site test of Codeml (PAML v4.4e) (Yang et al. 2000) was used to test for positive selection (null model M8a vs. alternative model M8) (Swanson et al. 2003, Wong et al. 2004). The functional categories enriched in positively selected genes in ants identified in this dataset are similar to the ones reported in Supplemental Table 20, supporting that our results are likely not artifactual.

CG compositional analysis

Genomic sequences were partitioned into domains using IsoPlotter (*http://code.google.com/p/isoplotter/*), which employs an algorithm that recursively segments chromosomes by maximizing the difference in CG-content between adjacent subsequences. The process of segmentation terminates when the difference in CG-content between two neighboring domains is no longer statistically significant.

Supplemental Text

Supplemental Text 1. Analysis of 64 TRGs found in all seven ant genomes.

Among the 28,581 TRGs specific to Formicidae, we identified a subset of 64 genes that display no protein sequence similarity to genes outside Formicidae but which have at least significant local similarity among all ants (BLASTP, E < 1e–3). Of these 64 orthologous gene clusters, 62 are strict single-copy gene clusters, i.e., they contain one protein sequence per species. The remaining two clusters are single-copy in six ant species but contain a duplication in one species. We could not detect any Pfam-A domains in these genes, indicating that these genes do not contain any known functional units, despite their broad conservation. For further classification of these 64 ant-specific TRGs, we aligned the 62 strict single-copy gene clusters using MUSCLE. To evaluate alignment conservation, we applied Gblocks (Castresana 2000) with default settings to identify only conserved sequence blocks (minimum length of 10 residues) from the protein multiple sequence alignments. Despite the relaxed homology criterion used to identify the ant-specific TRGs, the vast majority of clusters display substantial sequence conservation. 57 of the 64 gene clusters (89%) contain conserved blocks with a summed length of at least 50 residues, and in 52 of the 64 clusters (81%) at least 50% of all alignment positions are conserved (Fig. 2C). These results suggest that these ant-specific TRGs are present throughout Formicidae and contain highly conserved functional regions.

Supplemental Text 2. Codon usage bias.

The genetic code is redundant with multiple codons encoding the same amino acids. Codon usage bias reflects the fact that not all synonymous codons are used with equal frequencies, often with sharp preferences for some codons compared to others. This phenomenon is present in most organisms ranging from bacteria to animals (Hershberg and Petrov 2008, Duret 2002, Plotkin and Kudla 2011). Codon usage bias is thought to result from a balance between two major forces: selection for translational optimization and mutational biases (Duret 2002, Bulmer 1991, Drummond and Wilke 2008). Analysis of the 12 *Drosophila* species highlighted that selective forces were mainly responsible for codon usage bias in these genomes (Stark et al. 2007). Interestingly, variations in patterns of codon usage bias among these species reflect the variations of strength of translational selection across their phylogeny (Drosophila 12 Genomes Consortium 2007, Vicario et al. 2007, Heger and Ponting 2007). For example translational selection strength was shown to be highest for the species of the *D. melanogaster* group – although a slight genomic reduction in codon bias is observed for *D. melanogaster*. Another interesting example is a striking lineage-specific shift in codon preferences seen *D. willistoni*, which cannot be sufficiently explained by mutation alone, and may have involved directional selection (Vicario et al. 2007, Heger and Ponting 2007). Similarly to the *Drosophila* lineage, it is expected that the study of codon usage bias in the 7 ant species and their outgroups can give us valuable insights into the evolutionary history of these lineages.

To compare the levels of codon usage bias among different species, we measured the "effective number of codons" used in CDS sequences (ENC or N_C; Supplemental Fig. 9A) (Drosophila 12 Genomes Consortium 2007, Vicario et al. 2007, Heger and Ponting 2007). Though this is the measure of choice to implement multi-species comparisons

(Gingold et al. 2011), unfortunately it does not differentiate if codon usage bias results from selective forces or mutational bias. So we used three other complementary measures: First, we analyzed the GC content in CDS sequences (%GC; Supplemental Fig. 9C) and the G+C content at 3rd synonymous positions (%GC3s; Supplemental Fig. 9B), which reflect the overall mutational biases experienced by the genomes in their evolutionary history. Second, to better characterize the role of selective forces, we isolated codon usage bias levels of ribosomal genes (Supplemental Fig. 9A; red bars). Ribosomal genes are expected to be under strong selection for optimal codon usage because they are highly and constitutively expressed in most cells of the organism (Heger and Ponting 2007). A reduction of the levels of codon usage bias of these genes is likely to reflect a genome-wide relaxation of selection. Third, because both selective forces and mutational biases may be responsible for codon usage bias in a genome, and to know if nucleotide composition biases are sufficient to explain the observed patterns of codon bias, we created a randomized dataset by randomizing the codon usage in the sequences of the whole dataset, controlling for GC content of codons (see methods below). The ENC levels of genes in this dataset reflect the expectation in the absence of selective forces (Supplemental Fig. 9A; blue bars).

The 12 analyzed species can be gathered in three groups with similar patterns, the first "group" being *D. melanogaster* alone. This species displays a relatively high codon bias and it is well established that this pattern is essentially due to selective pressure acting on synonymous sites (Drosophila 12 Genomes Consortium 2007, Vicario et al. 2007, Heger and Ponting 2007, Duret 2002, Akashi 1994, Powell and Moriyama 1997). The observation of high levels of %GC and %GC3s in CDS sequences confirms this hypothesis, (i) because almost all optimal codons – corresponding to the most abundant tRNAs – are ending by cytosines or guanines (Duret 2002, Shields et al. 1988), (ii) because mutational events in *D. melanogaster* are biased toward A+T (Petrov and Hartl 1999). Selection on codon usage is also reflected by the very strong level of codon usage bias seen in ribosomal genes which are clearly skewed in the distribution of ENC values for protein coding genes. Consistently too, the randomized sequences display a lower codon usage bias.

Second, the seven ant species, *T. castaneum* and *N. vitripennis* display low levels of codon bias, consistent with a relaxation of selective pressure on synonymous sites on their genome. The nucleotide composition of these genomes is relatively balanced: the observed %GC3s is between 0.37 (*C. floridanus*) and 0.53 (*T. castaneum*); %GC is between 0.42 (*C. floridanus*) and 0.47 (*T. castaneum*). These values show that mutational forces were probably insufficient to change the composition of genomes and bias strongly codon usage. The relaxed levels of selection in these species is confirmed by the low level of codon usage bias observed in ribosomal genes sequences, as well as by the relatively low shift between real and randomized datasets.

Finally, strikingly high levels of codon bias are seen in *A. mellifera* and *P. humanus* genes. This is most probably due to strong mutational biases, which are reflected in very low %GC (0.34 and 0.36 respectively) and %GC3s (0.15 and 0.23 respectively) in these genomes. As shown for *A. mellifera* (Jorgensen et al. 2007), synonymous sites of genes tend to adopt the GC content of the region in which they reside and thus reflect the biased nucleotide composition of these genomes. The median levels of codon bias of ribosomal genes are very close to those of protein coding genes, showing that the selective pressure

on codon usage is drastically reduced, even on these genes which are usually under strong selection for optimized translation. Finally, the randomized sequences display similar ENC values as the real dataset, indicating that selective forces are not required to explain the codon bias patterns observed in these species.

Overall, this analysis provides evidence for strong selection on codon usage only in *D. melanogaster*. With the exception of *A. mellifera* and *P. humanus* genomes where codon usage is biased by a very extreme G+C content composition of the genome, all other genomes display relatively low levels of codon usage bias. For the 7 ant species in particular, the global reduction of codon usage bias most likely reflects a relaxation of purifying selection acting on these genomes. Interestingly, such a relaxation was previously predicted in relation to the reduction of effective population size (N_e) associated with social life (Bromham and Leys 2005), but no solid evidence of this phenomenon was found so far in eusocial organisms. We should also note that the genomic patterns seen in ants and in another social insect, *A. mellifera*, are drastically different. The reasons for this remain to be examined.

Supplemental Text 3. GC compositional analysis

Animal genomes are not uniform in their long-range sequence composition but are composed of a mosaic of sequence stretches of variable lengths that differ widely in their guanine and cytosine (GC) compositions. These sequences are referred to as compositional domains and are defined here as are genomic DNA segments that have a characteristic GC-content that differs significantly from the GC-content of adjacent compositional domains. Compositional domains can be divided into compositionally homogeneous and compositionally non-homogeneous domains, if their internal homogeneity is lower or higher than that of the chromosome on which they reside, respectively. In classical terminology, compositionally homogeneous domains that are larger than 300 kb are referred to as isochores (Bernardi 2000).

In all animal genomes studied so far, we found that the distribution of compositional-domain lengths showed an abundance of short domains and a paucity of long ones (Weinstock et al. 2006, Bernardi 2000, Richards et al. 2008, Sea Urchin Genome Sequencing Consortium 2006, Bovine Genome Sequencing and Analysis Consortium 2009). The three ant genomes we previously studied are not exceptions in this respect (CD Smith et al. 2011, CR Smith et al. 2011, Suen et al. 2011). Here we performed a comparative analysis of seven ant genomes along with two hymenopteran (*A. mellifera* and *N. vitripennis*) and three non-hymenopteran outgroups (*D. melanogaster*, *A. gambiae*, *T. castaneum*) to provide further insight into the evolution of GC compositional domain architecture.

We performed three analyses, described below. In the first analysis, we calculated the distribution of homogeneous domain lengths. For convenience, domains were divided according to the order of magnitude of their length into: short (10^3–10^4 bp), medium (10^4–10^5 bp), and long (10^5–10^7 bp). Based on the observed goodness-of-fit, we calculated a *p*-value that quantifies the probability that the data were drawn from the hypothesized distribution. In the second analysis, we compared the dispersal of domain GC-contents. In the last analysis, we compared the domain GC-content versus their sizes in a log scale.

Analysis of Compositional-Domain Sizes

The total number of compositional domains per genome varied from about 35,000 in *C. floridanus* to approximately 66,000 in *H. saltator* (Supplemental Table 10). The coefficient of variation for ant genomes is about 28%. We divided the compositional domains into four size classes: 1–10 kb, 10–100 kb, 100 kb to 1 Mb, and 1–10 Mb. Using a G-test goodness-of-fit test, we determined that none of the distributions of domain sizes is similar to any other ($p = 0.03$).

A comparison of the distributions of compositional domain lengths among ants, bee, wasp, beetle, mosquito, and fly showed that bee, wasp, and *H. saltator* have the smallest fraction (0.1–0.3%) of long domains (>100 kb). Long domains are abundant in the ant linage, with the leaf-cutters *A. cephalotes* and *A. echinatior* having the largest domains among all fully sequenced insect genomes (Supplemental Table 10, Supplemental Fig. 17).

Unlike vertebrate genomes, whose GC-content varies from 40% to 45%, ant genomes exhibit variable GC-content, with average GC-content ranging from 32.6% (*A. cephalotes*) to 45.2% (*H. saltator*) and a GC-content standard deviation of 8–10% (Supplemental Fig. 3). The distribution of GC-content within compositional domains varies greatly: in the bee, beetle, and most of the ant genomes, it is right-skewed due to a high frequency of GC-poor domains, in the wasp genome it is bimodal (Supplemental Fig. 18). The *H. saltator* genome is different than the other ant genomes, in that it is also bimodal. We used the Kolmogorov-Smirnov test (Sokal and Rohlf 1995) to determine that none of the compositional domain GC-content distributions is similar to any other ($p<0.01$).

The range of GC-content in hymenopteran domains was the widest among all invertebrates in the analysis, ranging from 1% to 75%, with *C. floridanus* domains setting the lower limit and *A. mellifera* domains setting the upper limit (Supplemental Fig. 18). Interestingly, the decrease in mean genomic GC-content in the ant genome is proportional to the increase in the number of large domains (>100 kb). This is not surprising, as the elimination of GC-rich domains increases the homogeneity of the genome indicated by longer homogeneous domains.

Analysis of Genome Architecture

Comparing the GC-content of compositional domains with their length distributions provides a general view of the invertebrate genomic architecture. Long GC-poor domains are rare among hymenopterans particularly in bee and wasp, compared to the beetle and the two dipterans. Although all genomes in the analysis have similar numbers of long domains (72 to 401) and isochoric domains (44 to 224), their GC-composition varies greatly (Supplemental Fig. 18, Supplemental Table 10). Nearly all long domains in beetle, mosquito, and fly have a GC-content that is within ±5% of their genomic mean GC-content, whereas in bee and wasp about half of the domains have GC-content above the 5% boundary. In ants, there is a trend of GC enrichment for long domains beginning with *H. saltator* and ending with *A. cephalotes*.

Distribution of Genes in Compositional Domains

We observed previously that genes in *A. mellifera* have a strong bias toward occurring in the more GC-poor regions of the genome (Weinstock et al. 2006). In contrast, the

genomes of all other species studied prior to the availability of an ant genome assembly (including human, fruit fly, worm, mosquito, yeast, body louse and sea urchin) showed either little bias with respect to GC content, or a slight bias toward occurring in more GC-rich regions of the genome (Weinstock et al. 2006, Bernardi 2000, Richards et al. 2008, Sea Urchin Genome Sequencing Consortium 2006, Bovine Genome Sequencing and Analysis Consortium 2009, Werren et al. 2010). We later found that genes in two ant genomes showed no bias (*A. cephalotes*) or a very slight bias (*L. humile* and *P. barbatus*) toward low GC regions (CD Smith et al. 2011, CR Smith et al. 2011, Suen et al. 2011). We therefore were interested in whether all of the currently available ant genomes were similar in this respect.

The relative percent GC of the GC compositional domains containing genes in each species recapitulate the relative percent GC of the overall genome of each species (Supplemental Fig. 17). For example, the cumulative distribution of GC content in compositional domains containing genes for *A. mellifera* lies to the left of that of *L. humile*, which in turn lies to the left of that of *N. vitripennis*. This is consistent with the fact that *A. mellifera* is more GC-poor than *L. humile*, which in turn is more GC-poor than *N. vitripennis*.

To assess whether genes in these species are biased toward occurring in GC compositional domains of high or low GC content, for each genome we overlaid cumulative distributions of the percent genome that is comprised of compositional domains below a given percent GC (thin lines) onto a similar distribution for only compositional domains that contain genes (thick lines; the same lines shown in Supplemental Fig. 19; Supplemental Fig. 20). Among the genomes studied, genes in the *A. mellifera* and *H. saltator* genomes show the strongest tendency to occur in more GC-poor regions of the genome (Supplemental Fig. 20). For example, about half of genes in *H. saltator* occur in compositional domains whose GC content is less than 40% (thick blue line, x = 40%, y = 0.5), but compositional whose GC content is less than 40% represents only about 25% of the genome (thin blue line, x = 40%, y = 0.20). Further, the cumulative distribution for the GC content of compositional domains containing genes lies to the left of the cumulative distribution for the GC content of all compositional domains (compare thick and thin lines for *A. mellifera* and *H. saltator*). Genes in the *C. floridanus* and *S. invicta* genomes, similar to the previously studied *P. barbatus*, *L. humile* and *N. vitripennis* genomes, showed a slight tendency to occur in GC-poor regions of the genome. (CD Smith et al. 2011, CR Smith et al. 2011, Werren et al. 2010). Genes in *A. echinatior* showed a very slight bias to GC rich regions, while, as previously reported, *A. cephalotes* did not show any bias toward lower percent GC regions (Suen et al. 2011).

Supplemental Text 4. Background on the salivary gland and wing development regulatory networks.

Glands derived from the ectodermal cell layer, including the mandibular, salivary (labial), and metapleural glands are essential for intracolonial communication and the interaction of individuals and their environment (Wurm et al. 2011). Phenotypic plasticity of these glands between specialized worker castes has been reported in some ants, predicting the acquisition of novel regulatory mechanisms (Pavon and Camargo-Mathias 2005, Niculita et al. 2008, Amaral and Machado-Santelli 2008). The underlying genetic regulation of the

specification, differentiation, and morphogenesis of these integumentary glands has best been studied in the salivary gland in *Drosophila* (Abrams et al. 2003). The complex interaction of transcriptional activators and repressors specify the pre-ductal cells, activate lineage-specific ductal and secretory morphogenic cassettes and remodeling glands during metamorphosis.

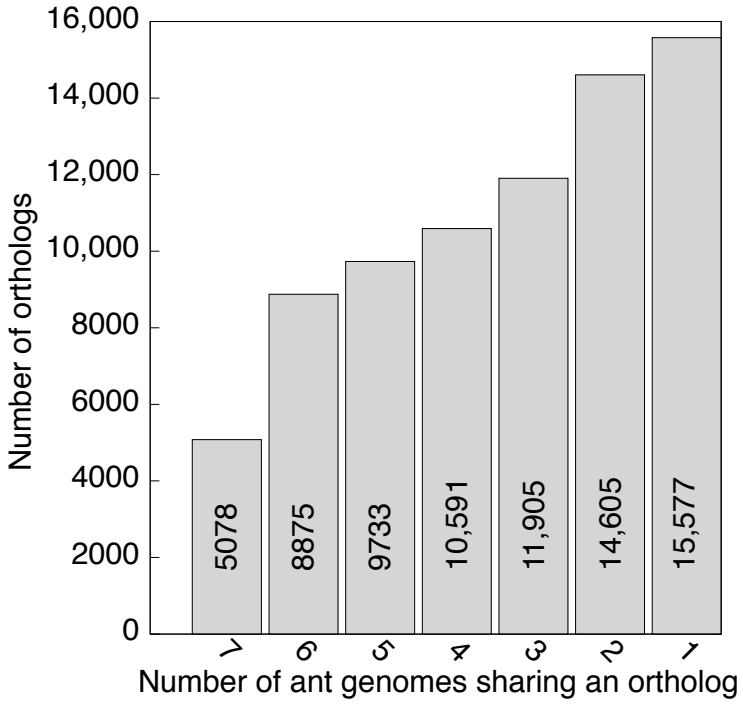

Supplemental Fig. 1. Variation in orthology among ant genomes. The number of orthologous genes shared among different ant genomes is shown as a function of the number of genomes in consideration (i.e., 7 denotes all seven ant genomes considered). Orthology assessed using OrthoDB.

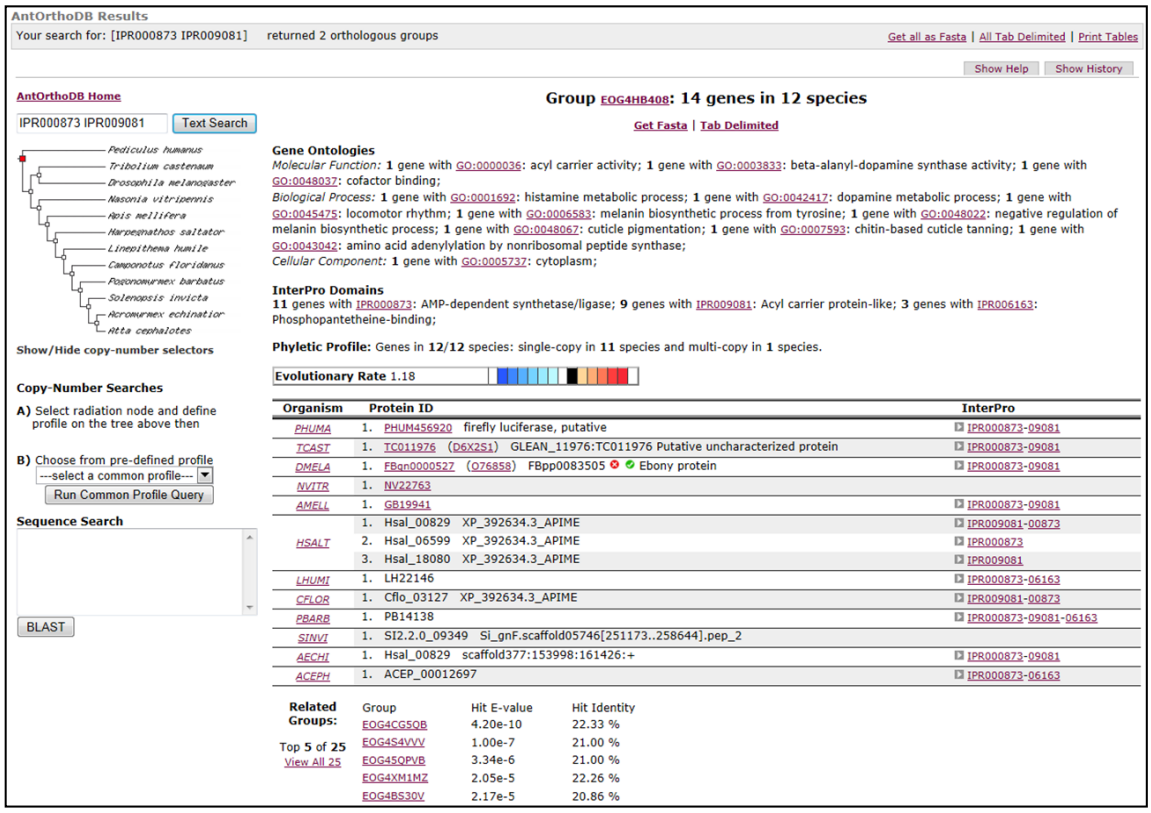

Supplemental Fig. 2. A screenshot from AntOrthoDB (*http://cegg.unige.ch/orthodbants*) shows an example orthologous group with protein descriptors, Gene Ontology and InterPro attributes, phyletic profile, evolutionary rate, and related groups.

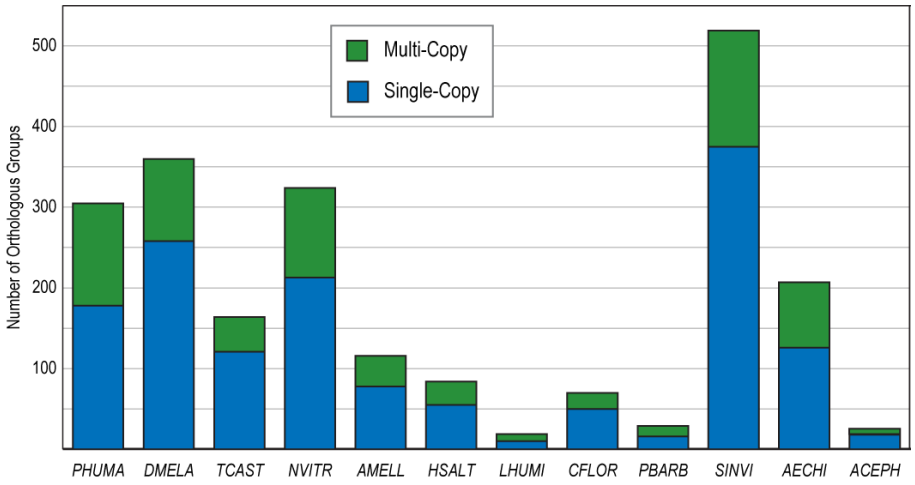

Supplemental Fig. 3. Identification of lost or missing genes by analysis of existing gene annotations. Orthologous groups were identified with genes from 11 out of the 12 species which contain (i) strictly one gene in each species (single-copy) and (ii) at least one species with more than one gene (multi-copy). See Supplemental Table 2 for species abbreviations.

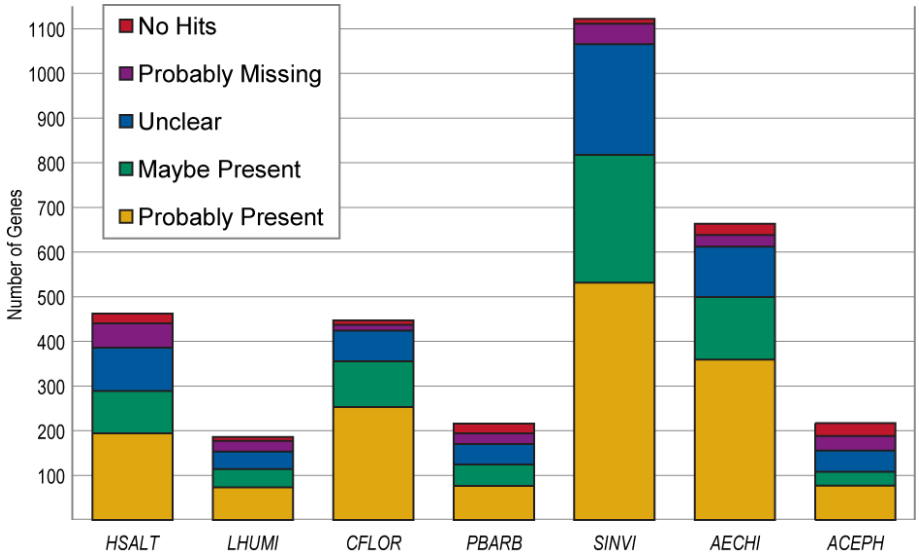

Supplemental Fig. 4. Assembled ant genomes were searched for potentially missing or missed genes (see Supplemental Table 2 for species abbreviations). No Hits: the seed gene had a significant BLAST hit to the 'outgroup' genome but none to the 'missing' genome, i.e. these orthologs are missing from the genome assemblies. Probably Missing: the seed gene BLAST hit was more significant to the 'outgroup' genome than to the 'missing' genome, i.e. the 'missing' genome hit may correspond to a homolog rather than an ortholog. Unclear: the differences between the seed gene BLAST hits to the 'missing' genomes and to the 'outgroup' genomes did not allow for clear distinctions to be made. Maybe Present: the seed gene BLAST hit was 'better' to the 'missing' genome than to the 'outgroup' genome, i.e. the 'missing' genome hit may correspond to the ortholog and hence these genes may be present. Probably Present: the seed gene BLAST hit was 'better' to the 'missing' genome than to the 'outgroup' genome, i.e. the 'missing' genome hit probably corresponds to the ortholog and hence these genes are probably present.

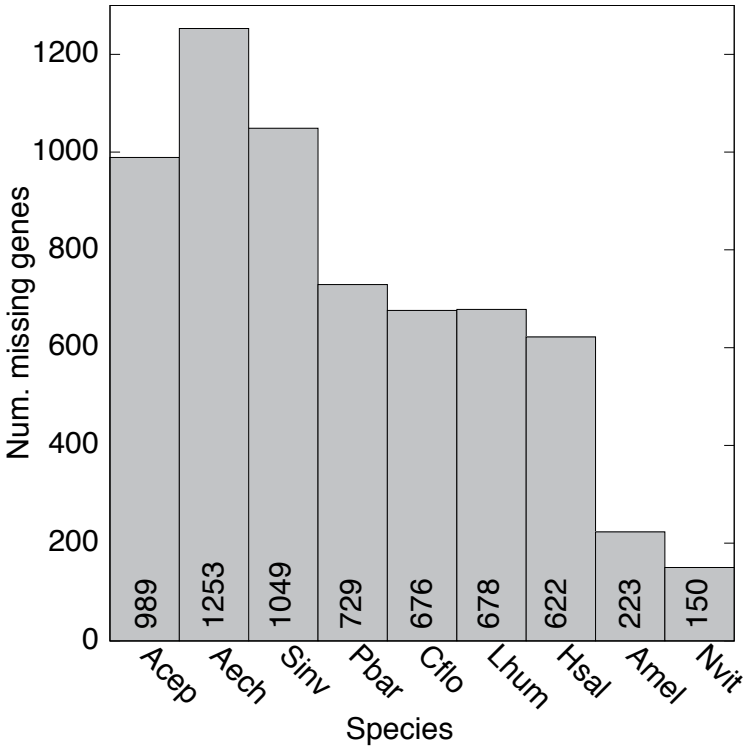

Supplemental Fig. 5. Newly annotated genes that were previously considered species-specific but are present in multiple Hymenoptera genomes. The number of newly annotated genes is shown for each species. See Materials and Methods (Identification of taxonomically restricted genes) for details on the identification procedure that included thirty published arthropod genomes.

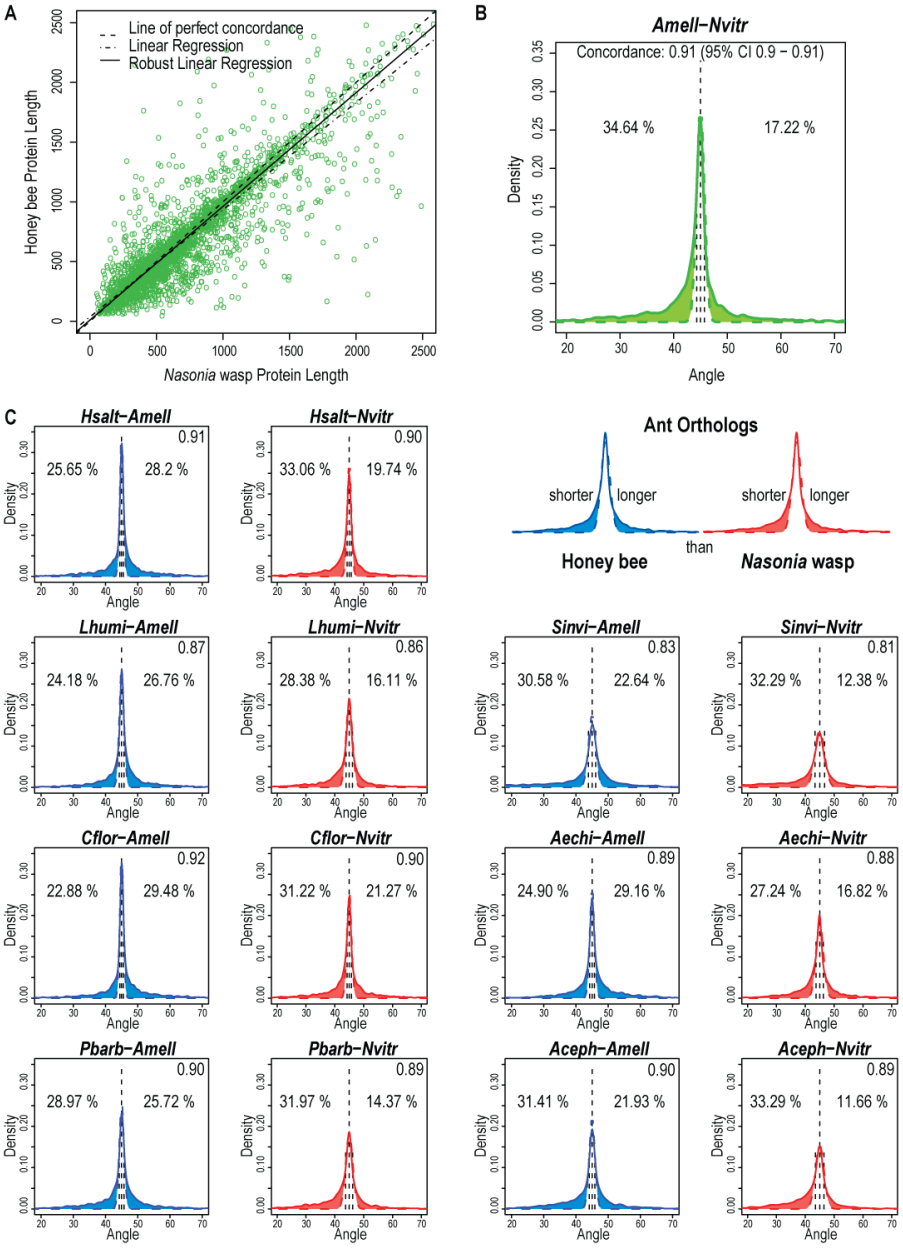

Supplemental Fig. 6. Concordance analysis of protein lengths between *A. mellifera* (blue) or *N. vitripennis* (red) genes and their ant orthologs. The bee-wasp comparison shows the distribution of compared lengths (**A**) with both regressions showing a tendency for bee proteins to be shorter than their wasp orthologs. Plotting the density of data points falling at each degree below and above 45 degrees (**B**) shows the distributions of the deviations from perfect agreement. Comparing to normal fittings of the data (dotted curves), with means fixed at 45 degrees, highlights proportions of significantly shorter bee proteins (**left**) and significantly longer bee proteins (**right**), given the underlying data. Each of the seven ant species is compared to bee and wasp in the same way (**C**). See Supplemental Table 2 for species abbreviations and Supplemental Table 3 for statistics.

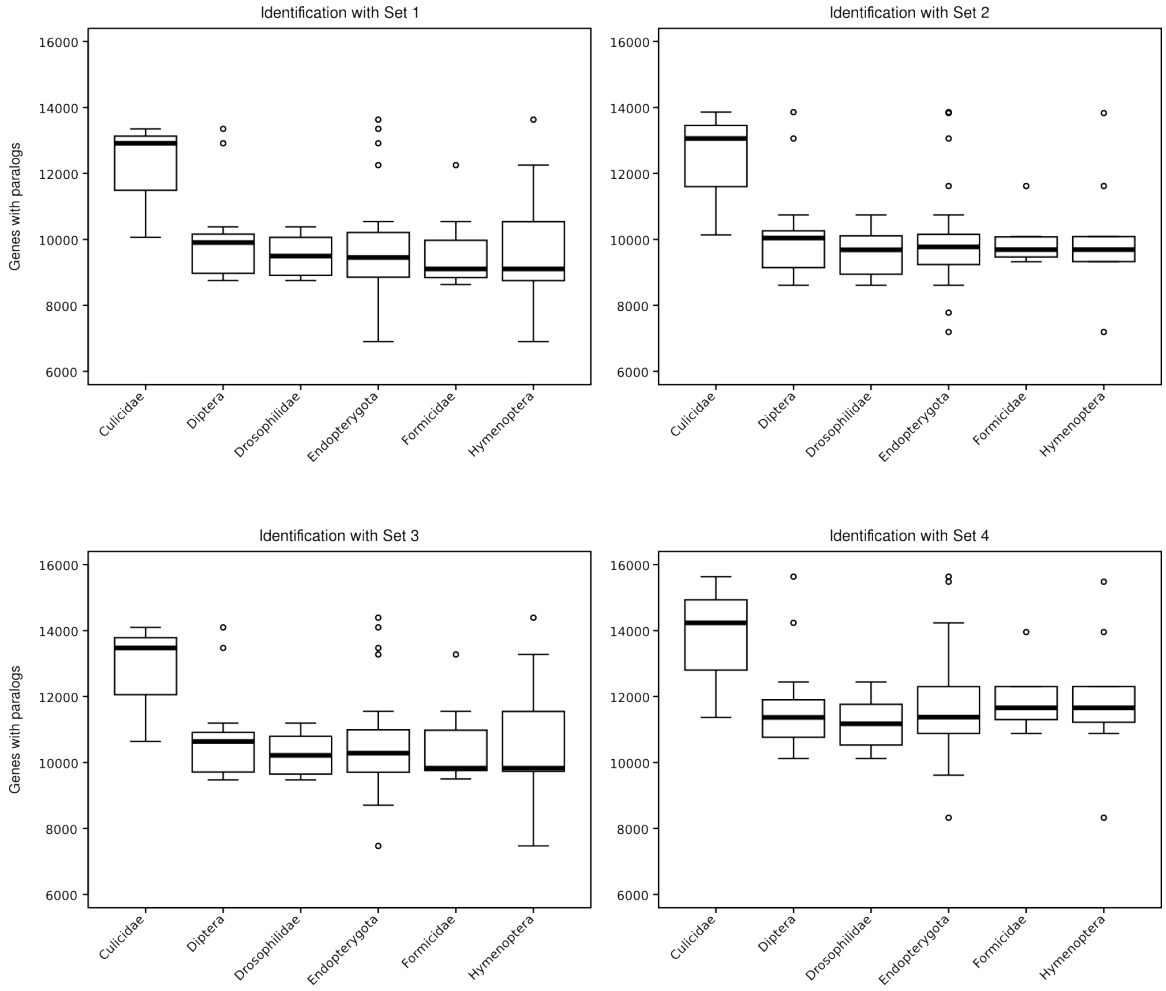

Supplemental Fig. 7. Genes with paralogs (GWP) counts across genomes of several partially overlapping groups of insects.

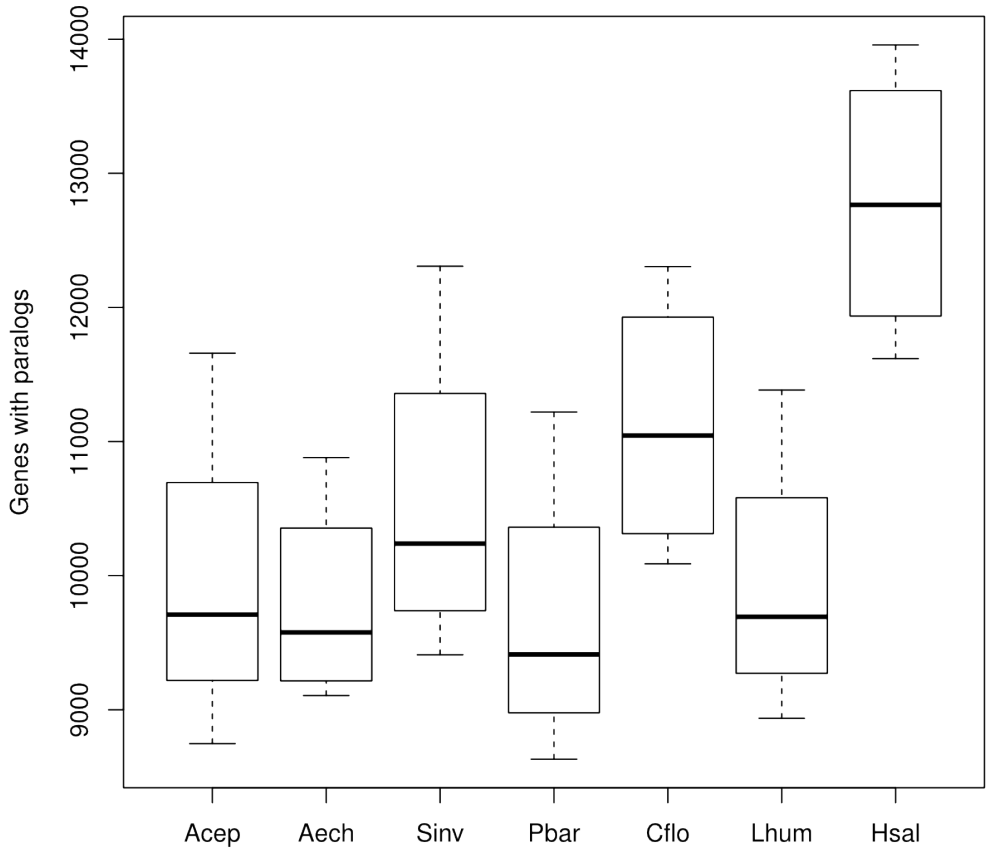

Supplemental Fig. 8. Genes with paralogs (GWP) counts among the seven ant genomes. The four sets of paralog definition were used as replicates per species.

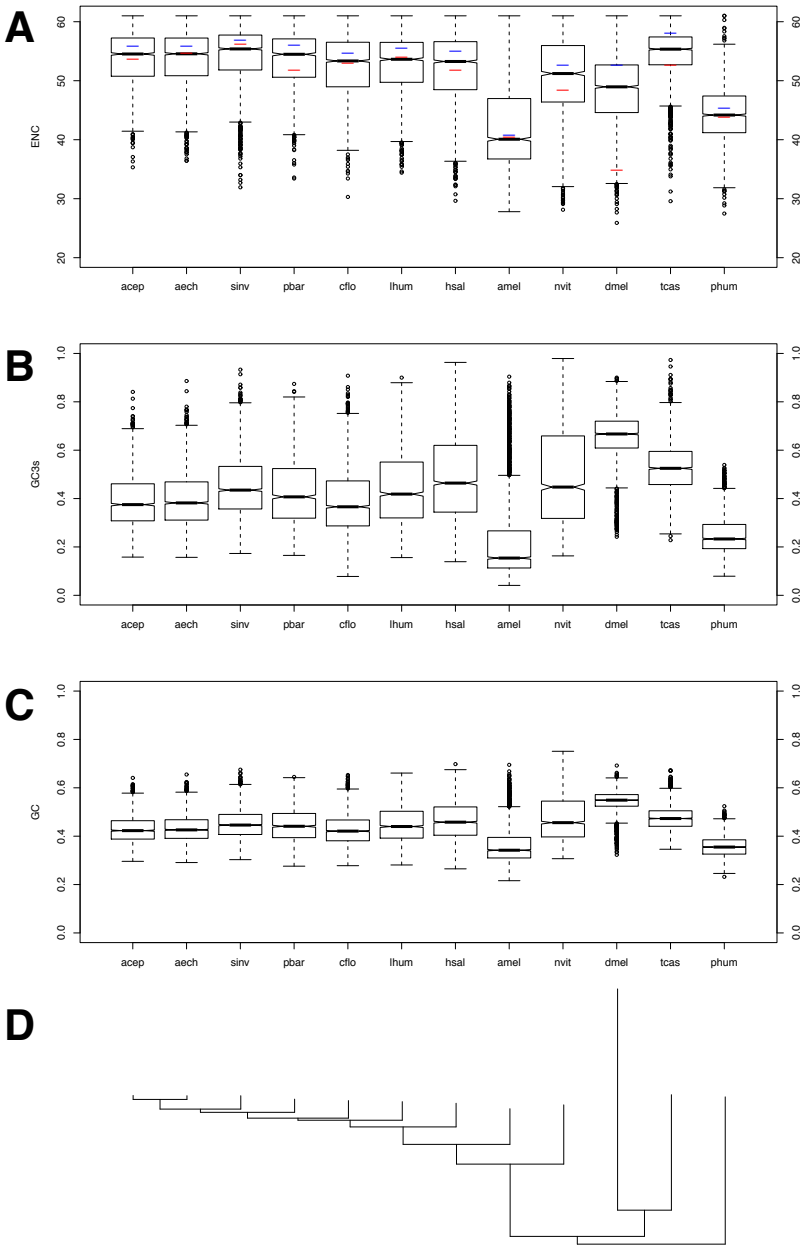

Supplemental Fig. 9. (**A**) Box plot of the distributions of ENC values of CDS sequences of the 12 genomes analyzed. ENC values range between 20 (strong codon usage bias) and 61 (no codon bias). Red bars indicate for each species the median level of ENC observed for CDS sequences of ribosomal genes. Blue bars indicate for each species the median level of ENC for the dataset of randomized CDS sequences. (**B**) Box plot of the distributions of the G+C content at 3rd positions of synonymous codons for CDS sequences of the 12 genomes analyzed. (**C**) Box plot of the distributions of the global G+C content of CDS sequences of the 12 genomes analyzed. (**D**) Phylogeny of the 12 species analyzed.

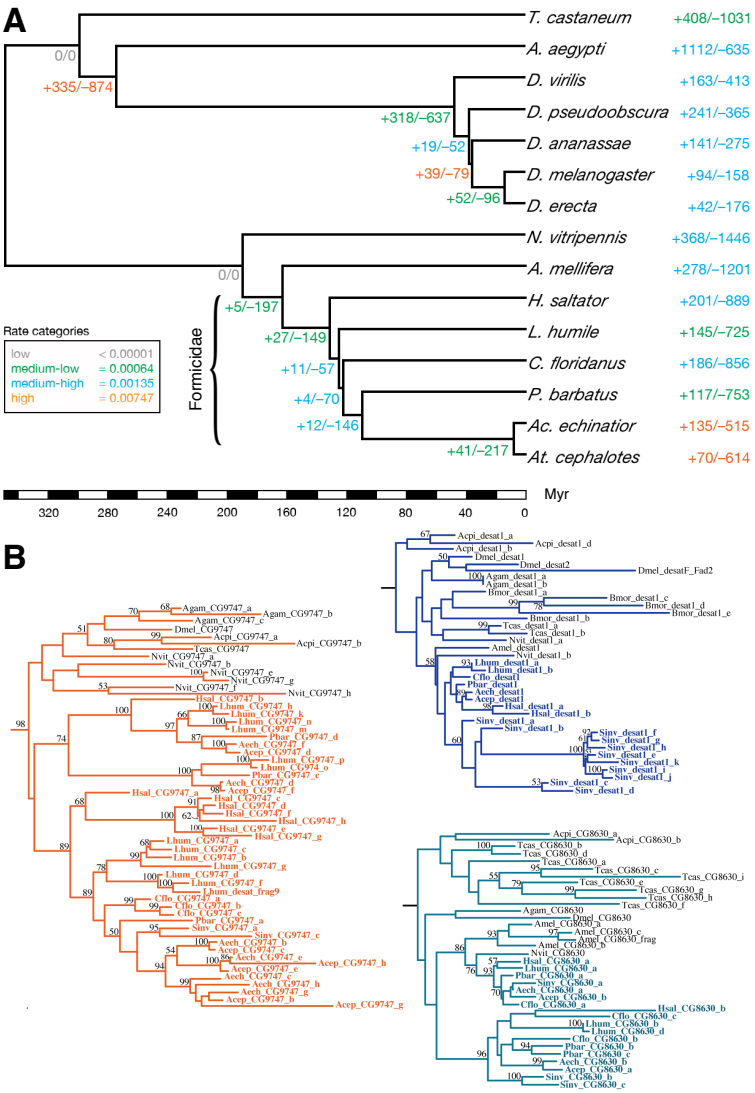

Supplemental Fig. 10. Gene family evolution along the insect phylogeny. (**A**) Number of gene families that have expanded (+) and contracted (–) along the insect tree of life, as inferred in a maximum likelihood framework (Supplemental Methods). Colors denote one of four estimated rates of average gene gain and loss per gene family per million years (Myr). A model assigning each branch to one of four rate categories fitted the data significantly better than any other model, assessed by likelihood ratio tests (Supplemental Table 6). Note, branches leading to "Formicoida" (six ant species excluding *H. saltator*) or Formicinae and Myrmicinae (excluding *H. saltator* and *L. humile*) proved too short to have accumulated significant changes in gene family size. (**B**) Phylogenetic reconstructions of three desaturase gene subfamilies characterized by both ancestral and recent lineage-specific expansions and contractions in ants. Shown are details of maximum likelihood trees inferred from a dataset encompassing all putatively functional Δ9 and Δ11 desaturase genes that could be identified in 14 holometabolous insect species. Ant genes are highlighted by colored labels; genes in other species are shown in black. Numbers denote nodal confidence values obtained from 500 rapid bootstrap replicates.

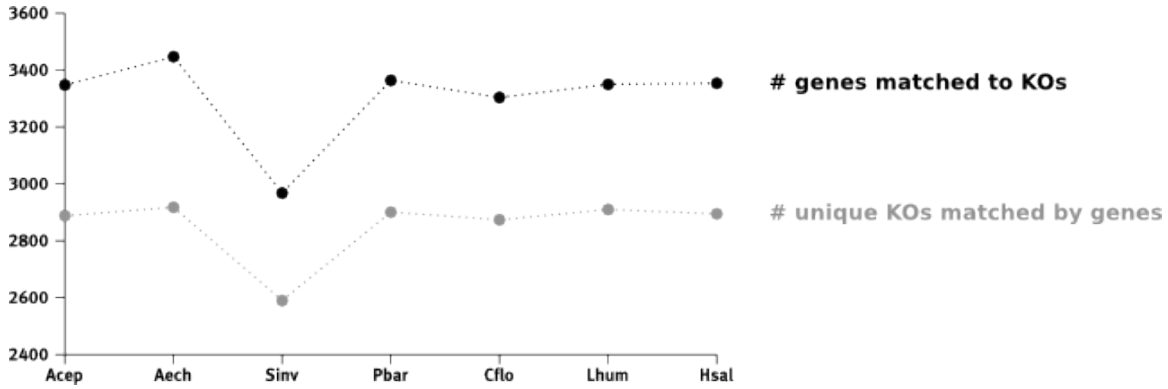

Supplemental Fig. 11. Coverage of KEGG annotation across the seven ant genomes. For each species, the number of annotated genes (black) and KEGG orthology (KO) terms (grey) are given, as multiple genes can map to the same KO term. The coverage is highly similar between all species except *S. invicta* (Sinv), which suggests incomplete genome annotation.

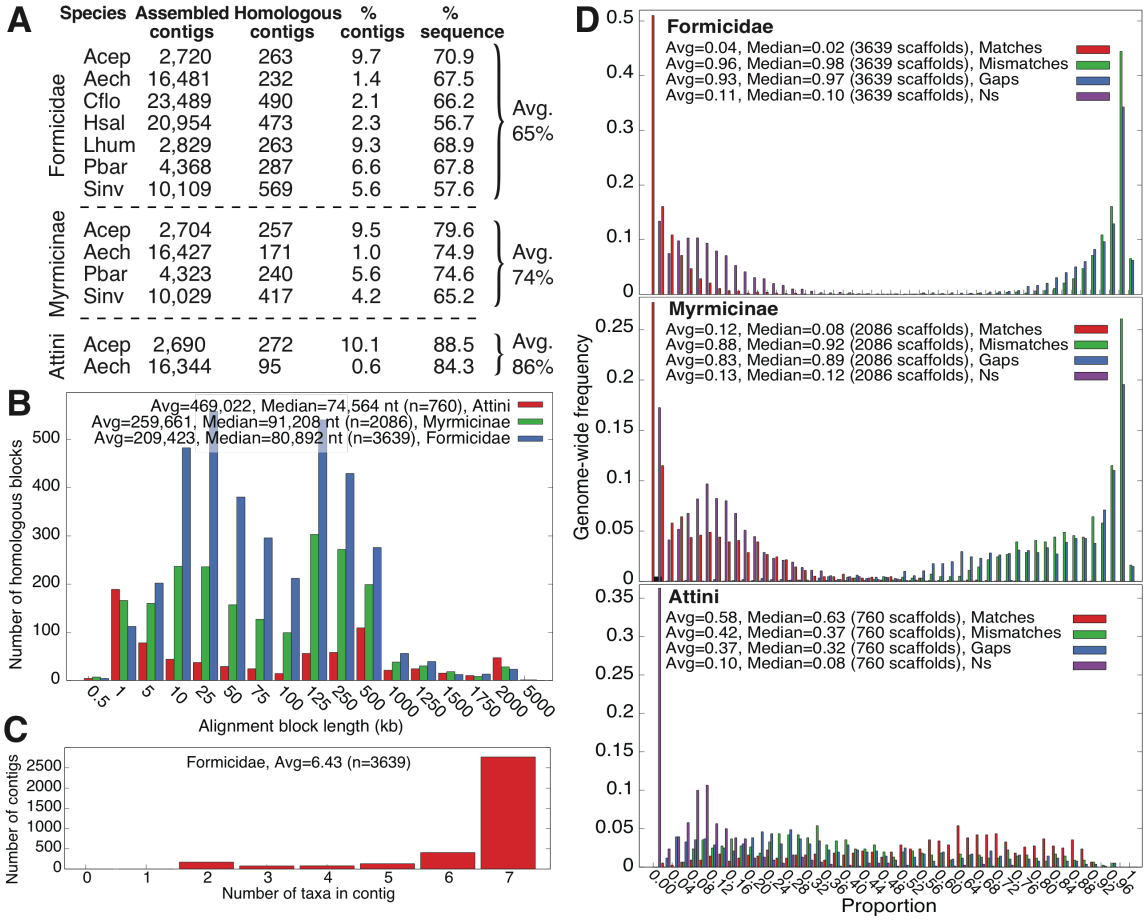

Supplemental Fig. 12. Multiple alignment of seven ant genomes. (**A**) Number of contigs and proportion of each ant genome identified as homologous among Formicidae, Myrmicinae, and Attini. Homologous contigs were determined using Mercator and subsequently aligned using Mavid. The number of homologous contigs identified for each evolutionary grouping are indicated. (**B**) Sequence length distribution of homologous, aligned contigs for each evolutionary grouping. (**C**) Species representation among homologous contigs; average number of species per homologous contig group is indicated. (**D**) Distribution of nucleotide matches, mismatches, gaps, and missing nucleotides (N) across the 7 Formicidae (**top**), 4 Myrmicinae (*Acep*, *Aech*, *Pbar*, *Sinv*) (middle), and 2 Attini (*Acep*, *Aech*) (**bottom**) genomes.

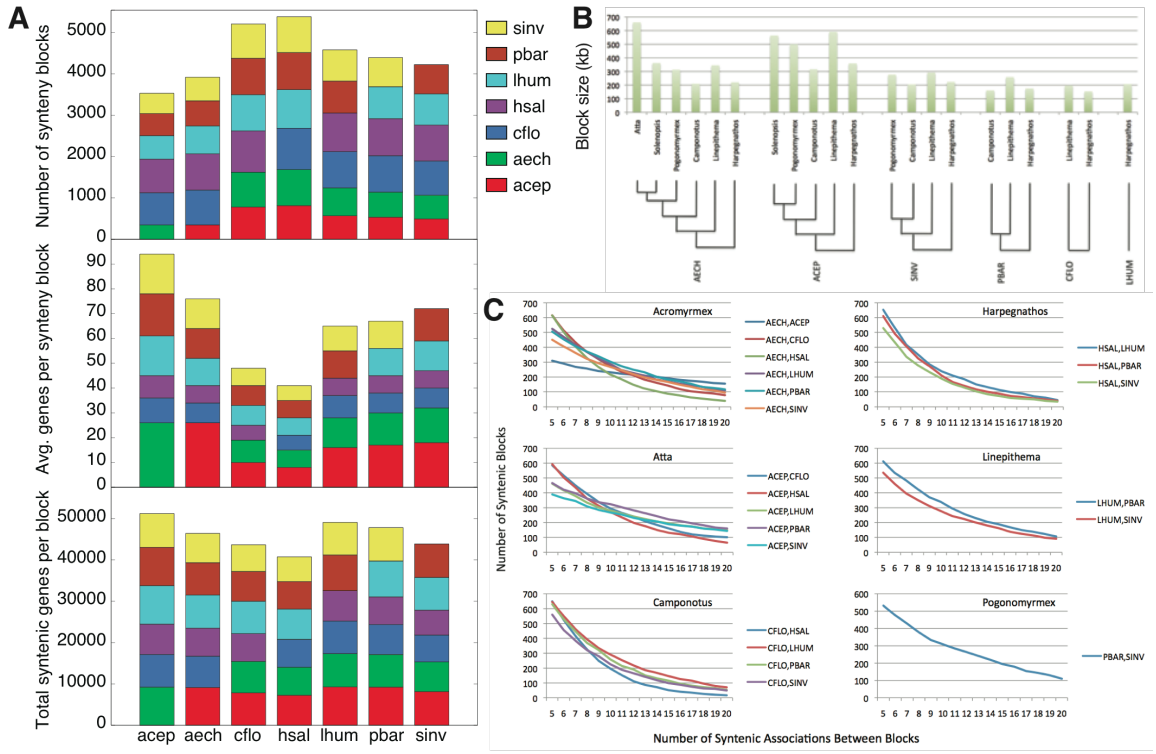

Supplemental Fig. 13. Characteristics of ant synteny blocks. (**A**) Number of synteny blocks for each ant species relative to one other species (top); Average number of genes per synteny block for each ant species relative to another species (middle); Total syntenic genes per synteny block for each ant species relative to another species (bottom). (**B**) Average length of synteny blocks (kilobases, kb). (**C**) Relationship between number of synteny blocks for each species versus the number of syntenic associations between blocks, used as a cutoff for synteny block identification.

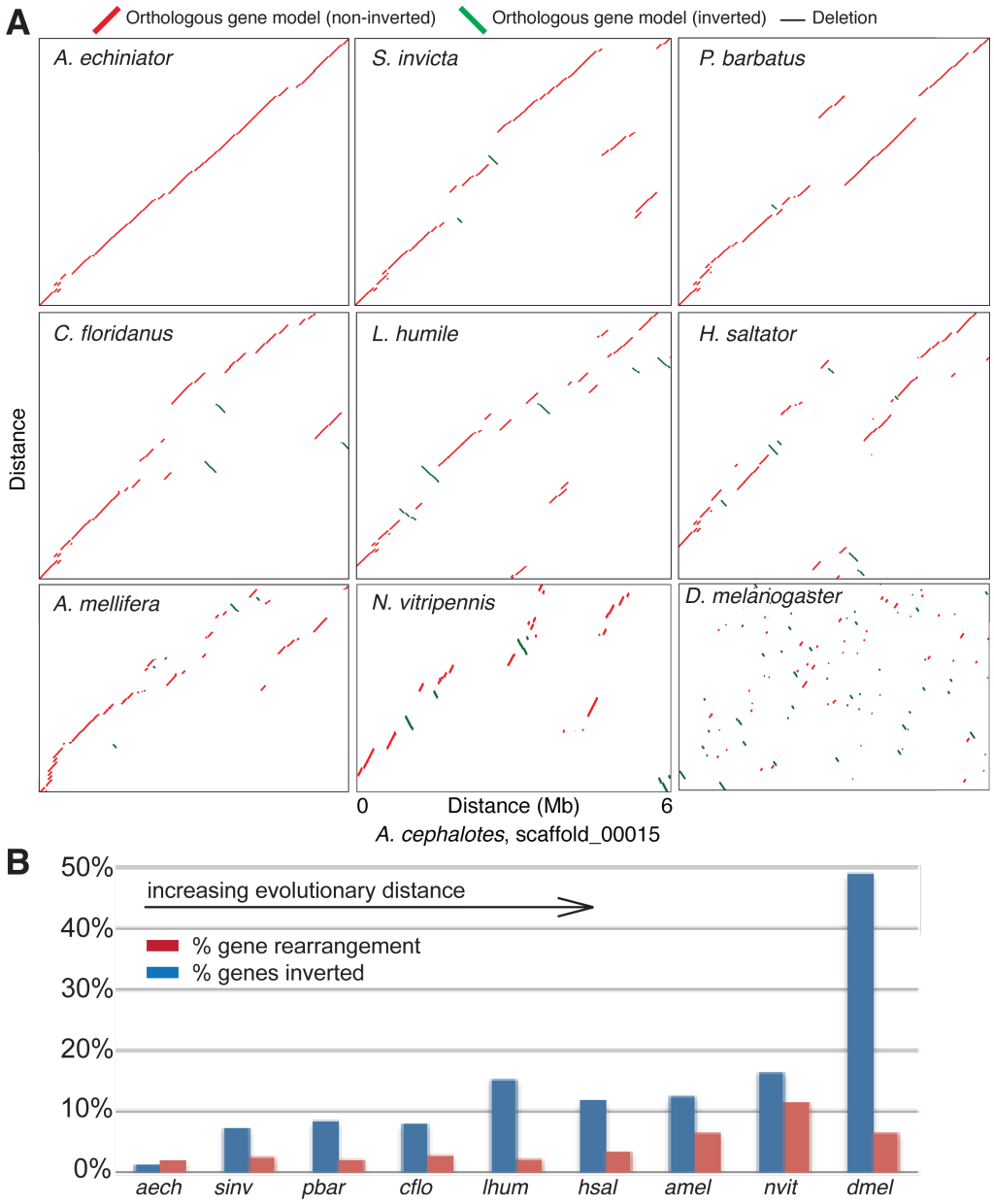

Supplemental Fig. 14. Syntenic fragmentation with increasing evolutionary distance. (**A**) Synteny plots for scaffold 00015 in *A. cephalotes* compared to six other ant and three other insect genomes. Horizontal axes show *A. cephalotes* gene order and vertical axes map orthologous gene models in the respective species. Red and green lines represent gene models in the same or reverse orientation to *A. cephalotes*, respectively. Horizontal gaps represent deletions in the other species. (**B**) Genome-wide proportion of genes inverted (blue) or rearranged (red) between *A. cephalotes* and other species, for all scaffolds greater than one megabase in size. Gene rearrangement is quantified for a target species by ranking genes by order along *A. cephalotes* scaffolds, counting the shift in each gene's rank order relative to *A. cephalotes*, and normalizing this rank shift to the maximum possible number of shifts over all genes. Species are arranged in order of increasing evolutionary distance to *A. cephalotes*.

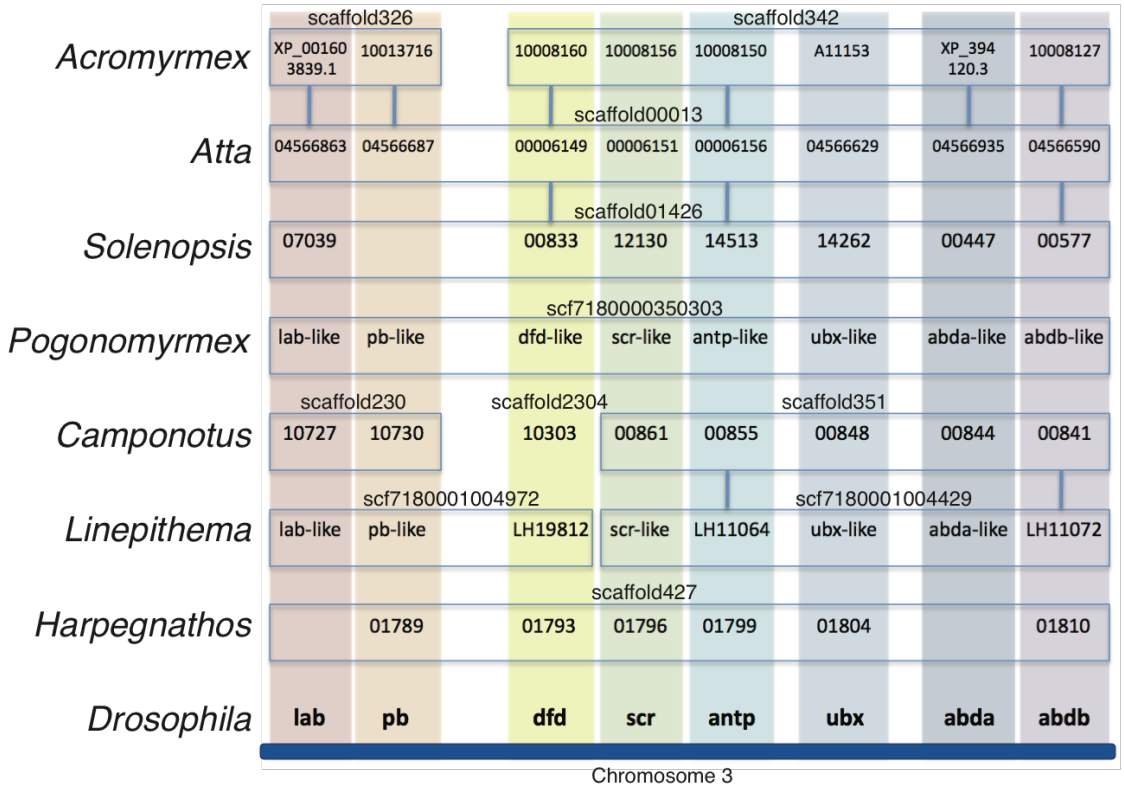

Supplemental Fig. 15. Hox cluster gene order is conserved among ants. Bottom row shows Hox cluster gene order along chromosome 3 in *D. melanogaster.* Columns indicate gene orthology among species. Boxes indicate individual scaffolds in the current genome assembly for each ant specices. Vertical lines denote syntenic links between species (see Methods).

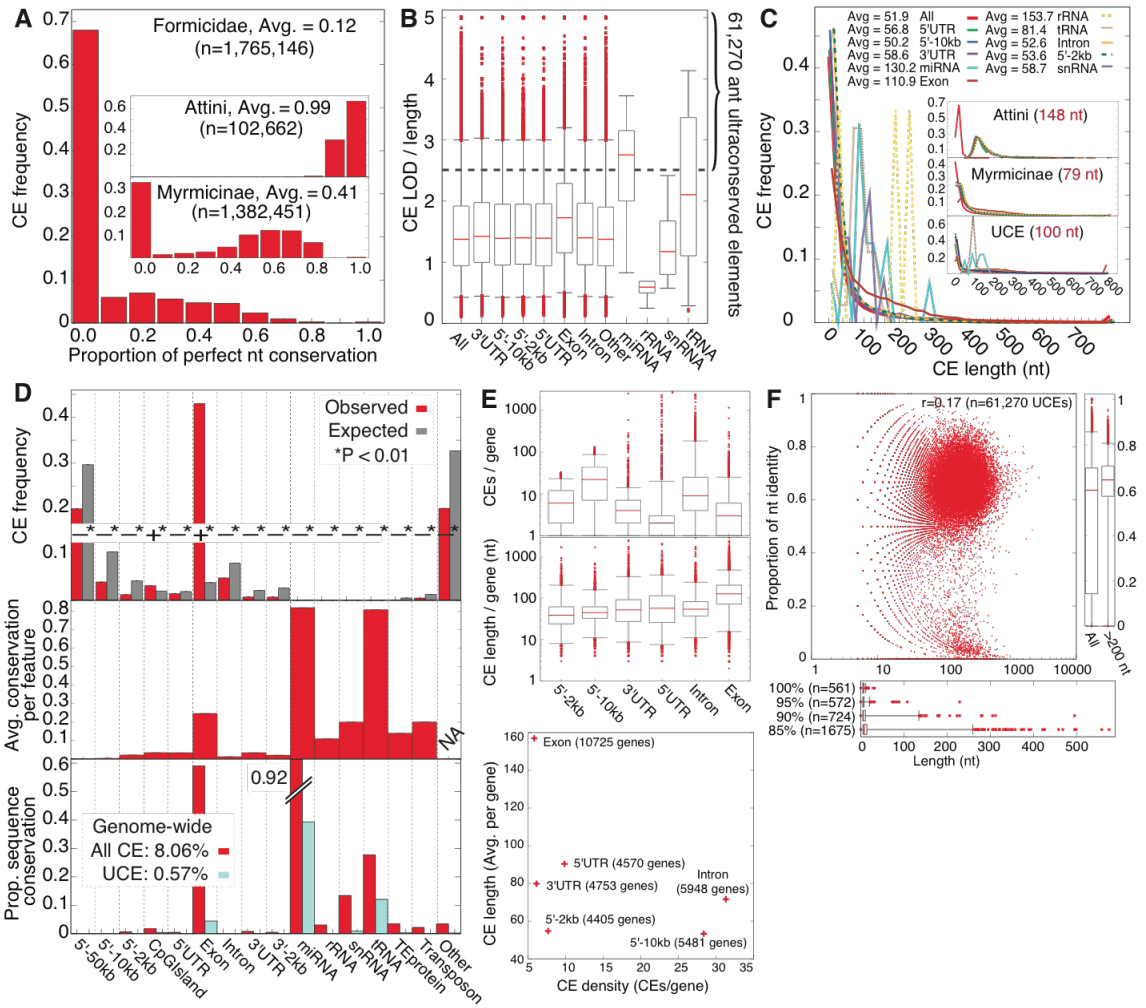

Supplemental Fig. 16. Distribution of conserved elements in ants. (**A**) Number of conserved elements (CEs) and proportion of perfect nucleotide conservation identified from aligned ant genomes (posterior probability of conservation > 0.95) for each of three evolutionary groupings: Formicidae (n=7), Myrmicinae (n=4), Attini (n=2). (**B**) CE conservation scores for Formicidae, estimated by LOD score normalized by CE length. Whiskers indicate outer 5% of distributions. Dashed line indicates 95% cutoff for isolation of ultra-conserved elements (UCEs; n=61,270). (**C**) CE length distributions, grouped by genic feature: Exon, Intron, 5' UTR, 3' UTR, proximal (2 kb) and distal (10 kb) promoters. Noncoding gene classes (miRNA, rRNA, tRNA, snRNA) are also included for CEs in Formicidae. Inside panels show length distributions for Attine and Myrmicine CEs and for auCEs (**bottom**). (**D, top**) Distribution of CEs over annotated genic regions (red), compared to random expectation (gray). Expected distributions were generated by randomly sampling sequences (with the same length distribution as observed CEs) from the 7 genome alignment and assessing genic feature distribution over 100 replicates. Genic regions significantly enriched (+) or depleted (–) for CEs are indicated ($P > 0.99$). (**Middle**) Conservation of each annotated genic feature, assessed as the proportion of DNA sequence for each genic feature that is covered by a single CE, averaged over all features for a given region. (**Bottom**) Estimates of the proportion of

each genic region with sequence conservation (thus under purifying selection). Overall estimates of proportion of genome-wide conservation using CEs or UCEs are indicated; note these estimates are based on the total aligned nucleotide sequence among the seven ant genomes. Error bars indicate 1 SE. (**E**) Distributions of number (**left**) and length (**right**) of CEs per protein-coding gene. Whiskers indicate outer 5% of distributions. Right, scatterplot of average CE density vs. length per protein-coding gene; sample sizes are indicated for each genic region. (**F**) Scatterplot of CE length vs. proportion of perfect (7-way) nucleotide identity for 61,270 ultraconserved elements (UCEs). Right, length distribution for all UCEs and the subset of 11,574 UCEs greater than 200 nt in length. Bottom, length distributions for UCEs grouped by minimum percent nucleotide identity.

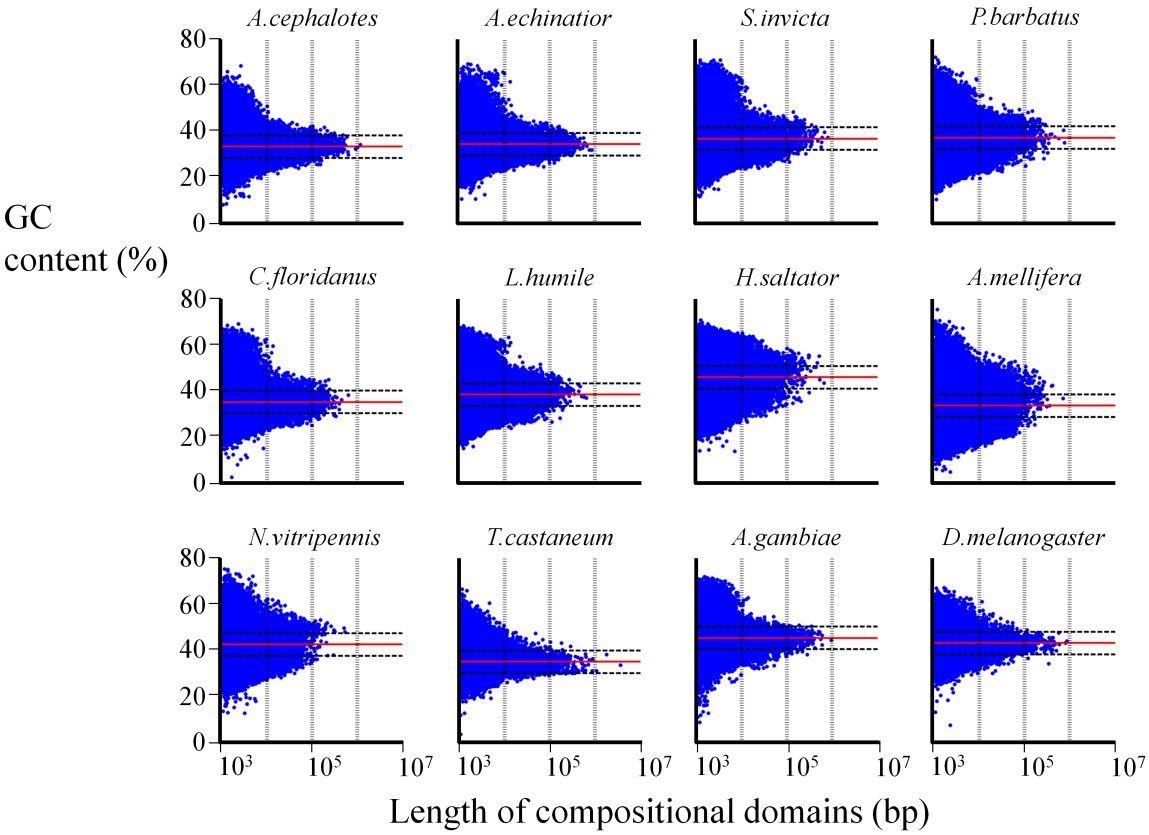

Supplemental Fig. 17. Compositional domain GC-content versus domain lengths on a log scale. The middle horizontal line (solid red) represents the mean genome GC-content within margins of ±5% (dashed black).

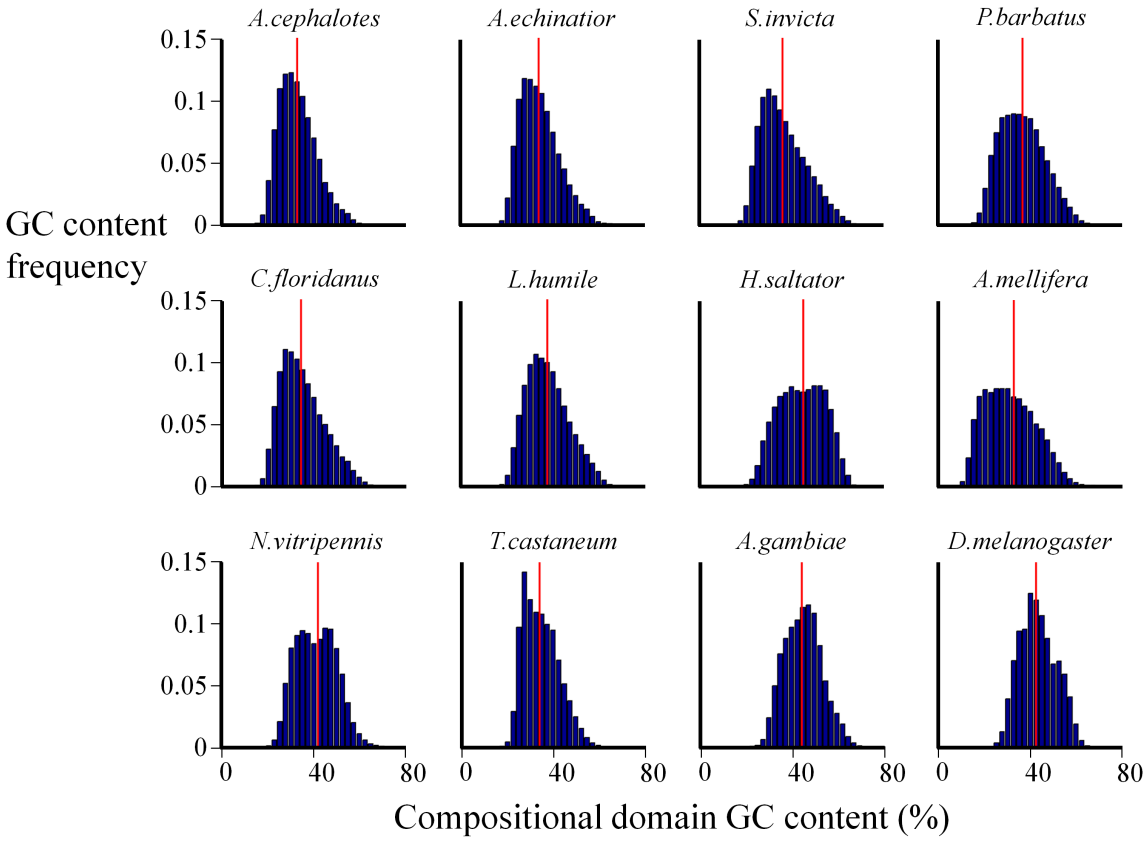

Supplemental Fig. 18. Compositional domain GC-content frequency distribution. The middle horizontal line (solid red) represents the mean genome GC-content.

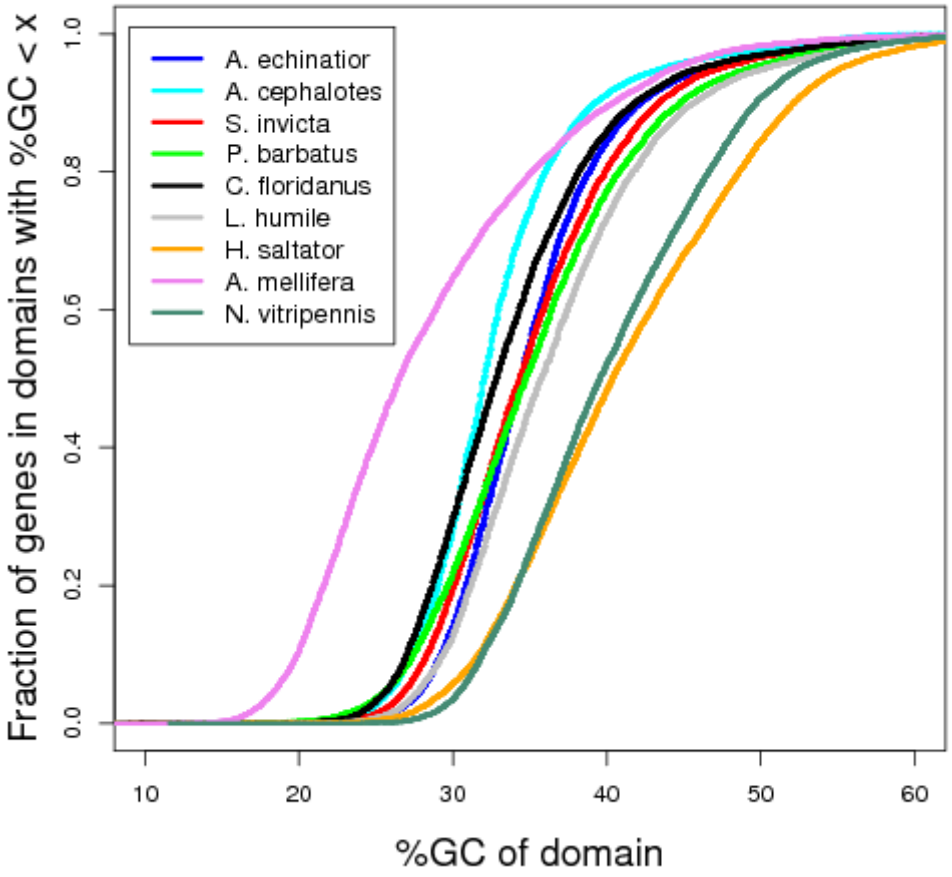

Supplemental Fig. 19. Cumulative distribution of the percent GC of all the genes in the nine species studied. Any point on this curve as the fraction of genes that exists in compositional domains less than a given percent GC. For example, a point on the *L. humile* curve at x = 33 and y = 0.4 indicates that 0.4 (40%) of genes are in poor compositional domains (GC_u<33%).

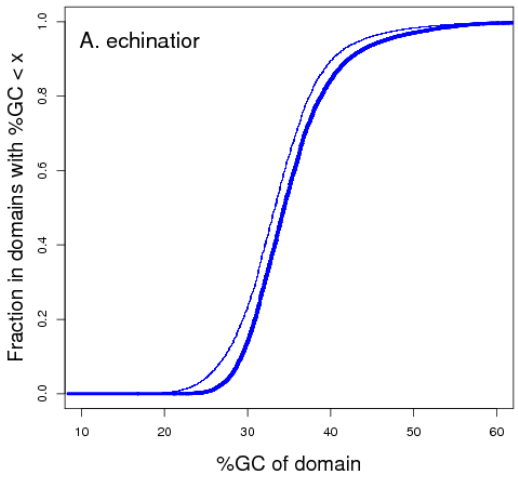
A. echinatior
Fraction in domains with %GC < x
%GC of domain

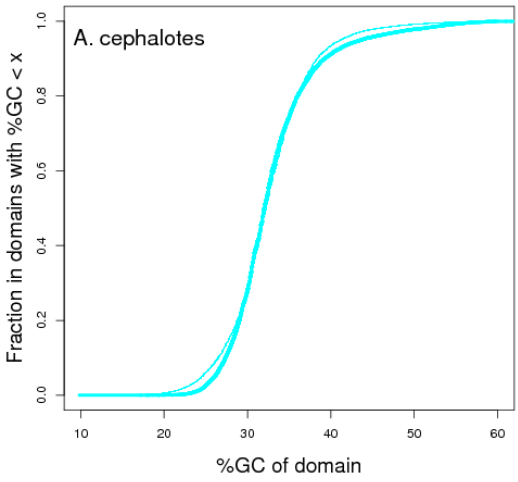
A. cephalotes
Fraction in domains with %GC < x
%GC of domain

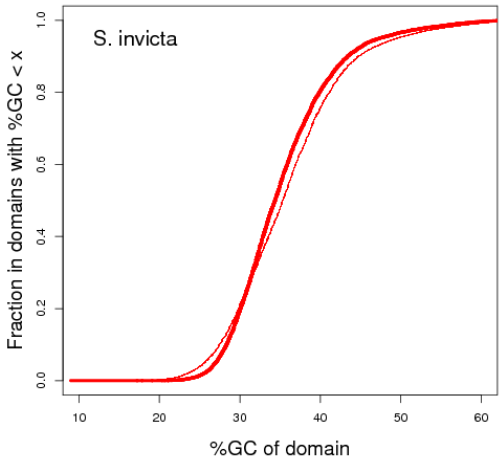
S. invicta
Fraction in domains with %GC < x
%GC of domain

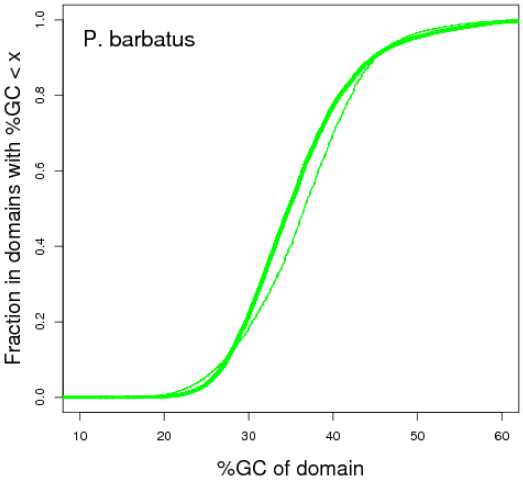
P. barbatus
Fraction in domains with %GC < x
%GC of domain

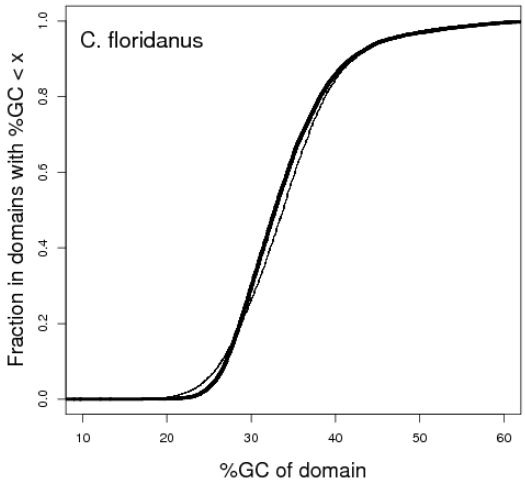
C. floridanus
Fraction in domains with %GC < x
%GC of domain

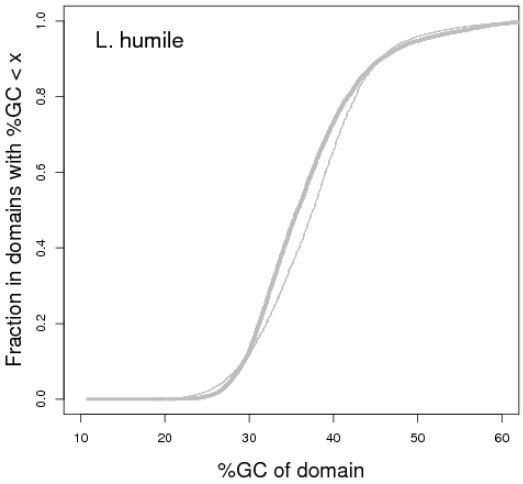
L. humile
Fraction in domains with %GC < x
%GC of domain

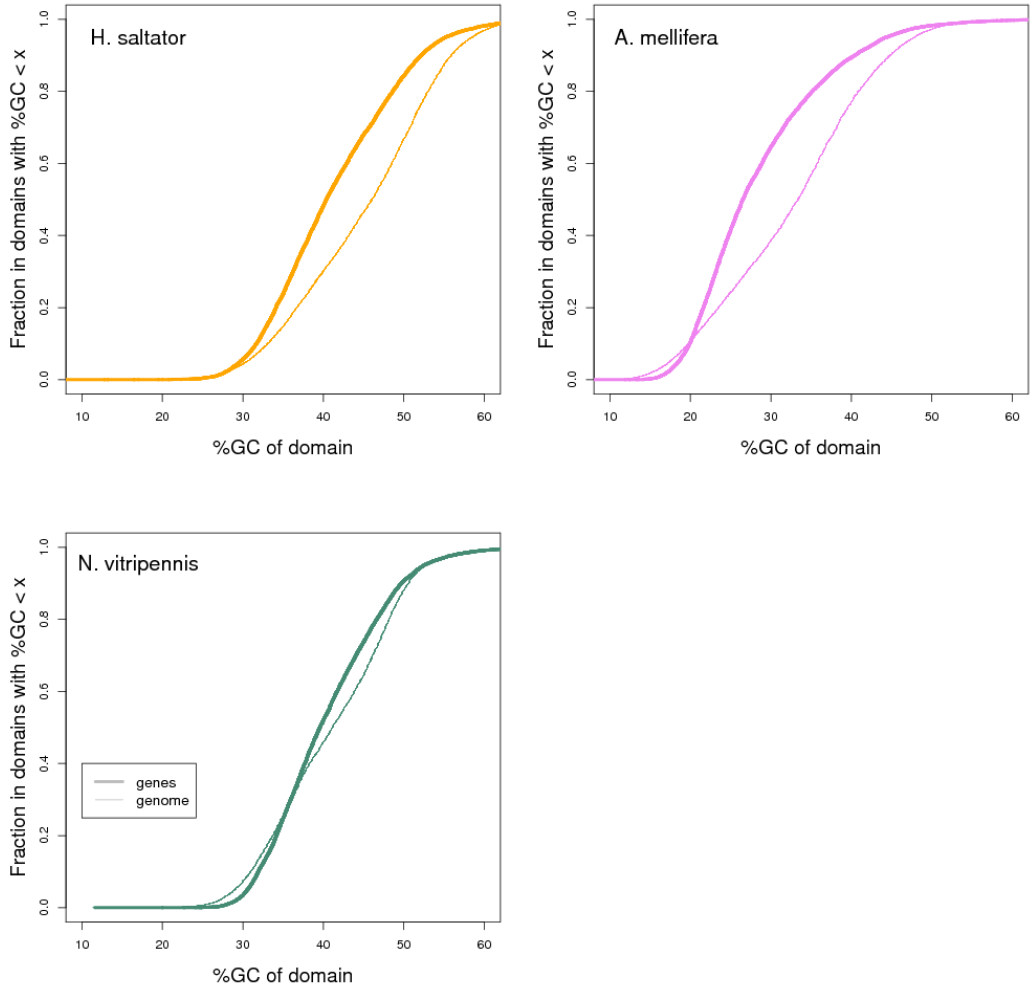

Supplemental Fig. 20. Cumulative distribution of the percent of each genome that is comprised of compositional domains below a given percent GC (thin lines) and the similar distribution for only compositional domains that contain genes (thick lines). If there is no tendency for genes to occur in compositional domains of a particular GC content, these two curves will be essentially the same.

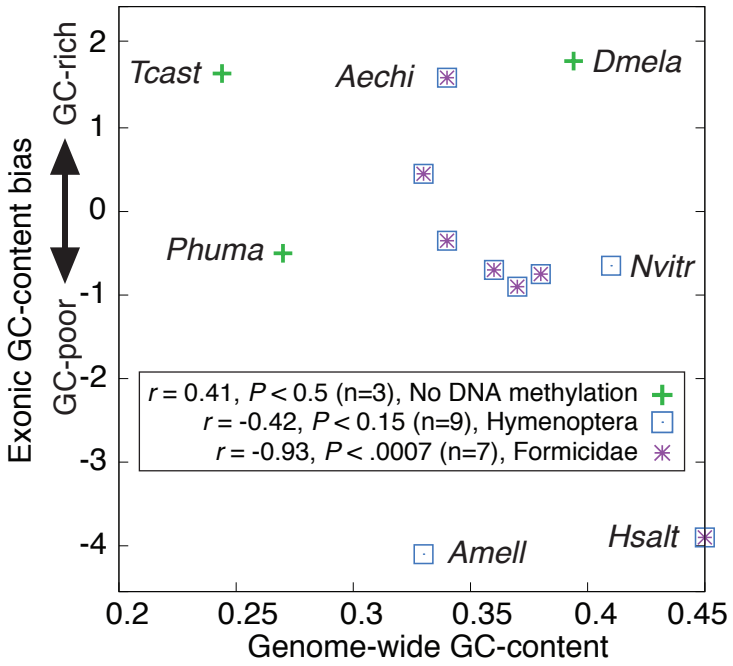

Supplemental Fig. 21. Scatterplot of genome-wide GC-content versus average GC-content bias for all protein-coding genes in 12 insect genomes. GC-content bias was computed as the difference in GC dinucleotide frequency of individual genes compared to the genome-wide background (Supplemental Fig. 20). Unexpectedly, ants cover the whole range of GC-content bias observed in animals. Pearson correlations were computed for three groups: insects lacking DNA methylation (Dmela, Phum, Tcast), Hymenoptera (n=9), and Formicidae (n=7). P-values computed using one-sample T-test.

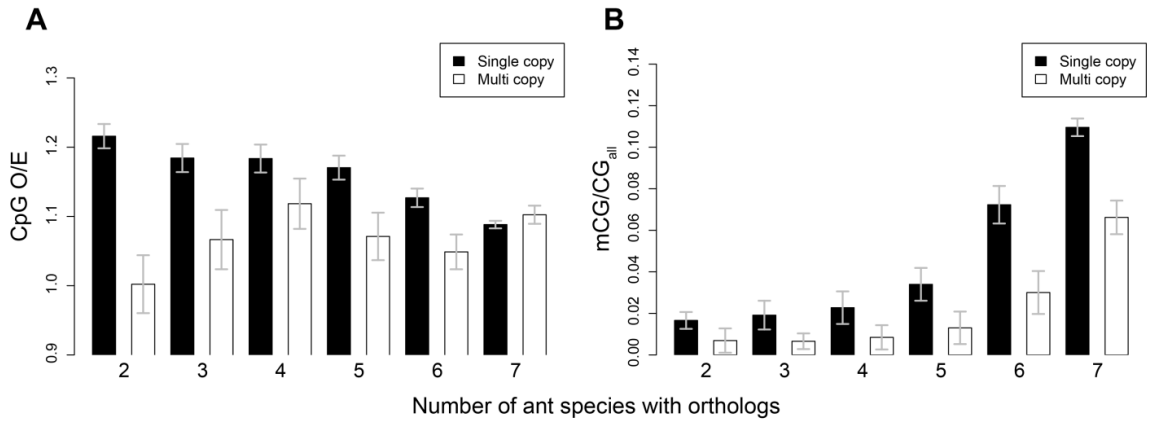

Supplemental Fig. 22. Normalized CpG content (CpG O/E) faithfully reflects DNA methylation of single copy, but not multi copy, genes. (**A**) *Solenopsis invicta* CpG O/E values of coding sequences suggest orthologs that are single copy in all lineages (single copy) exhibit increasing methylation with increasing prevalence of orthology among seven ant taxa, but this pattern does not hold for orthologs that are multi-copy in some lineages (multi copy). (**B**) In contrast, fractional methylation data (mCG/CG$_{all}$) demonstrate that methylation is correlated with the taxonomic prevalence of orthologs for single copy and multi copy genes. Notably, genes with orthologs in all seven ant genomes exhibit the highest methylation levels among single copy and multi copy orthologs. These results suggest that CpG O/E is not a good indicator of DNA methylation for multi copy genes (see Supplemental Table 8). Means and 95% confidence intervals are plotted.

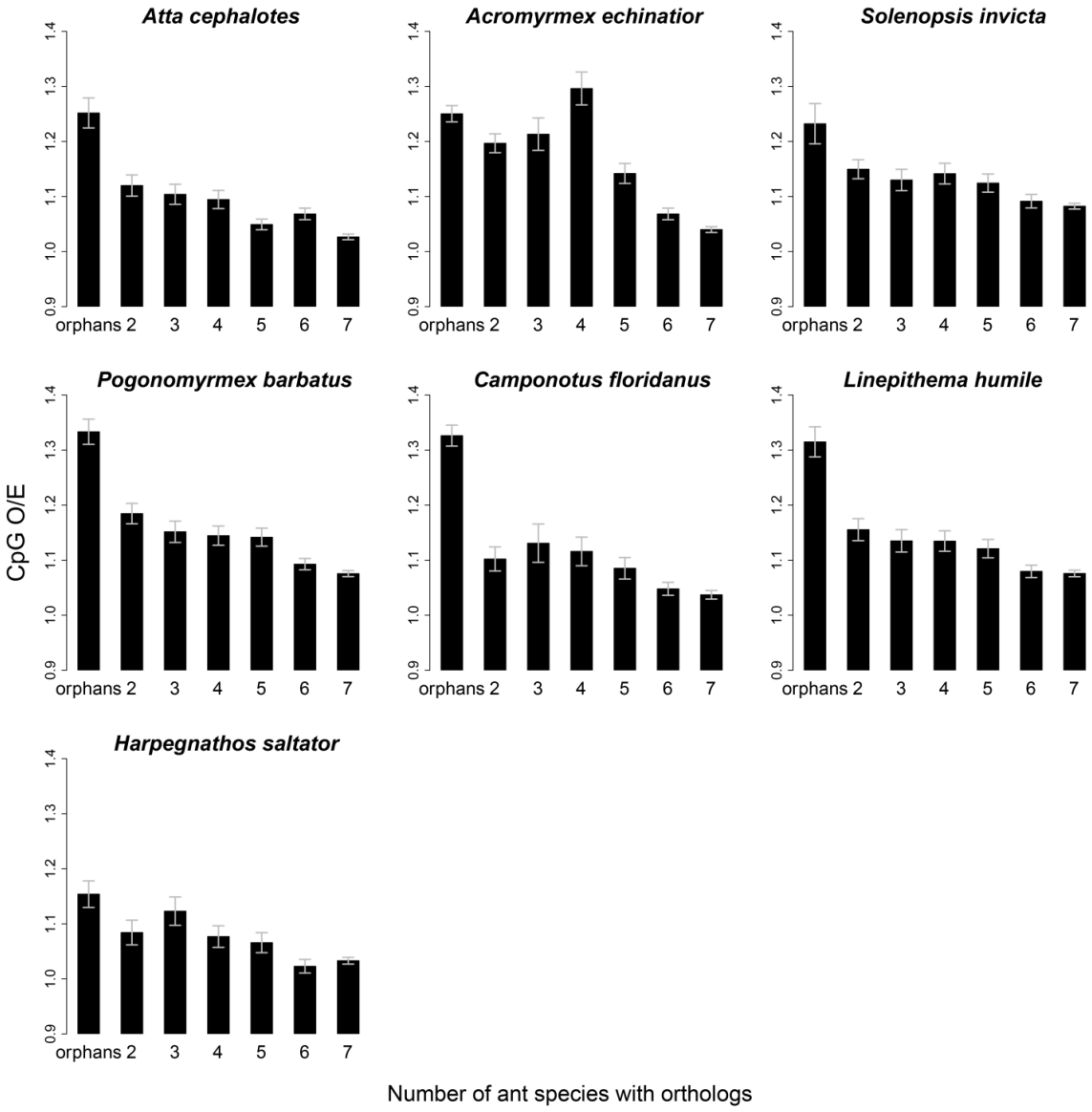

Supplemental Fig. 23. DNA methylation levels differ according to gene conservation. Normalized CpG content of coding sequences within genes (CpG O/E) are grouped according to the number of species with orthology. The relatively high CpG O/E values in orphan genes suggest they are largely unmethylated, whereas the relatively low CpG O/E values suggest seven-species orthologs are the primary targets of DNA methylation. Differences are highly significant in each species (Kruskal-Wallis $P < 0.0001$). Means and 95% confidence intervals are plotted.

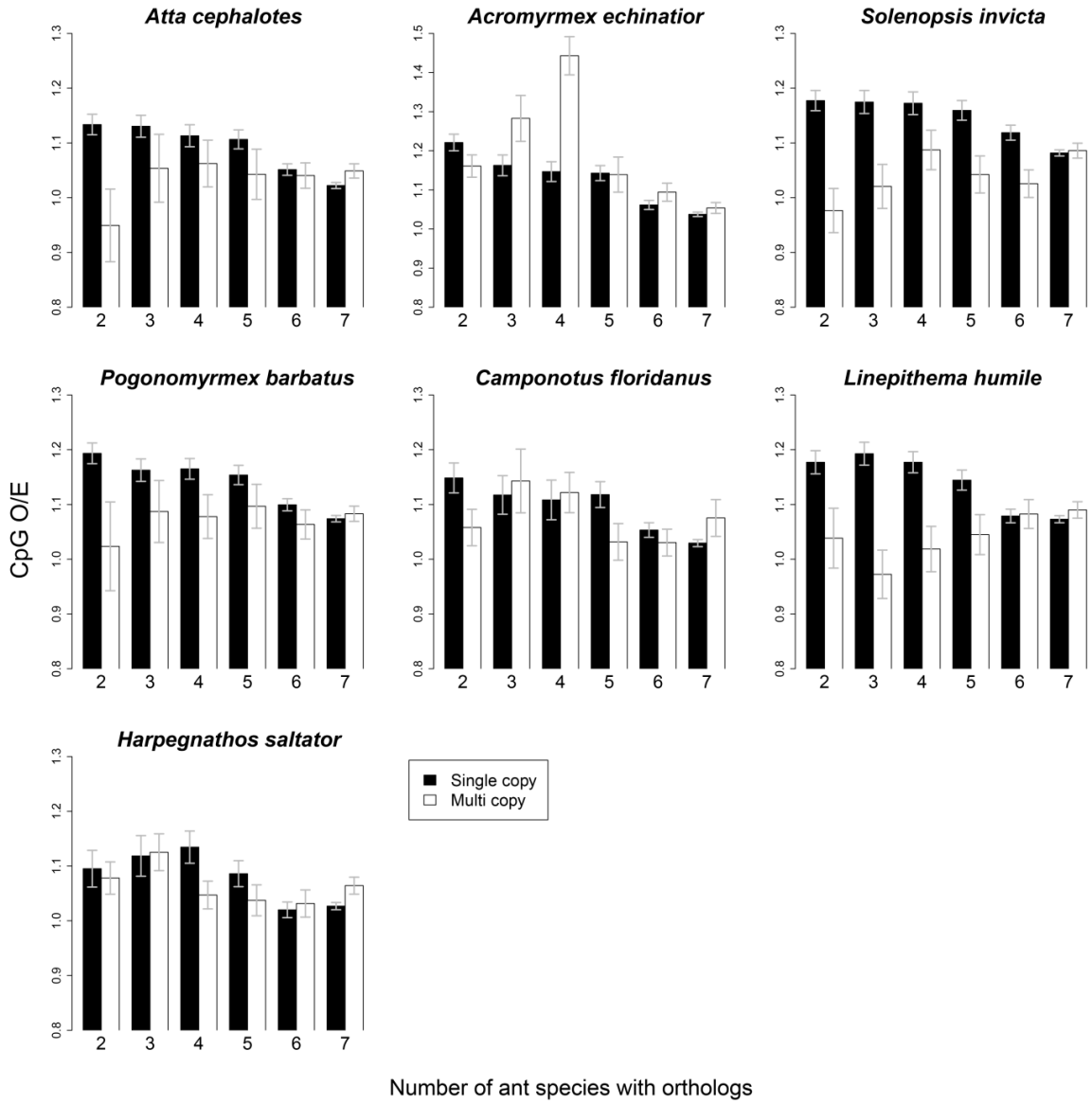

Supplemental Fig. 24. Normalized CpG content (CpG O/E) of coding sequences grouped according to the number of species with orthologs that are either multi copy in some lineages (multi copy) or single copy in all lineages (single copy). Estimates of methylation from single copy orthologs (see Supplemental Fig. 21) consistently suggest that seven-way orthologs are the primary targets of DNA methylation, and that DNA methylation infrequently targets taxonomically restricted or fast evolving genes. In contrast, CpG O/E of multi copy orthologs does not follow this trend and may not reflect methylation status (see Supplemental Fig. 21). Differences are highly significant in all species among single-copy orthologs (Kruskal-Wallis $P < 0.0001$) and are significant in each species except *P. barbatus* among multi-copy orthologs (Kruskal-Wallis $P < 0.05$). Means and 95% confidence intervals are plotted.

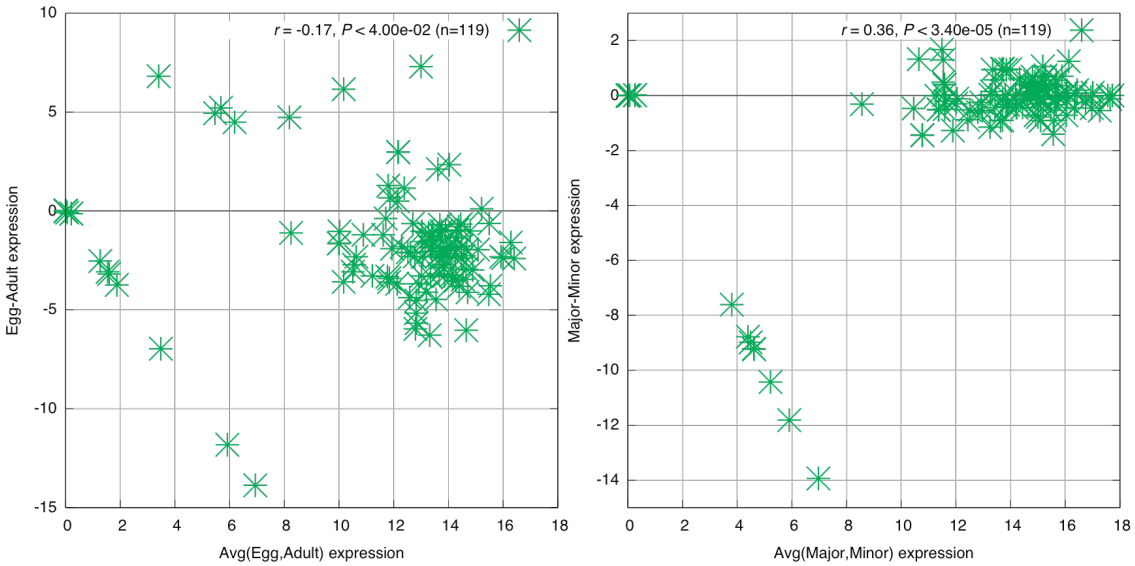

Supplemental Fig. 25. Expression of miRNA genes in *C. floridanus*. Left panel compares miRNA expression averaged over egg and adult stages (major, minor, male) with differential expression between egg and adult stages. Right panel compares miRNA expression averaged over female worker castes (major, minor) with differential expression between these castes. Expression estimates derived from small RNA-Seq data and quantified as $\log_2$(FPKM+1).

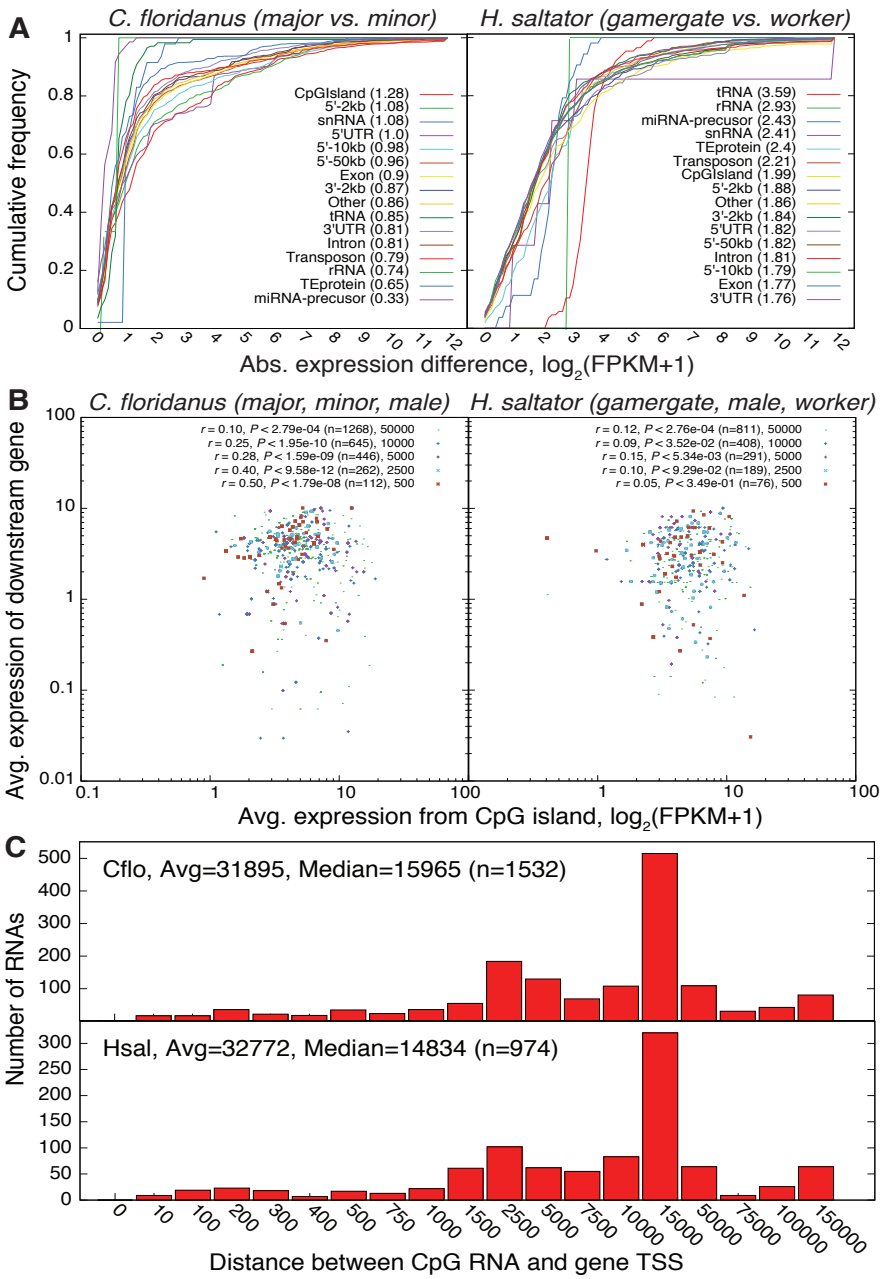

Supplemental Fig. 26. Expression of noncoding RNAs that overlap CEs. (**A**) Cumulative distributions of worker caste variation in gene expression of noncoding RNAs overlapping different genic regions, for *C. floridanus* on left and *H. saltator* on right. Values in parentheses indicate absolute difference in caste expression for the 50th percentile of features for a given region; regions are ranked by this statistic. (**B**) Relationship between expression level of small RNAs overlapping CpG islands and expression level of nearest downstream protein-coding gene, grouped by distance to nearest gene. Expression levels reflect average $\log_2$(FPKM+1) over three castes, as indicated. Pearson correlation coefficients are reported. (**C**) Distribution of distances between conserved CpG RNAs and nearest downstream protein-coding genes.

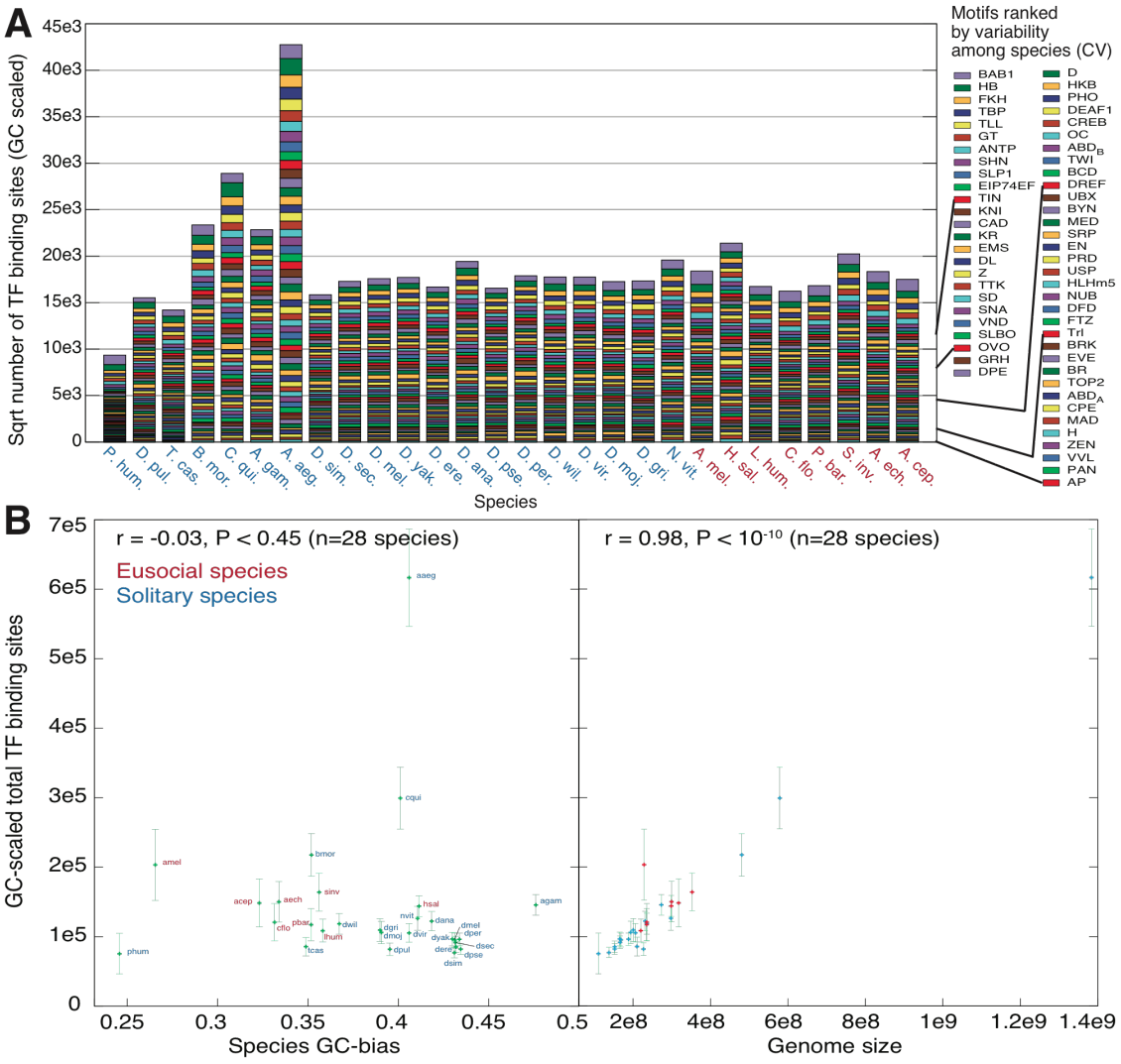

Supplemental Fig. 27. Genome-wide distribution of TF binding sites in insects. (**A**) Genome-wide distributions of total binding sites predicted for each species, separated by TF. TFs are ranked by species variability, Variance(|TFBS_i|)/Mean(|TFBS_i|), for each TF i. Mean and variance are computed across species. (**B**) Comparison of GC-bias (left) and Genome size (right) versus number of binding sites predicted for 28 insect species, averaged over 59 motifs. Binding site number for each motif is scaled by the ratio GC(x)/avg(GC), which corrects for variation in GC-bias among species. Error bars indicate 1 SEM over TFs. Red and blue text indicates eusocial and solitary species, respectively. Most genomes show very similar TFBS distributions (A), and we found no significant relationship to GC-content (P<0.45), though GC content is variable (B, left). However, 96% of observed variation in the number of TFBSs among species is explained by overall genome-size ($P<10^{-10}$) (B, right), as expected by our assumption of constant TFBS occurrence probability among species (1 TFBS per 5000nt).

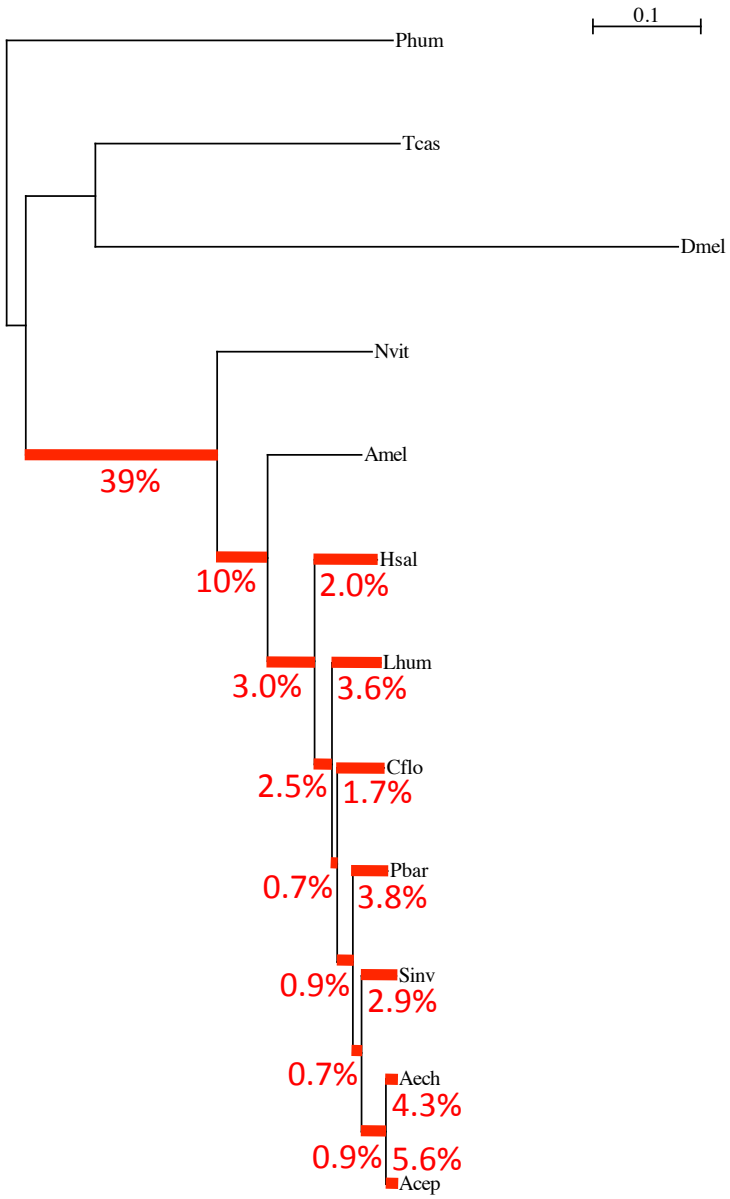

Supplemental Fig. 28. Phylogeny of the 12 species used in the positive selection analysis (see section on phylogeny above). All families tested did not include duplications, so their topology is following the species tree. In red are the 15 branches which were used as foreground branches in successive runs of the branch-site test for each families. The percentages indicated on each of these branches represent the proportion of gene families that display a significant signal for positive selection at a FDR threshold of 10%.

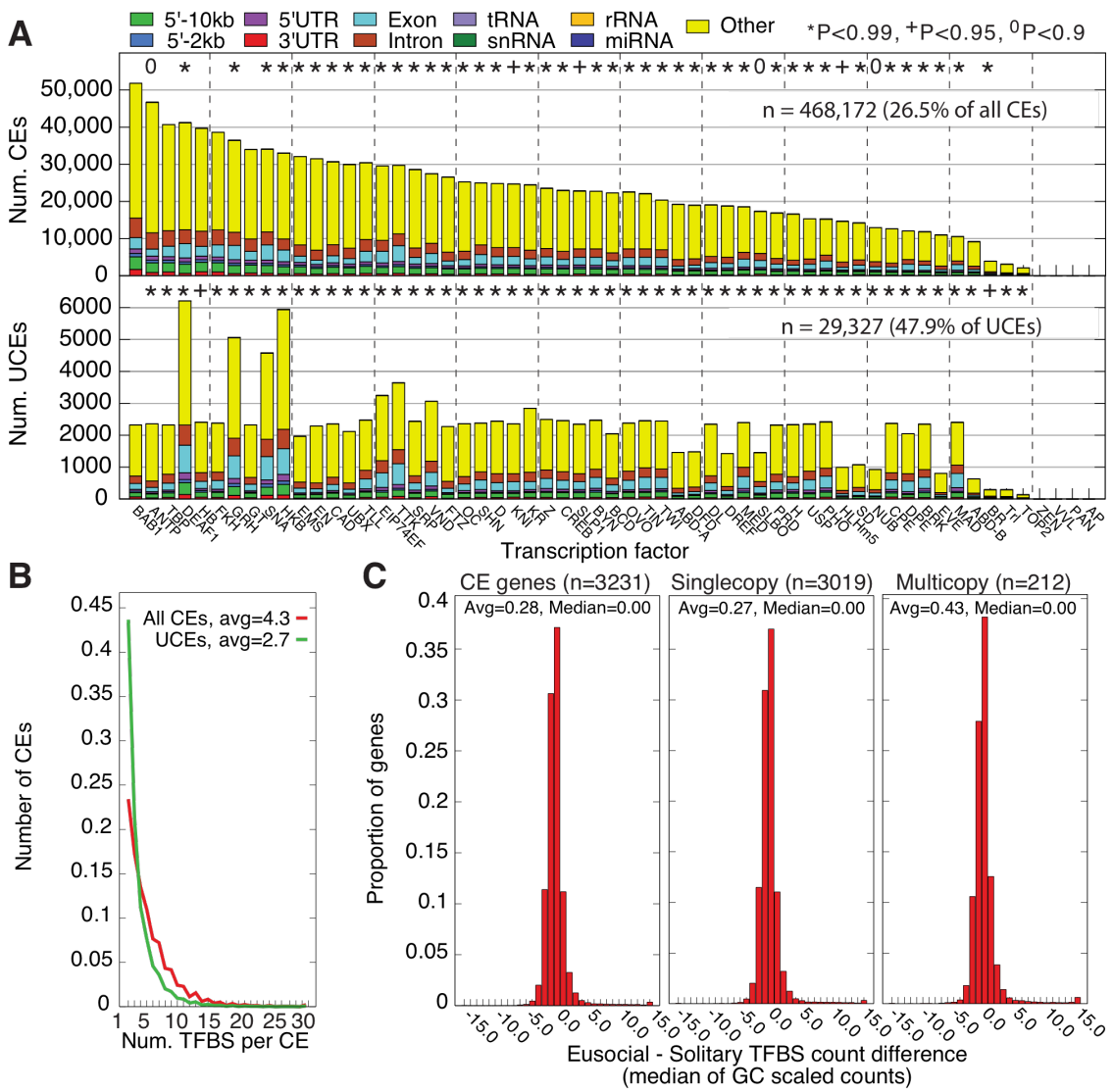

Supplemental Fig. 29. Genome-wide distribution of TF binding sites over genic regions. (**A**) Distribution of predicted TF binding sites (TFBSs) among ant conserved elements (CEs) for 59 TF sequence elements, sorted by total binding sites. Each stacked bar shows the binding site proportions among genic regions. Results for all CEs (**top**) and ultra-conserved elements (UCEs; **bottom**). P-values indicate whether more binding sites for a TF were found among CEs than among random sequences, computed by randomly sampling homologous sequences from the whole-genome alignment and counting predicted TFBSs (n=100; random sequences match the CE length distribution); $^{*}P < 0.99$; $^{+}P < 0.95$; $^{o}P < 0.9$. (**B**) Distributions of number of binding sites per individual CE, for all CEs (red) and the subset of ultraconserved elements (auCEs). (**C**) Distributions of the difference in GC-scaled number of TF binding sites between eusocial and solitary species per gene, pooling differences for all 59 TFs. Only binding sites occurring within 2 kb of the predicted transcription start site of homologous protein-coding genes were included. Genome-wide distributions for all (**left**), single-copy (**middle**), and multi-copy (**right**) genes are shown.

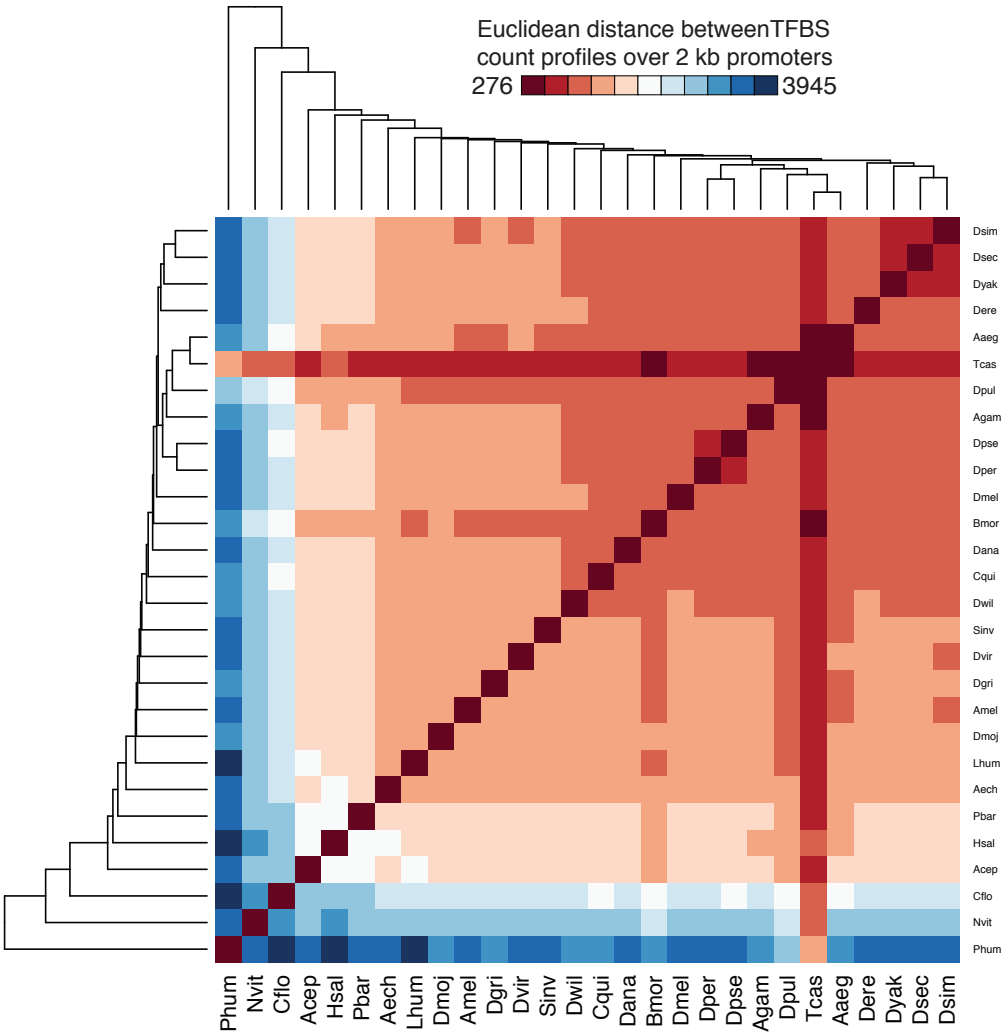

Supplemental Fig. 30. Hierarchical clustering of insect species using TFBS count profiles in 2kb promoters of protein-coding genes for 57 TFs. Clustering was performed using average linkage and Euclidean distance.

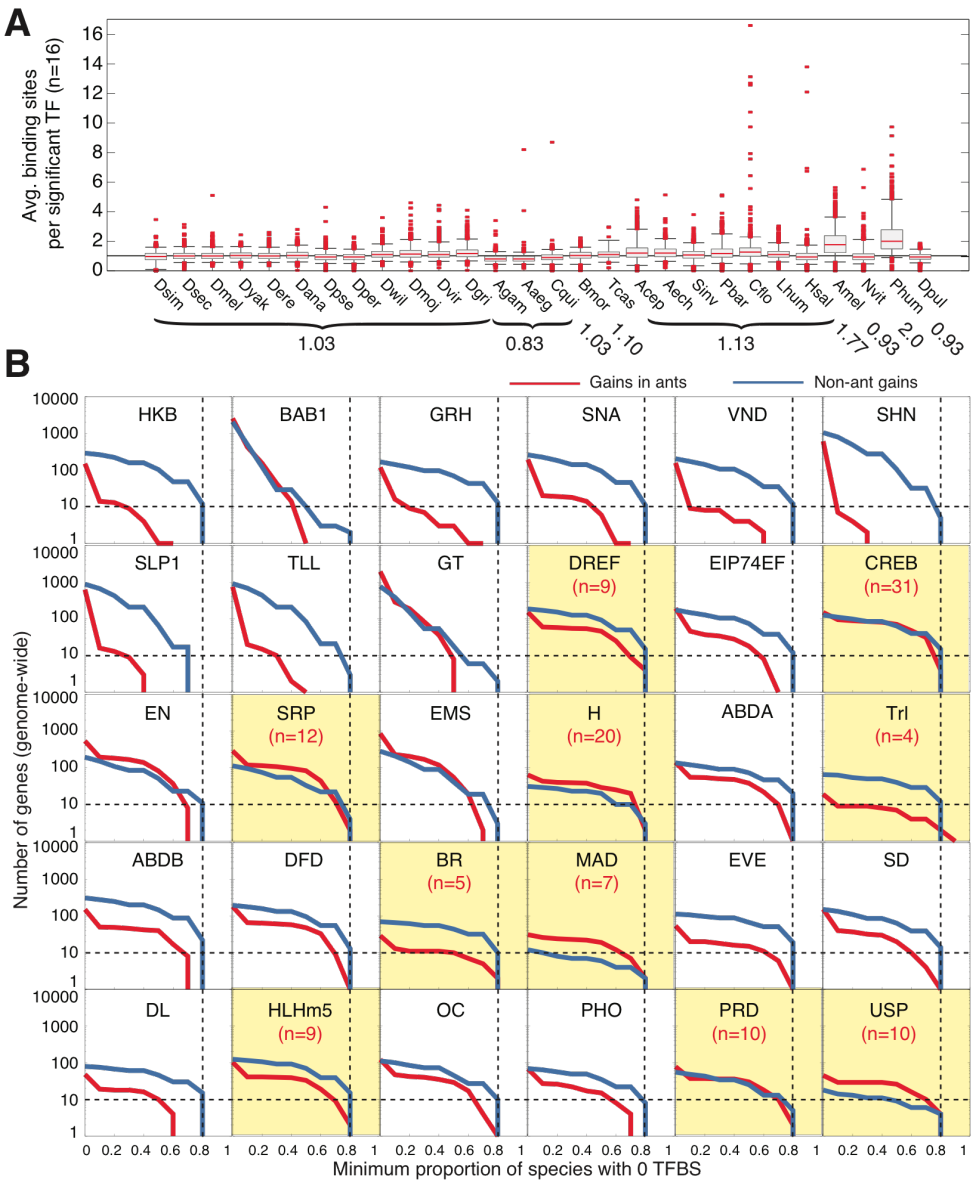

Supplemental Fig. 31. Conservation and divergence of TFBSs for significant TFs. (**A**) Distributions of the average number of TFBSs per gene among target genes for the top 16 TFs significantly associated with eusocial regulatory evolution (see Fig. 5B). Boxes denote 25–75% percentiles; whiskers denote inner 95% of data; outliers shown as red dots. The overall mean number of binding sites per TF is reported for major taxonomic groups and is computed as the median binding sites for each species, averaging over species per taxonomic group as indicated. (**B**) Genome-wide distributions of the number of genes associated with gains (red) or losses (blue) in TF binding sites in the ant lineages (n=7), compared to all other insect species (n=21). X-axis denotes the proportion of species, either ants (blue) or non-ants (red) for which the specified TF shows 0 predicted binding sites. Distributions for the 30 TFs associated with significant regulatory evolution are shown. 10 TFs highlighted in yellow have a positive number of genes with at least 80% of species showing 0 binding sites (blue, ants; red, non-ants).

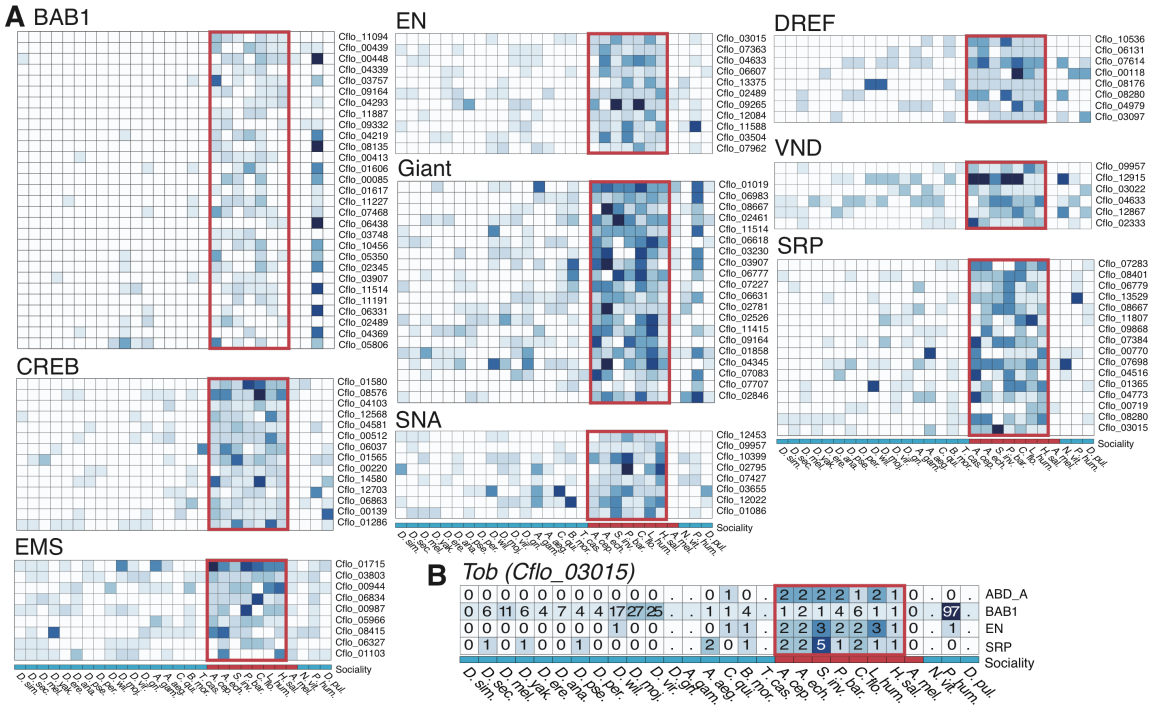

Supplemental Fig. 32. Heatmaps illustrating number of TF binding sites per gene across insect species (n=28) for genes that show significantly increased binding sites in eusocial lineages without concordant increases in *A. mellifera*. A total of 141 genes met this criteria. (**A**) Heatmaps for nine TFs associated with at least 5 genes are shown. (**B**) Heatmap for a single gene *Tob,* which shows 0 predicted binding sites in *A. mellifera* for four TFs (ABD_A, BAB1, EN, SRP), despite significant changes in ants compared to solitary species. *Tob* encodes a cell antiproliferative protein that interacts with multiple signaling proteins to regulate cell proliferation (Jia and Meng 2007).

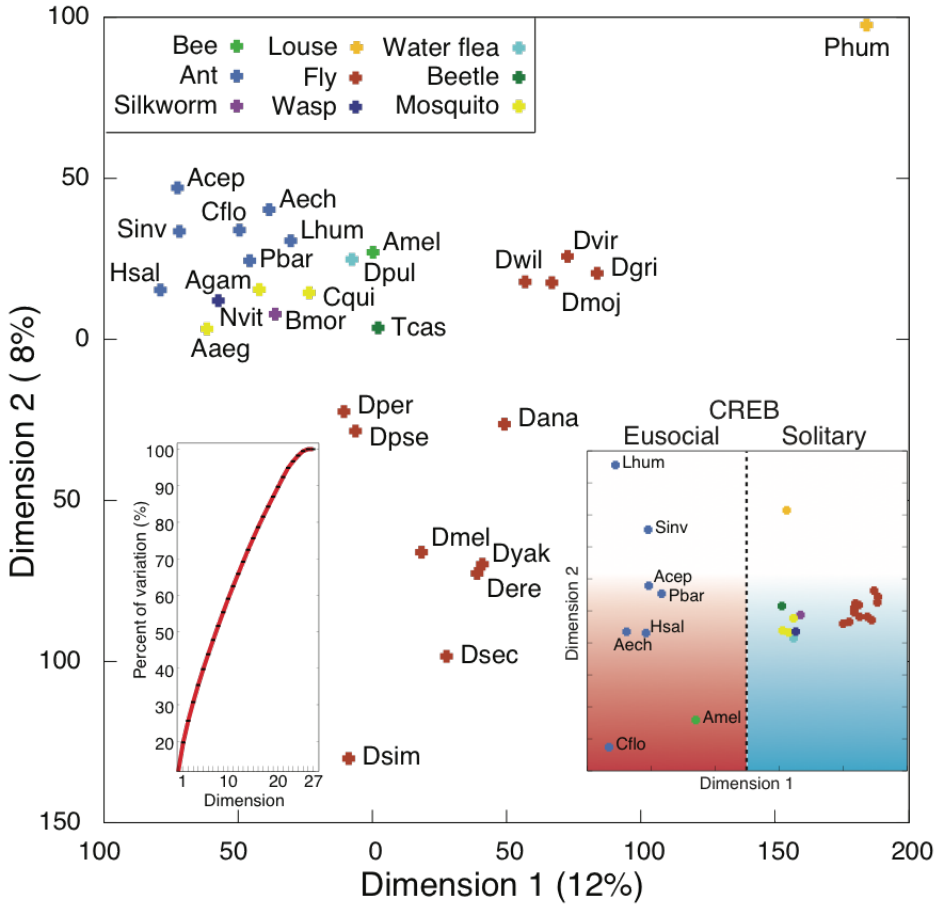

Supplemental Fig. 33. Principle components visualization of TF binding site evolution among insects. Singular value decomposition was applied to the 1955 gene x 28 species matrix whose values represent the total number of TF binding sites for the 16 TFs with significant binding site evolution (see Fig. 5B). Resulting species vectors were projected onto the top 2 eigenvectors (dimensions of covariation), as shown. Proportion of variation in TF binding sites among species explained by each dimension is shown on axes and in left inset plot. Right inset plot shows similar analysis of TF binding sites for a single TF, CREB. Vertical dashed line separates eusocial from solitary insects.

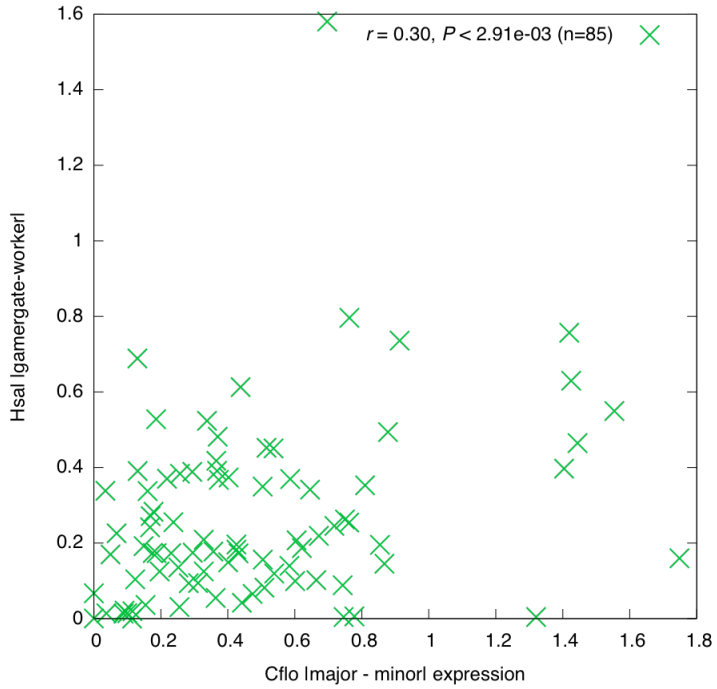

Supplemental Fig. 34. Correlation of variation in worker caste expression between species. Plasticity in worker caste gene expression was computed as the absolute value of the standard deviation in $\log_2$(FPKM+1) expression levels between major and minor samples (*C. floridanus*) and gamergate and worker samples (*H. saltator*). 85 of the 96 genes with concentrated regulatory evolution in TFBSs for multiple TFs per gene are shown (those with data in both species). Correlation computed using Pearson metric.

Supplemental Table 1. Organism and gene set information for the twelve insects included in AntOrthoDB (*http://cegg.unige.ch/orthodbants*).

Organism	Common Name	Code	Gene Set	Gene Count
Pediculus humanus	Body Louse	*PHUMA*	PhumU1.2	10,773
Drosophila melanogaster	Fruit Fly	*DMELA*	FB5.29	13,752
Tribolium castaneum	Flour Beetle	*TCAST*	Tcas_3.0	16,645
Nasonia vitripennis	Jewel Wasp	*NVITR*	OGS_v1.2	18,731
Apis mellifera	Honey Bee	*AMELL*	Amel_pre_release2	10,699
Harpegnathos saltator	Jumping Ant	*HSALT*	OGS_3.3	18,564
Linepithema humile	Argentine Ant	*LHUMI*	OGS_1.2	16,116
Camponotus floridanus	Carpenter Ant	*CFLOR*	OGS_3.3	17,064
Pogonomyrmex barbatus	Harvester Ant	*PBARB*	OGS_1.2	17,189
Solenopsis invicta	Fire Ant	*SINVI*	OGS_2.2.3	16,522
Acromyrmex echinatior	Leaf-cutter Ant	*AECHI*	OGS_1.0	20,243
Atta cephalotes	Leaf-cutter Ant	*ACEPH*	OGS_1.2	18,093

Supplemental Table 2. Orthologous protein length agreement between each of the seven ant species and the honeybee *A. mellifera* (*AMELL*) and the wasp *N. vitripennis* (*NVITR*). Concordances with 95% confidence limits (Conf. Lim.) are shown, as well as proportions of longer or shorter ant proteins compared to their bee or wasp orthologs.

	AMELL			
Species	Concordance	Conf. Lim.	Longer	Shorter
HSALT	0.91	0.90–0.91	28.20%	25.65%
LHUMI	0.87	0.86–0.87	26.76%	24.18%
CFLOR	0.92	0.91–0.92	29.48%	22.88%
PBARB	0.90	0.89–0.91	25.72%	28.97%
SINVI	0.83	0.82–0.84	22.64%	30.58%
AECHI	0.89	0.88–0.89	29.16%	24.90%
ACEPH	0.90	0.90–0.91	21.93%	31.41%

	NVITR			
Species	Concordance	Conf. Lim.	Longer	Shorter
HSALT	0.90	0.89–0.90	19.74%	33.06%
LHUMI	0.86	0.85–0.87	16.11%	28.38%
CFLOR	0.90	0.89–0.90	21.27%	31.22%
PBARB	0.89	0.89–0.90	14.37%	31.97%
SINVI	0.81	0.80–0.82	12.38%	32.29%
AECHI	0.88	0.87–0.88	16.82%	27.24%
ACEPH	0.89	0.88–0.89	11.66%	33.29%

Supplemental Table 3. Genes with paralog (GWP) counts for different definitions of paralogs (Set 1–4) across 30 arthropod species.

Species	GWPs for Set 1	GWPs for Set 2	GWPs for Set 3	GWPs for Set 4
Aaeg	12915	13060	13474	14234
Acep	8748	9690	9729	11659
Acyp	22313	21498	24038	25322
Aech	9106	9325	9829	10880
Agam	10061	10137	10637	11368
Amel	6900	7192	7471	8327
Bmor	7872	7780	8705	9615
Cflo	10539	10088	11551	12304
Cqui	13352	13860	14098	15636
Dana	9287	9237	10047	10884
Dere	8978	9054	9716	10645
Dgri	9705	9856	10388	11313
Dmel	8754	8610	9475	10123
Dmoj	8773	8826	9504	10364
Dper	10383	10743	11194	12442
Dpse	10213	10154	10992	11862
Dpul	19803	19648	21036	22434
Dsec	10015	10370	10757	11945
Dsim	8964	9512	9704	11037
Dvir	8854	8832	9594	10415
Dwil	10111	10065	10842	11669
Dyak	9905	10042	10643	11616
Hsal	12253	11618	13276	13957
Isca	9671	9007	10868	11442
Lhum	8936	9607	9779	11384
Nvit	13632	13830	14392	15481
Pbar	8632	9323	9502	11220
Phum	5731	5785	6363	7135
Sinv	9410	10068	10410	12307
Tcas	9496	9526	10182	11005

Supplemental Table 4. Summary of the dataset used for codon usage bias analysis (asterisks indicate genes that passed all quality filters).

Acro-nym	***Species name***	***Gene set version***	***No. of genes****	***Proportion of genes****	***Proportion of 1-copy orthologs****	***No. of ribosomal genes****
Acep	*Atta cephalotes*	OGS_1.2	15401	85.1	82.4	19
Aech	*Acromyrmex echinatior*	OGS_1.0	19926	98.4	94.6	68
Amel	*Apis mellifera*	Amel_pre_release2	9930	92.8	93.6	70
Cflo	*Camponotus floridanus*	OGS_3.3	16355	95.8	99.9	85
Dmel	*Drosophila melanogaster*	FB5.29	13687	99.5	99.9	89
Hsal	*Harpegnathos saltator*	OGS_3.3	17191	92.6	99.9	114
Lhum	*Linepithema humile*	OGS_1.2	11917	74.0	69	5
Nvit	*Nasonia vitripennis*	OGS_v1.2	14086	75.2	64.5	7
Pbar	*Pogonomyrmex barbatus*	OGS_1.2	12252	71.3	58.3	14
Phum	*Pediculus humanus*	PhumU1.2	10725	99.6	99.7	77
Sinv	*Solenopsis invicta*	OGS_2.2.3	15817	95.7	97.9	66
Tcas	*Tribolium castaneum*	T cas_3.0	16609	99.8	97.4	98

Supplemental Table 5. Rates of gene gain and loss estimated by considering each branch at a time independently from all others. Branches were assigned to rate categories based on *k*-means clustering with $k = 4$. The subsequent model with four rate categories (Fig. 2B) fitted the data significantly better than all other tested models.

Branch leading to	**Branch-specific rate**	**Rate category**
T. castaneum	0.00048	2
Non-hymenopteran Holometabola	0.00000	1
D. virilis	0.00126	3
Drosophilidae	0.00077	2
D. melanogaster	0.00216	3
D. melanogaster + *D. erecta*	0.00091	2
D. erecta	0.00177	3
D. melanogaster group	0.00666	4
D. ananassae	0.00122	3
Drosophila subgenus *Sophophora*	0.00105	3
D. pseudoobscura	0.00231	3
Diptera	0.00380	4
A. aegypti	0.00126	3
P. barbatus	0.00092	2
Myrmicinae	0.00152	3
A. echinatior	0.01192	4
Attini	0.00026	2
A. cephalotes	0.01224	4
Myrmicinae + Formicinae	0.00228	3
C. floridanus	0.00130	3
Formicoida	0.00106	3
L. humile	0.00086	2
Formicidae	0.00061	2
H. saltator	0.00134	3
Aculeata	0.00077	2
A. mellifera	0.00113	3
Hymenoptera	0.00000	1
N. vitripennis	0.00159	3

Supplemental Table 6. Immune gene families and their sizes in selected insects (taxon abbreviations as in Supplemental Table 4). For explanations of gene family acronyms see Material and Methods, Immune Genes. Values for *A. mellifera*, *T. castaneum* and *D. melanogaster* were obtained from published analyses (CR Smith et al. 2012, Pauli et al. 2011, Elango et al. 2009).

	Aech	***Acep***	***Cflo***	***Hsal***	***Lhum***	***Pbar***	***Sinv***	***Amel***	***Nvit***	***Tcas***	***Bmor***	***Dmel***
	Social Hymenoptera											
Recognition												
GNBP	2	2	2	2	4	2	4	4	3	3	4	5
PGRP	4	4	4	4	6	5	3	4	13	8	12	13
FREP	1	1	1	1	1	1	1	2	1	7	3	14
Galectins	2	3	3	3	3	3	2	3	3	3	4	6
SCR-B	8	9	12	8	9	9	10	10	12	16	13	13
SCR-C	1	1	1	1	1	1	1	1	1	1	1	4
CTL*	11	11	12	12	12	13	10	10	28	16	21	33
TEP	3	3	3	3	3	3	3	3	3	4	3	13
Modulation												
cSP†	8	6	9	14	8	7	4	18 (10)	13	48 (20)	15	46 (22)
Serpin	8	7	11	8	7	7	9	7	12	31	26	30
Effectors												
Abaecin	1	1	0	1	0	2	1	1	3	0	0	0
defensin	1	1	2	1	1	5	2	2	6	4	1	1
hymenoptaecin	1	1	1	1	1	1	1	1	2	0	0	0
other AMPs*	0	0	0	0	0	0	0	0	33	8	29	20
lysozyme	4	5	2	1	2	2	4	3	2	4	4	13
PPO*	1	1	1	1	1	1	1	1	2	3	2	3

† Numbers in parenthesis are gene family counts obtained using the same HMMER profile as used for the ants and *N. vitripennis*.
* Denotes significant difference in family size between eusocial (n=8) and solitary (n=4) species using a Mann-Whitney U-test (FDR < 0.1).

Supplemental Table 7. GO terms enriched among ant ultra-conserved elements.

Name	GOID	P	Q(GW)	Q(FG)	Count
regulation of multicellular organismal process	GO:0051239	3.86E–11	0.326	0.076	283
cell development	GO:0048468	1.07E–09	0.310	0.086	323
organ morphogenesis	GO:0009887	5.81E–09	0.314	0.073	274
cellular component movement	GO:0006928	6.55E–09	0.329	0.056	209
localization of cell	GO:0051674	6.55E–09	0.329	0.056	209
cell surface receptor linked signaling pathway	GO:0007166	8.11E–09	0.305	0.085	318
generation of neurons	GO:0048699	1.10E–08	0.321	0.063	234
calcium ion binding	GO:0005509	1.28E–08	0.326	0.056	211
regulation of transcription, DNA-dependent	GO:0006355	1.88E–08	0.294	0.105	393
regulation of RNA metabolic process	GO:0051252	1.94E–08	0.293	0.108	403
neurogenesis	GO:0022008	2.06E–08	0.317	0.064	240
cell adhesion	GO:0007155	3.04E–08	0.330	0.050	187
biological adhesion	GO:0022610	3.51E–08	0.330	0.050	187
neuron differentiation	GO:0030182	3.99E–08	0.320	0.058	218
integral to plasma membrane	GO:0005887	6.27E–08	0.310	0.068	255
intrinsic to plasma membrane	GO:0031226	6.66E–08	0.310	0.069	257
embryonic development	GO:0009790	7.46E–08	0.309	0.070	261
cell morphogenesis	GO:0000902	9.97E–08	0.325	0.050	188
transcription, DNA-dependent	GO:0006351	1.11E–07	0.288	0.111	417
molecular transducer activity	GO:0060089	1.49E–07	0.297	0.086	323
signal transducer activity	GO:0004871	1.49E–07	0.297	0.086	323
RNA biosynthetic process	GO:0032774	1.59E–07	0.287	0.112	419
synapse	GO:0045202	2.21E–07	0.335	0.041	153
cellular component morphogenesis	GO:0032989	3.98E–07	0.316	0.054	202
cell motility	GO:0048870	7.09E–07	0.327	0.042	158
cell-cell signaling	GO:0007267	8.39E–07	0.315	0.051	192
system process	GO:0003008	8.99E–07	0.292	0.087	324
neuron development	GO:0048666	9.62E–07	0.320	0.046	173
locomotion	GO:0040011	1.13E–06	0.317	0.048	180
transmembrane receptor activity	GO:0004888	1.13E–06	0.324	0.043	159
cell projection organization	GO:0030030	1.60E–06	0.317	0.047	176
regulation of cell differentiation	GO:0045595	1.90E–06	0.325	0.040	150
receptor activity	GO:0004872	2.23E–06	0.300	0.065	245
embryonic morphogenesis	GO:0048598	2.91E–06	0.326	0.038	142
regulation of neuron differentiation	GO:0045664	2.91E–06	0.374	0.020	76
cell migration	GO:0016477	3.30E–06	0.327	0.037	139
cell morphogenesis involved in differentiation	GO:0000904	3.30E–06	0.327	0.037	139
cell fate commitment	GO:0045165	3.32E–06	0.361	0.023	87
transcription regulator activity	GO:0030528	3.84E–06	0.285	0.091	342
transcription factor activity	GO:0003700	5.08E–06	0.301	0.059	220
regulation of neurogenesis	GO:0050767	5.17E–06	0.361	0.022	84
central nervous system development	GO:0007417	6.69E–06	0.313	0.045	168

cell projection	GO:0042995	7.12E–06	0.297	0.064	238
muscle system process	GO:0003012	7.19E–06	0.362	0.021	80
cell proliferation	GO:0008283	7.21E–06	0.295	0.067	251
regulation of biological quality	GO:0065008	8.56E–06	0.278	0.109	408
heart development	GO:0007507	9.06E–06	0.341	0.027	102
pattern specification process	GO:0007389	9.12E–06	0.330	0.032	121
positive regulation of developmental process	GO:0051094	1.10E–05	0.311	0.044	165
metal ion binding	GO:0046872	1.18E–05	0.260	0.226	844
sequence-specific DNA binding	GO:0043565	1.31E–05	0.313	0.042	156
neuron projection	GO:0043005	1.51E–05	0.318	0.037	140
tissue development	GO:0009888	1.54E–05	0.301	0.053	199
muscle contraction	GO:0006936	1.60E–05	0.361	0.020	75
regulation of cell communication	GO:0010646	1.61E–05	0.295	0.061	229
regulation of cell development	GO:0060284	1.71E–05	0.345	0.024	91
receptor binding	GO:0005102	1.84E–05	0.313	0.041	152
chordate embryonic development	GO:0043009	2.14E–05	0.318	0.036	136
embryonic development ending in birth or egg hatching	GO:0009792	2.31E–05	0.313	0.040	148
cell morphogenesis involved in neuron differentiation	GO:0048667	2.34E–05	0.323	0.033	123
regulation of nervous system development	GO:0051960	2.42E–05	0.345	0.023	87
neuron projection development	GO:0031175	2.45E–05	0.318	0.036	133
regulation of system process	GO:0044057	2.55E–05	0.328	0.030	111
cell junction	GO:0030054	2.65E–05	0.317	0.036	135
regulation of localization	GO:0032879	2.82E–05	0.307	0.043	162
regulation of cellular component organization	GO:0051128	3.12E–05	0.311	0.040	150
ion binding	GO:0043167	3.14E–05	0.258	0.230	861
locomotory behavior	GO:0007626	3.17E–05	0.337	0.025	95
transmission of nerve impulse	GO:0019226	3.24E–05	0.309	0.041	155
cation binding	GO:0043169	3.35E–05	0.258	0.228	852
sensory organ development	GO:0007423	3.44E–05	0.317	0.035	132
cell part morphogenesis	GO:0032990	3.48E–05	0.319	0.034	126
transcription factor binding	GO:0008134	3.63E–05	0.308	0.041	155
neuron projection morphogenesis	GO:0048812	3.80E–05	0.322	0.032	119
cell projection morphogenesis	GO:0048858	3.80E–05	0.320	0.033	122
ion channel activity	GO:0005216	4.21E–05	0.333	0.026	97
muscle organ development	GO:0007517	4.32E–05	0.328	0.028	105
behavior	GO:0007610	4.77E–05	0.305	0.043	161
synapse part	GO:0044456	4.98E–05	0.327	0.028	105
protein amino acid phosphorylation	GO:0006468	5.11E–05	0.300	0.048	178
cytoskeletal part	GO:0044430	5.28E–05	0.291	0.059	222
regulation of transcription from RNA polymerase II promoter	GO:0006357	5.29E–05	0.296	0.052	196
channel activity	GO:0015267	5.50E–05	0.330	0.026	99
passive transmembrane transporter activity	GO:0022803	5.50E–05	0.330	0.026	99
substrate-specific channel activity	GO:0022838	6.01E–05	0.330	0.026	98

neurological system process	GO:0050877	6.38E–05	0.287	0.067	249
cation channel activity	GO:0005261	6.85E–05	0.351	0.019	71
brain development	GO:0007420	7.21E–05	0.316	0.033	122
protein kinase activity	GO:0004672	7.53E–05	0.307	0.039	145
phosphate metabolic process	GO:0006796	8.25E–05	0.281	0.078	291
phosphorus metabolic process	GO:0006793	8.88E–05	0.280	0.078	291
cell fate determination	GO:0001709	9.24E–05	0.404	0.011	40
synaptic transmission	GO:0007268	9.35E–05	0.310	0.036	133
negative regulation of developmental process	GO:0051093	9.77E–05	0.301	0.043	160
gated channel activity	GO:0022836	1.02E–04	0.339	0.021	80
blood vessel morphogenesis	GO:0048514	1.03E–04	0.341	0.021	78
vasculature development	GO:0001944	1.05E–04	0.331	0.024	90
axonogenesis	GO:0007409	1.08E–04	0.322	0.028	104
phosphorylation	GO:0016310	1.09E–04	0.283	0.068	256
death	GO:0016265	1.11E–04	0.283	0.070	260
regulation of cell proliferation	GO:0042127	1.13E–04	0.299	0.045	167
cell death	GO:0008219	1.19E–04	0.283	0.069	258
regulation of anatomical structure morphogenesis	GO:0022603	1.19E–04	0.338	0.021	80
regulation of cellular component movement	GO:0051270	1.23E–04	0.356	0.017	62
negative regulation of gene expression	GO:0010629	1.25E–04	0.306	0.037	139
negative regulation of cell differentiation	GO:0045596	1.26E–04	0.344	0.019	72
response to external stimulus	GO:0009605	1.29E–04	0.290	0.056	208
regulation of cell projection organization	GO:0031344	1.40E–04	0.385	0.012	45
cytoskeletal protein binding	GO:0008092	1.43E–04	0.308	0.035	132
regulation of neuron projection development	GO:0010975	1.45E–04	0.394	0.011	41
blood vessel development	GO:0001568	1.45E–04	0.330	0.024	88
regulation of locomotion	GO:0040012	1.49E–04	0.354	0.017	62
extracellular region	GO:0005576	1.57E–04	0.281	0.072	268

Supplemental Table 8. Structure, length, and location of EvoFold predicted conserved RNA structures within the conserved elements (CEs) from the seven-way genome alignments. A total of 3318 putative RNA structures were identified, 1223 of which were considered high-confidence. A database of specific structures may be viewed with the following URL: *http://people.binf.ku.dk/jeanwen/data/ants/*.

	All predictions (n=3318)	**High confidence (n=1223)**
Structure shapes		
Hairpin	2980	1049
Clover shaped	15	7
Complex shaped	154	73
Y shaped	169	94
Structure length		
Short (≤ 15 bp)	3007	1118
Long (> 15 bp)	311	105
Structure location		
3' UTR	132	42
5' UTR	47	13
Intron	745	283
Intergenic	2003	694
CDS	391	191

Supplemental Table 9. Top 25 enriched GO categories of the EvoFold predicted conserved structural RNAs. While the P-values reported are not corrected for multiple testing, they were estimated using the TopGO "elim" method, which reduces redundancy in the GO analysis. The full table (less significant hits and the Molecular Function and Cell Component hierarchies), as well as tables of enriched categories for both the high-confidence structure set and for only intronic or UTR structures, can be browsed at the following URL: *http://people.binf.ku.dk/jeanwen/data/ants/evofold/*.

Accession	GO Biological Process	P-value
GO:0048870	cell motility	0.000042
GO:0007476	imaginal disc-derived wing morphogenesis	0.000093
GO:0009792	embryo development ending in birth or egg hatching	0.001300
GO:0007380	specification of segmental identity, head	0.001500
GO:0035295	tube development	0.001600
GO:0048598	embryonic morphogenesis	0.001700
GO:0007166	cell surface receptor linked signaling pathway	0.001700
GO:0016477	cell migration	0.002000
GO:0030182	neuron differentiation	0.002300
GO:0048675	axon extension	0.003400
GO:0007631	feeding behavior	0.004200
GO:0002251	organ or tissue specific immune response	0.004300
GO:0048468	cell development	0.004300
GO:0001745	compound eye morphogenesis	0.004400
GO:0010927	cellular component assembly involved in morphogenesis	0.005400
GO:0035220	wing disc development	0.005400
GO:2000026	regulation of multicellular organismal development	0.006700
GO:0007431	salivary gland development	0.006800
GO:0048569	post-embryonic organ development	0.007300
GO:0006928	cellular component movement	0.008100
GO:0009628	response to abiotic stimulus	0.009200
GO:0010556	regulation of macromolecule biosynthetic process	0.009500
GO:0006935	chemotaxis	0.009600
GO:0035071	salivary gland cell autophagic cell death	0.009900
GO:0030902	hindbrain development	0.009900

Supplemental Table 10. Distribution of GC/AT compositional-domain lengths.

Order	Species	Number of compositional domains				Total number	Assembly size (Mb)*
		1-–10 kb (%)	10–100 kb (%)	100 kb–1 Mb (%)	1–10 Mb (%)		
Hymenoptera	*A. cephalotes*	32,887 (88)	4,042 (11)	399 (1.1)	2 (0.01)	37,330	281
	A. echinatior	36,282 (88)	4,411 (11)	372 (0.9)	0 (0)	41,065	289
	S. invicta	54,878 (92)	4,376 (7)	294 (0.5)	0 (0)	59,548	311
	P. barbatus	35,604 (90)	3,637 (9)	192 (0.5)	0 (0)	39,433	220
	C. floridanus	30,714 (88)	3,804 (11)	202 (0.6)	0 (0)	34,720	221
	L. humile	31,978 (89)	3,755 (10)	188 (0.5)	0 (0)	35,921	213
	H. saltator	61,849 (94)	3,985 (6)	144 (0.2)	0 (0)	65,978	281
	A. mellifera	42,006 (91)	3,944 (9)	150 (0.3)	0 (0)	46,100	230
	N. vitripennis	51,064 (93)	3,870 (7)	72 (0.1)	0 (0)	55,006	238
Coleoptera	*T. castaneum*	15,432 (90)	1,535 (9)	183 (1)	3 (0.02)	17,153	131
Diptera	*A. gambiae*	36,941 (92)	3,185 (8)	231 (0.6)	0 (0)	40,357	223
	D. melanogaster	12,297 (85)	1,973 (14)	154 (1.1)	0 (0)	14,424	120

* Number of non-ambiguous nucleotides in the assembly

Supplemental Table 11. Spearman's rank correlations between bisulfite-seq fractional methylation levels and CpG O/E of genes in *Solenopsis invicta* males according to orthology data. CpG O/E is a strong predictor of empirically obtained levels of methylation for conserved single copy genes, but not multi copy genes.

Number of taxa with orthology	**Transcription unit (exons and introns)**		**Coding sequence**	
	Single copy	**Multi copy**	**Single copy**	**Multi copy**
1 [a]	0.1029 *		0.0791 ^{NS}	
2	0.056 ^{NS}	0.153 ^{NS}	0.011 ^{NS}	0.1555 *
3	0.061 ^{NS}	0.172 *	0.0257 ^{NS}	0.0917 ^{NS}
4	–0.023 ^{NS}	0.118 ^{NS}	–0.0658 ^{NS}	0.1004 ^{NS} 4
5	–0.175 ****	0.147 *	–0.1624 ****	0.036 ^{NS}
6	–0.456 ****	0.016 ^{NS}	–0.3678 ****	–0.0042 ^{NS}
7	–0.669 ****	–0.291 ****	–0.5545 ****	–0.2644 ****

^{NS} $P > 0.05$, * $P < 0.05$, **** $P < 0.0001$

[a] Orphan genes have not been annotated as single copy or multi copy

Supplemental Table 12. Bisulfite-seq fractional methylation levels (mCG/CG_{all}) of coding sequences in *Solenopsis invicta* males according to different CpG O/E cutoffs (among genes with single copy orthologs present in seven species). CpG O/E values differ among genes according to empirically obtained levels of methylation.

Cutoff	**CpG o/e cutoff value**	**Direction**	**Number of genes**	**Mean fractional methylation (± SEM)**
Mean CpG o/e	1.088	above	2525	0.041 (±0.001)
Mean CpG o/e + 0.5 SD	1.193	above	1822	0.029 (±0.001)
Mean CpG o/e + 1 SD	1.298	above	792	0.020 (±0.002)
Mean CpG o/e + 2 SD	1.507	above	70	0.018 (±0.005)
Mean CpG o/e	1.088	below	2525	0.193 (±0.004)
Mean CpG o/e – 0.5 SD	0.983	below	1546	0.249 (±0.005)
Mean CpG o/e – 1 SD	0.878	below	866	0.311 (±0.008)
Mean CpG o/e – 2 SD	0.669	below	229	0.436 (±0.018)

Supplemental Table 13. Gene Ontology functional enrichment for putatively methylated genes according to the presence of lower than mean coding sequence CpG O/E values in all seven ant taxa (among single copy orthologs present in seven species). P-value calculated by the Benjamini and Hochberg FDR method.

Accession	GO Biological Process	Fold enrichment in class	P-value
GO:0010467	gene expression	1.54	2.32E –05
GO:0016070	RNA metabolic process	1.75	3.93E –05
GO:0006461	protein complex assembly	2.48	1.78E –04
GO:0070271	protein complex biogenesis	2.48	1.78E –04
GO:0009987	cellular process	1.12	2.69E –04
GO:0044260	cellular macromolecule metabolic process	1.28	2.85E –04
GO:0044237	cellular metabolic process	1.22	3.18E –04
GO:0006367	transcription initiation from RNA polymerase II promoter	3.16	3.18E –04
GO:0006366	transcription from RNA polymerase II promoter	2.67	3.59E –04
GO:0006352	transcription initiation	3.08	4.77E –04
GO:0043933	macromolecular complex subunit organization	1.95	9.42E –04
GO:0044249	cellular biosynthetic process	1.38	0.001
GO:0006139	nucleobase, nucleoside, nucleotide and nucleic acid metabolic process	1.39	0.001
GO:0032774	RNA biosynthetic process	2.33	0.001
GO:0034645	cellular macromolecule biosynthetic process	1.46	0.001
GO:0065003	macromolecular complex assembly	2.02	0.001
GO:0006351	transcription, DNA-dependent	2.34	0.001
GO:0009059	macromolecule biosynthetic process	1.45	0.001
GO:0009058	biosynthetic process	1.35	0.002
GO:0034641	cellular nitrogen compound metabolic process	1.31	0.007
GO:0043170	macromolecule metabolic process	1.19	0.012
GO:0006412	Translation	1.76	0.013
GO:0044085	cellular component biogenesis	1.46	0.037
GO:0006974	response to DNA damage stimulus	2.19	0.038
GO:0006281	DNA repair	2.25	0.039
GO:0006807	nitrogen compound metabolic process	1.26	0.040

Supplemental Table 14. Gene Ontology functional enrichment for putatively unmethylated genes according to the presence of higher than mean coding sequence CpG O/E values in all seven ant taxa (among single copy orthologs present in seven species). P-value calculated by the Benjamini and Hochberg FDR method.

Accession	GO Biological Process	Fold enrichment in class	P-value
GO:0048856	anatomical structure development	1.35	5.61E –08
GO:0048731	system development	1.38	5.74E –08
GO:0032501	multicellular organismal process	1.27	6.82E –08
GO:0030154	cell differentiation	1.41	8.70E –07
GO:0007166	cell surface receptor linked signal transduction	1.64	1.05E –06
GO:0048869	cellular developmental process	1.38	1.67E –06
GO:0048468	cell development	1.48	1.72E –06
GO:0007165	signal transduction	1.48	4.60E –06
GO:0007275	multicellular organismal development	1.27	5.03E –06
GO:0007399	nervous system development	1.47	5.11E –06
GO:0009653	anatomical structure morphogenesis	1.35	6.07E –06
GO:0032502	developmental process	1.24	1.09E –05
GO:0022008	Neurogenesis	1.52	2.32E –05
GO:0048699	generation of neurons	1.51	7.89E –05
GO:0048513	organ development	1.33	1.28E –04
GO:0007186	G-protein coupled receptor protein signaling pathway	1.93	1.80E –04
GO:0009887	organ morphogenesis	1.44	1.83E –04
GO:0007610	Behavior	1.64	1.90E –04
GO:0007411	axon guidance	1.95	4.43E –04
GO:0007409	Axonogenesis	1.73	9.19E –04
GO:0030182	neuron differentiation	1.48	0.001
GO:0048666	neuron development	1.50	0.003
GO:0009888	tissue development	1.46	0.004
GO:0007155	cell adhesion	1.76	0.005
GO:0022610	biological adhesion	1.76	0.005
GO:0030030	cell projection organization	1.45	0.005
GO:0065007	biological regulation	1.14	0.005
GO:0006928	cell motion	1.56	0.006
GO:0007626	locomotory behavior	1.78	0.007
GO:0051239	regulation of multicellular organismal process	1.52	0.007
GO:0000902	cell morphogenesis	1.38	0.009
GO:0030534	adult behavior	2.00	0.010
GO:0042221	response to chemical stimulus	1.56	0.011
GO:0003008	system process	1.41	0.014
GO:0050794	regulation of cellular process	1.14	0.015

GO:0007167	enzyme linked receptor protein signaling pathway	1.74	0.018
GO:0050789	regulation of biological process	1.13	0.021
GO:0050877	neurological system process	1.39	0.024
GO:0006468	protein amino acid phosphorylation	1.49	0.029
GO:0008407	bristle morphogenesis	2.33	0.032
GO:0048812	neuron projection morphogenesis	1.46	0.032
GO:0032989	cellular component morphogenesis	1.31	0.040
GO:0031175	neuron projection development	1.45	0.040
GO:0048858	cell projection morphogenesis	1.41	0.043
GO:0048667	cell morphogenesis involved in neuron differentiation	1.44	0.044
GO:0007169	transmembrane receptor protein tyrosine kinase signaling pathway	1.80	0.045

Supplemental Table 15. Species-level Gene Ontology functional enrichment (Benjamini and Hochberg FDR P-value < 0.05) for putatively methylated genes with low coding sequence CpG O/E according to a cutoff of one SD below the mean (among single copy orthologs present in seven species). Functional enrichment associated with lineage-specific methylation does not appear to deviate qualitatively from patterns of functional enrichment observed for genes that are methylated in all ants (Supplemental Table 13).

Accession	GO Biological Process	*Acep*	*Aech*	*Sinv*	*Pbar*	*Cflo*	*Lhum*	*Hsal*
GO:0009987	cellular process	×	×	×	×	×	×	×
GO:0010467	gene expression	×	×	×	×	×	×	×
GO:0016070	RNA metabolic process	×	×	×	×	×	×	×
GO:0044237	cellular metabolic process	×		×	×	×	×	×
GO:0044260	cellular macromolecule metabolic process	×		×	×	×	×	×
GO:0006461	protein complex assembly	×	×		×	×		×
GO:0065003	macromolecular complex assembly	×	×		×	×		×
GO:0070271	protein complex biogenesis	×	×		×	×		×
GO:0006139	nucleobase, nucleoside, nucleotide and nucleic acid metabolic process	×		×	×		×	
GO:0006351	transcription, DNA-dependent				×	×	×	×
GO:0006366	transcription from RNA polymerase II promoter				×	×	×	×
GO:0006396	RNA processing	×			×	×	×	
GO:0006412	Translation			×		×	×	×
GO:0009058	biosynthetic process				×	×	×	×
GO:0032774	RNA biosynthetic process				×	×	×	×
GO:0034660	ncRNA metabolic process	×			×	×	×	
GO:0043933	macromolecular complex subunit organization		×		×	×		×
GO:0044249	cellular biosynthetic process				×	×	×	×
GO:0006352	transcription initiation				×	×		×
GO:0006367	transcription initiation from RNA polymerase II promoter				×	×		×
GO:0006399	tRNA metabolic process				×	×	×	
GO:0006807	nitrogen compound metabolic process	×			×		×	
GO:0008152	metabolic process				×		×	×
GO:0009059	macromolecule biosynthetic process				×		×	×
GO:0022613	ribonucleoprotein complex biogenesis			×		×	×	
GO:0034641	cellular nitrogen compound metabolic process	×			×		×	
GO:0034645	cellular macromolecule biosynthetic process				×		×	×
GO:0043170	macromolecule metabolic process				×		×	×

GO:0034470	ncRNA processing		×	×	
GO:0042254	ribosome biogenesis		×	×	
GO:0044238	primary metabolic process	×		×	
GO:0000022	mitotic spindle elongation				×
GO:0000279	M phase				×
GO:0007051	spindle organization				×
GO:0007052	mitotic spindle organization				×
GO:0022403	cell cycle phase				×
GO:0051231	spindle elongation				×

Supplemental Table 16. Genomic coordinates of novel miRNA conserved across ant species. (*) denotes miRNA conserved in all Hymenoptera. (#) denotes Aculeata-specific miRNA. (Table continues on next page.)

ID	*A. cephalotes*	*A. echinatior*	*S. invicta*	*P. barbatus*	*C. floridanus*
1*	Scaffold00009 298195:298279:–	scaffold12 255692:255776:–	Si_gnF.scaffold00206 1720505:1720587:–	scf7180000350292 641659:641741:–	scaffold1446 156946:157025:–
2*	Scaffold00011 1845047:1845144:+	scaffold327 41375:41465:+	Si_gnF.scaffold03557 488207:488300:–	scf7180000350374 732174:732267:–	scaffold493 518629:518713:–
3*	Scaffold00015 526022:526097:–	scaffold99 3513473:3513548:+	Si_gnF.scaffold03776 230425:230499:+	scf7180000350301 242704:242777:–	scaffold1141 50615:50690:–
4*	Scaffold00004 4279845:4279928:+	scaffold527 608040:608121:–	Si_gnF.scaffold06788 607865:607946:+	scf7180000350270 1181197:1181276:–	scaffold710 227009:227091:+
5*	Scaffold00076 524670:524762:–	scaffold39 883344:883434:–	Si_gnF.scaffold03949 26730:26821:+	scf7180000349939 285288:285373:+	scaffold620 8460:8550:–
6#	Scaffold00074 740977:741075:–	scaffold293 677141:677238:–	Si_gnF.scaffold06735 264755:264844:–	scf7180000350310 231490:231569:–	scaffold56 38359:38422:+
7#	Scaffold00018 2590478:2590566:+	scaffold140 2023033:2023122:–	Si_gnF.scaffold06792 466767:466850:+	scf7180000350289 171709:171792:–	scaffold487 1168024:1168090:+
8#	Scaffold00022 176789:176876:–	scaffold88 511352:511439:–	Si_gnF.scaffold05788 503497:503574:–	scf7180000349970 430080:430158:–	scaffold316 1103878:1103956:–
9#	Scaffold00022 176741:176822:–	scaffold88 511304:511394:–	Si_gnF.scaffold05788 503438:503531:–	scf7180000349970 430030:430123:–	scaffold316 1103820:1103905:–
10#	Scaffold00053 1140357:1140443:–	scaffold182 221834:221922:+	Si_gnF.scaffold03294 1453491:1453581:–	scf7180000350222 916084:916171:–	scaffold409 110435:110520:+
11	Scaffold00015 521926:522004:–	scaffold99 3517560:3517640:+	Si_gnF.scaffold03776 234724:234803:+	scf7180000350301 241823:241901:–	scaffold1141 45851:45928:–
12	Scaffold00019 2075903:2075977:+	scaffold485 554961:555033:–	Si_gnF.scaffold01122 1466372:1466445:+	scf7180000350360 189174:189248:+	scaffold1001 129602:129677:–
13	Scaffold00019 476958:477050:–	scaffold294 521785:521877:+	Si_gnF.scaffold06340 384039:384131:+	scf7180000349958 1228972:1229064:+	scaffold1221 174724:174815:–
14	Scaffold00005 5055741:5055775:+	scaffold288 1120031:1120094:+	Si_gnF.scaffold04519 2131:2203:+		scaffold486 352289:352360:–
15	Scaffold00001 822537:822628:–	scaffold220 1135597:1135687:–	Si_gnF.scaffold02694 1023049:1023140:–	scf7180000350285 165772:165862:+	scaffold437 196606:196694:+
16	Scaffold00076 525036:525113:–	scaffold39 883701:883779:–	Si_gnF.scaffold03949 26440:26515:+	scf7180000349939 284934:285012:+	scaffold620 9595:9671:–
17	Scaffold00013 3558919:3558992:+	scaffold342 709632:709710:+	Si_gnF.scaffold01426 531424:531497:+	scf7180000350303 1673055:1673128:+	scaffold351 990202:990279:+
18	Scaffold00034 3145482:3145580:–	scaffold50 2574310:2574385:–	Si_gnF.scaffold07124 468044:468141:–	scf7180000350378 2077483:2077580:+	scaffold372 172336:172416:+
19	Scaffold00008 22919:23005:–	scaffold309 1033552:1033638:–	Si_gnF.scaffold06738 1922595:1922674:+	scf7180000350035 171683:171768:–	scaffold263 930276:930361:–
20	Scaffold00026 1206522:1206599:–	scaffold310 219997:220074:+	Si_gnF.scaffold06207 3421852:3421935:–	scf7180000350381 2220671:2220743:–	scaffold1357 1047:1118:–
21	Scaffold00049 228114:228198:+	scaffold758 168792:168876:+	Si_gnF.scaffold06735 1026055:1026141:–	scf7180000349994 401180:401265:–	scaffold407 1874944:1875027:+
22	Scaffold00015 4711497:4711578:+	scaffold283 1722440:1722522:–	Si_gnF.scaffold06899 487914:487990:–	scf7180000350119 179725:179806:–	scaffold1533 86168:86242:+
23	Scaffold00011 1922519:1922590:–	scaffold327 115890:115961:–	Si_gnF.scaffold03557 396658:396715:+	scf7180000350374 676678:676739:+	
24	Scaffold00088 497795:497871:–	scaffold39 385467:385545:–	Si_gnF.scaffold05266 353110:353186:+	scf7180000350371 729092:729168:–	scaffold770 87970:88047:– scaffold770 93493:93570:–
25	Scaffold00002 498215:498307:–		Si_gnF.scaffold00514 2519367:2519456:–	scf7180000349954 628272:628364:+	scaffold1826 717945:718036:–
26	Scaffold00021 84547:84629:–	scaffold574 412982:413064:–	Si_gnF.scaffold06735 1597341:1597423:–	scf7180000349994 928090:928172:–	scaffold407 1304940:1305021:+
27	Scaffold00055 319865:319943:+	scaffold18 939140:939218:–	Si_gnF.scaffold05266 161013:161078:–	scf7180000349880 101508:101590:+	scaffold1702 155864:155929:+
28	Scaffold00015 4711359:4711446:+	scaffold283 1722572:1722660:–	Si_gnF.scaffold06899 488038:488123:–	scf7180000350119 179857:179941:–	scaffold1533 86038:86116:+
29	Scaffold00032 2852256:2852333:+	scaffold501 525447:525521:+	Si_gnF.scaffold01506 313600:313680:+	scf7180000350194 706179:706249:–	scaffold638 184201:184276:–

Supplemental Table 16. Continued.

ID	*L. humile*	*H. saltator*
1*	scf7180001004419 138805:138885:+	scaffold186 184082:184161:+
2*	scf7180001004917 825128:825213:–	scaffold155 695798:695882:–
3*	scf7180001004993 1158427:1158503:+	scaffold2362 45806:45882:–
4*	scf7180001004868 673945:674024:–	scaffold2261 400323:400405:–
5*	scf7180001004958 44294:44380:+	scaffold355 180638:180696:+
6#	scf7180001005010 75718:75789:+	scaffold846 496341:496429:+
7#	scf7180001004973 699038:699104:–	scaffold896 110866:110932:–
8#	scf7180001005077 16454:16531:–	scaffold1632 34670:34756:+
9#	scf7180001005077 16395:16484:–	scaffold1632 34714:34806:+
10#	scf7180001004914 983486:983570:–	scaffold829 1445687:1445772:–
11	scf7180001004993 1161141:1161219:+	scaffold2362 41385:41464:–
12	scf7180001004913 318801:318875:–	scaffold125 1186156:1186236:–
13	scf7180001004905 218388:218479:+	scaffold31 451061:451152:–
14	scf7180001004659 1548615:1548687:+	scaffold120 133411:133482:–
15	scf7180001004947 294745:294831:–	scaffold1545 18020:18101:–
16	scf7180001004958 43895:43973:+	scaffold355 180456:180530:+
17	scf7180001004429 567555:567632:–	scaffold427 997677:997754:–
18	scf7180001004715 877351:877431:+	scaffold284 273801:273881:+
19	scf7180001005010 600479:600566:+	scaffold710 107334:107414:+
20		scaffold220 172582:172655:+
21	scf7180001004456 483993:484075:+	
22	scf7180001004952 137094:137167:–	
23	scf7180001004917 740996:741065:+	
24	scf7180001004940 2630045:2630122:–	
25	scf7180001004986 193126:193198:–	
26		
27		
28		
29		

Supplemental Table 17. Transcription of ant conserved elements. See Materials and Methods for data sets and analysis parameters.

		C. floridanus			*H. saltator*		
Sample	**CEs**	**Transcripts**	**Expr. CE %**	**CE overlap %**	**Transcripts**	**Expr. CE %**	**CE overlap %**
5' 50kb	620,248	16,042	2.6%	91.0%	17,231	2.8%	92.0%
5' 10kb	190,210	5,540	2.9%	89.7%	5,392	2.8%	90.4%
5' 2kb	52,268	1,655	3.2%	87.8%	1,366	2.6%	88.4%
5' UTR	34,375	932	2.7%	87.6%	718	2.1%	88.6%
CpG island	64,016	2,284	3.6%	90.3%	1,570	2.5%	88.2%
Exon	763,028	20,430	2.7%	86.6%	20,288	2.7%	88.3%
Intron	96,431	1,877	1.9%	90.6%	1,831	1.9%	91.7%
3' UTR	33,878	1,636	4.8%	91.5%	1,636	4.8%	91.2%
3' 2kb	39,988	2,820	7.1%	91.9%	2,923	7.3%	91.8%
miRNA	63	63	100.0%	73.6%	53	84.1%	65.1%
rRNA	4	3	75.0%	100.0%	1	25.0%	100.0%
snRNA	47	47	100.0%	97.6%	7	14.9%	82.3%
tRNA	134	127	94.8%	94.5%	84	62.7%	90.6%
TEprotein	4,260	1,499	35.2%	91.8%	802	18.8%	93.2%
Transposon	15,506	1,239	8.0%	90.8%	919	5.9%	90.6%
Other	596,098	17,169	2.9%	90.7%	16,571	2.8%	92.1%
Total		**73,363**			**71,392**		
Non-exonic		**52,933**			**51,104**		
Intergenic		**45,510**			**45,053**		

Supplemental Table 18. GO terms enriched among 118 genes nearest to conserved transcribed CpG islands.

Name	GOID	P	Q(GO)	Q(FG)	Count
regulation of primary metabolic process	GO:0080090	0.0	0.02	0.314	37
regulation of neuron differentiation	GO:0045664	0.0	0.067	0.076	9
regulation of nervous system development	GO:0051960	0.0	0.057	0.085	10
regulation of macromolecule metabolic process	GO:0060255	0.0	0.02	0.305	36
negative regulation of cellular process	GO:0048523	0.0	0.025	0.203	24
regulation of metabolic process	GO:0019222	0.0	0.019	0.322	38
regulation of neurogenesis	GO:0050767	0.0	0.057	0.076	9
regulation of biological process	GO:0050789	0.0	0.016	0.466	55
regulation of cellular biosynthetic process	GO:0031326	0.0	0.02	0.271	32
regulation of biosynthetic process	GO:0009889	0.0	0.02	0.271	32
negative regulation of metabolic process	GO:0009892	0.0	0.032	0.136	16
regulation of cellular metabolic process	GO:0031323	0.0	0.019	0.305	36
regulation of macromolecule biosynthetic process	GO:0010556	0.0	0.021	0.263	31
regulation of cellular component organization	GO:0051128	0.0	0.038	0.11	13
negative regulation of biological process	GO:0048519	0.0	0.023	0.212	25
negative regulation of steroid hormone receptor signaling pathway	GO:0033144	0.0	0.375	0.025	3
biological regulation	GO:0065007	0.0	0.015	0.483	57
multicellular organismal development	GO:0007275	0.0	0.018	0.305	36
developmental process	GO:0032502	0.0	0.018	0.339	40
regulation of protein metabolic process	GO:0051246	0.0	0.033	0.119	14
cellular developmental process	GO:0048869	0.0	0.022	0.22	26
regulation of multicellular organismal process	GO:0051239	0.0	0.028	0.144	17
regulation of cell development	GO:0060284	0.0	0.05	0.076	9
regulation of cellular process	GO:0050794	0.0	0.016	0.441	52
cell differentiation	GO:0030154	0.0	0.022	0.212	25
regulation of cell differentiation	GO:0045595	0.0	0.037	0.102	12
negative regulation of macromolecule metabolic process	GO:0010605	0.0	0.031	0.127	15
cellular macromolecule biosynthesis	GO:0034961	0.0	0.018	0.305	36
negative regulation of cell differentiation	GO:0045596	0.0	0.055	0.068	8
anatomical structure development	GO:0048856	0.0	0.019	0.28	33
macromolecule biosynthesis	GO:0043284	0.0	0.018	0.305	36
multicellular organismal process	GO:0032501	0.0	0.017	0.347	41
regulation of steroid hormone receptor signaling pathway	GO:0033143	0.0	0.3	0.025	3
regulation of gene expression	GO:0010468	0.0	0.019	0.254	30
negative regulation of cellular metabolic process	GO:0031324	0.0	0.031	0.119	14
translation elongation factor activity	GO:0003746	0.0	0.133	0.034	4
negative regulation of signal transduction	GO:0009968	0.0	0.056	0.059	7
regulation of cellular protein metabolic process	GO:0032268	0.0	0.033	0.102	12
system development	GO:0048731	0.0	0.019	0.254	30
response to reactive oxygen species	GO:0000302	0.0	0.067	0.051	6
protein complex binding	GO:0032403	0.0	0.055	0.059	7
regulation of transcription from RNA polymerase II promoter	GO:0006357	0.0	0.029	0.119	14
cellular macromolecule biosynthetic process	GO:0034645	0.0	0.017	0.305	36
regulation of translation	GO:0006417	0.0	0.053	0.059	7
macromolecule biosynthetic process	GO:0009059	0.0	0.017	0.305	36
negative regulation of developmental process	GO:0051093	0.0	0.031	0.102	12

Supplemental Table 19. TF gene loci are broadly conserved among insects.

	Name	TF	Gene copy number																									
			Dsim	Dsec	Dmel	Dyak	Dere	Dana	Dpse	Dper	Dwil	Dmoj	Dvir	Dgri	Agam	Aaeg	Cqui	Bmor	Tcas	Acep	Aech	Slnv	Pbar	Cflo	Lhum	Hsal	Amel	Nvit	Phum	Dpul
1	abdominal A	ABD_A	1	1	1	1	1	1	1	1	1	1	1	1	1?	?	?	1	1	1	?	?	1	?	1	1	1	1	?
2	abdominal B	ABD_B	1	1	1	1	1	1	1	1	1	1	1	1	1	1?	1	1	1	1	1	1	?	1	1	1	?	1	?
3	bric-a-brac1	BAB1	1	1	1	1	1	1	1	1	1	1	1	1	?	1	1	1	1	1	1	1	1	1	1	1	1	1	1
4	broad	BR	?	?	1	?	1	1	1	1	1	1	?	1	1	1	1	1	1	?	1	?	?	1	?	1	2?	1	1
	cyclic-AMP response element binding protein	CREB	1																										
5		DFD	1	1	1	1	1	1	1	1	1	1	1	1	1	1	1	1	1	1	1	1	1	1	1	1	1	1	1
6	deformed	DL	1	1	1	1	1	1	1	1	?	1	1	?	1	2?	3?	1	1	1?	1	1	1	1	1?	1	2?	1	1
7	dorsal	DNA replication-related element factor	1	1	1	1	1	1	1	1	1	1	1	1	1	?	?	?	?	?	1	1	1	1?	1	1?	1	1?	1
8		DREF	1	1	1	1	1	1	1	1	1	1	1	1	1	?	?	?	?	?	1	1	1	1?	1	1?	1	1?	1
9	Ecdysone-induced protein 74EF	E(spl) region transcript m5	1	1	1	1	1	1	1	1	1	1	1	1	1	1	1	1	1	1	1	1	1	1	1	1	1	1	1
10	empty spiracles	EMS	1	1	1	1	1	1	1	1	1	1	1	1	1	?	1	1	1	1	?	1	1	1	1	?	1	1	1
11	engrailed	EN	1	1	1	1	1	1	1	1	1	1	1	1	1	1	1	1	1	1	1	1	1	1	1	1	1	1	1
12	even skipped	EVE	?	1	1	1	1	1	1	1	1	1	1	1	1	1	1	1	1	?	1	1	1	1	1	1	1	1	?
13	grainy head	GRH	1	1	1	1	1	1	1	1	1	1	1	1	1	1	1	1	1	1	1	1	1	1	1	1	1	1	1
14	giant	GT	?	1	1	1	1	?	?	?	?	?	?	?	?	?	?	?	?	1	1	1	?	1	1	1	1	?	?
15	hairy	H	1	1	1	1	1	1	1	?	1	1	1	1	1	1	1	1	1	1	1	1	1	1	1	1	1	1	?
16	huckebein	HKB	1	1	1	1	1	1	1	1	1	1	1	1	1	1	1	1	1	1	1	1	1	1	1	?	2?	1	1
17	mothers against m5	HLHm5	1	1	1	1	1	1	1	1	1	1?	1	1	?	?	?	?	?	?	1	1	1	1	1	1	1	?	?
18	decapentaplegic	MAD	1	1	1	1	1	1	1	1	1	1	1	1	1	1	1	1	1?	1	1	1	?	1	1	1	1	2?	1
19	ocellilless	OC	1	1	1	1	1	1	1	1	1	1	1	1	?	1	1	?	1?	1	1	1	1	1	1	1	1	1	1
20	pleiohomeotic	PHO	1	1	1	1	1	1	1	1	1	1	1	1	?	?	1?	1	1	?	1	1?	?	?	2?	1	?	1	1
21	paired	PRD	1	1	1	1	1	1	1	1	1	1	1	1	1	2?	1	1	1	?	1	1	?	?	1	?	1?	1	1
22	scalloped	SD	1	1	1	1	1	1	1	1	1	1	1	1	1	?	1	1	1	1	1	1	1	1	1	?	1?	1	1
23	scnnurri	SHN	1	1	1	1	1	1	1	1	1	1	1	1	?	?	1	?	1	?	1	1	?	?	1	?	?	1	1
24	sloppy paired 1	SLP1	1	1	1	1	1	1	?	?	1	1	?	?	?	?	?	?	?	?	1	1	?	?	1	?	?	1	1?
25	snail	SNA	1	1	1	1	1	1	1	1	1	1	1	1	1?	1?	?	?	1?	1?	?	1?	1?	1?	1?	1?	1?	1?	1?
26	serpent	SRP	1?	1?	1	1	1	1	1	1	1	1	1?	1	?	?	?	?	?	?	?	?	?	?	?	?	1	?	?
27	tailless	TLL	1	1	1	1	1	1	1	1	1	1	1	1	1	1	1	1	1	1	1	1	1	1	1	1	1	1	1
28	trithorax-like	TRL	1	1	1	1	1	1	1	?	1	1	1	1	1	1	1	1	1	1	1	?	1	1	1	1	1	?	?
29	ultraspiracle	USP	1	1	1	1	1	1	1	1	1	1	1	1	1	1	1	1	1	1	1	?	1	1	1	1	1	1	1
30	ventral nervous system defective	VND	1?	1	1	1	1	1	1	1	1	1	1	1	1?	?	?	?	?	?	1?	1?	?	1?	1?	1?	?	?	?

Supplemental Table 20. Gene Ontology category enrichment for positively selected genes in ants. False discovery rates are calculated based on randomizations (100 tests with permutation of the scores attributed to genes). Categories with FDR < 20% are reported.

GO ID	Ontology	GO name	p	FDR
GO:0000313	CC	organellar ribosome	1.43E–10	0
GO:0006120	BP	mitochondrial electron transport, NADH to ubiquinone	1.05E–09	0
GO:0005759	CC	mitochondrial matrix	1.63E–09	0
GO:0005762	CC	mitochondrial large ribosomal subunit	1.09E–07	0.0025
GO:0005746	CC	mitochondrial respiratory chain	4.53E–07	0.003333333
GO:0005747	CC	mitochondrial respiratory chain complex I	1.26E–06	0.003333333
GO:0008137	MF	NADH dehydrogenase (ubiquinone) activity	3.21E–05	0.012857143
GO:0005763	CC	mitochondrial small ribosomal subunit	0.000178056	0.047272727
GO:0008038	BP	neuron recognition	0.000228635	0.047272727
GO:0008344	BP	adult locomotory behavior	0.000819594	0.086153846
GO:0042254	BP	ribosome biogenesis	0.001112847	0.099333333
GO:0003735	MF	structural constituent of ribosome	0.001159211	0.099333333
GO:0044459	CC	plasma membrane part	0.001581373	0.115625
GO:0006508	BP	proteolysis	0.002209659	0.143529412
GO:0006412	BP	translation	0.002519768	0.1455
GO:0016491	MF	oxidoreductase activity	0.002753425	0.1455
GO:0004872	MF	receptor activity	0.002823959	0.1455
GO:0055114	BP	oxidation-reduction process	0.003831834	0.164583333
GO:0008237	MF	metallopeptidase activity	0.003874749	0.164583333
GO:0061134	MF	peptidase regulator activity	0.004628046	0.178461538
GO:0002520	BP	immune system development	0.005283503	0.185666667
GO:0048534	BP	hemopoietic or lymphoid organ development	0.005283503	0.185666667
GO:0016616	MF	oxidoreductase activity, acting on the CH-OH group of donors, NAD or NADP as acceptor	0.00531916	0.185666667
GO:0016836	MF	hydro-lyase activity	0.005464343	0.185666667

Supplemental Table 21. TFs and genes associated with TFBS evolution in eusocial genomes. Highlighted rows indicate significant TFs. Significance assessed using Mann-Whitney U-test (FDR < 0.25). NS, not significant.

		Genome-wide (n=6673)					Genes with promoter CEs (n=1966)				
TF	Overall change, P	Total sig.	Gains	Losses	Prop. gain	Prop. 1 copy	Total sig.	Gains	Losses	Prop. gain	Prop. 1 copy
ABD_A	+, 6.6e–2	111	81	30	0.73	0.883	97	60	37	0.62	0.928
ABD_B	+, 1.4e–2	74	65	9	0.88	0.838	24	21	3	0.88	0.958
ANTP	+, 1e–10	0	0	0	NA	NA	0	0	0	NA	NA
AP	NS	0	0	0	NA	NA	0	0	0	NA	NA
BAB1	+, 1e–10	0	0	0	NA	NA	1243	1187	56	0.95	0.893
BCD	NS	0	0	0	NA	NA	0	0	0	NA	NA
BR	NS	0	0	0	NA	NA	7	7	0	1.00	0.857
BRK	–, 1.2e–5	0	0	0	NA	NA	0	0	0	NA	NA
BYN	–, 7e–3	0	0	0	NA	NA	0	0	0	NA	NA
CAD	NS	0	0	0	NA	NA	0	0	0	NA	NA
CPE	–, 5.1e–2	0	0	0	NA	NA	0	0	0	NA	NA
CREB	+, 6.9e–2	436	295	141	0.68	0.876	188	123	65	0.65	0.920
D	–, 5.9e–6	0	0	0	NA	NA	0	0	0	NA	NA
DEAF1	–, 1.1e–3	0	0	0	NA	NA	0	0	0	NA	NA
DFD	+, 4.6e–3	20	18	2	0.90	0.9	12	9	3	0.75	0.833
DL	–, 2.4e–6	0	0	0	NA	NA	3	1	2	0.33	1.000
DPE	NS	0	0	0	NA	NA	0	0	0	NA	NA
DREF	NS	0	0	0	NA	NA	266	135	131	0.51	0.887
EIP74EF	–, 5.1e–2	0	0	0	NA	NA	201	18	183	0.09	0.910
EMS	+, 1.6e–11	513	424	89	0.83	0.858	132	109	23	0.83	0.932
EN	+, 8.5e–4	0	0	0	NA	NA	182	108	74	0.59	0.901
EVE	NS	18	16	2	0.89	0.833	5	3	2	0.60	1.000
FKH	+, 2e–12	0	0	0	NA	NA	0	0	0	NA	NA
FTZ	NS	0	0	0	NA	NA	0	0	0	NA	NA
GRH	–, 1e–10	0	0	0	NA	NA	1208	24	1184	0.02	0.897
GT	+, 1e–10	0	0	0	NA	NA	458	389	69	0.85	0.910
H	NS	305	254	51	0.83	0.862	127	104	23	0.82	0.906
HB	NS	0	0	0	NA	NA	0	0	0	NA	NA
HKB	–, 1e–10	0	0	0	NA	NA	1330	27	1303	0.02	0.898
HLHm5	+, 1.1e–2	15	13	2	0.87	0.933	4	4	0	1.00	1.000
KNI	–, 1.6e–3	0	0	0	NA	NA	0	0	0	NA	NA
KR	–, 4.8e–6	0	0	0	NA	NA	0	0	0	NA	NA
MAD	NS	55	48	7	0.87	0.855	7	7	0	1.00	1.000
MED	–, 1.5e–9	0	0	0	NA	NA	0	0	0	NA	NA
NUB	+, 1.7e–2	174	129	45	0.74	0.879	0	0	0	NA	NA
OC	NS	0	0	0	NA	NA	4	3	1	0.75	0.750
OVO	NS	0	0	0	NA	NA	0	0	0	NA	NA
PAN	NS	0	0	0	NA	NA	0	0	0	NA	NA
PHO	–, 5.8e–8	0	0	0	NA	NA	4	1	3	0.25	0.750
PRD	NS	0	0	0	NA	NA	4	4	0	1.00	0.750
SD	NS	3	3	0	1.00	1	5	4	1	0.80	1.000
SHN	–, 1e–10	0	0	0	NA	NA	937	25	912	0.03	0.904
SLBO	–, 3.8e–2	0	0	0	NA	NA	0	0	0	NA	NA
SLP1	–, 1.1e–12	0	0	0	NA	NA	855	31	824	0.04	0.904
SNA	–, 1e–10	0	0	0	NA	NA	1083	38	1045	0.04	0.887
SRP	+, 4.8e–2	0	0	0	NA	NA	179	104	75	0.58	0.872
TBP	+, 1e–10	0	0	0	NA	NA	0	0	0	NA	NA
TIN	–, 3.8e–14	0	0	0	NA	NA	0	0	0	NA	NA
TLL	–, 5.9e–10	0	0	0	NA	NA	730	22	708	0.03	0.908

TOP2	NS	319	279	40	0.87	0.828	0	0	0	NA	NA
TRL	NS	77	74	3	0.96	0.909	33	31	2	0.94	0.939
TTK	–, 2.3e–3	0	0	0	NA	NA	0	0	0	NA	NA
TWI	–, 6.8e–7	0	0	0	NA	NA	0	0	0	NA	NA
UBX	NS	0	0	0	NA	NA	0	0	0	NA	NA
USP	–, 4.8e–2	6	6	0	1.00	1	3	2	1		1.000
VND	–, 7.8e–16	0	0	0	NA	NA	1065	20	1045	0.02	0.908
VVL	NS	0	0	0	NA	NA	0	0	0	NA	NA
Z	–, 3.6e–3	0	0	0	NA	NA	0	0	0	NA	NA
ZEN	NS	0	0	0	NA	NA	0	0	0	NA	NA

Supplemental Table 22. GO analysis of genes exhibiting TFBS evolution in eusocial genomes, by comparing 1793 OrthoDB groups (genes) showing significant promoter-associated social evolution and conservation against 9236 genes with conservation (non-significant eusocial changes). GO terms pass FDR < 0.01.

Name	GOID	P	Q(GO)	Q(FG)	Count
cellular_component	GO:0005575	7.31E–20	0.200	0.791	1609
molecular_function	GO:0003674	1.36E–19	0.200	0.794	1614
Cell	GO:0005623	5.55E–17	0.201	0.742	1508
cell part	GO:0044464	5.55E–17	0.201	0.742	1508
binding	GO:0005488	1.55E–16	0.203	0.692	1406
biological_process	GO:0008150	2.78E–16	0.200	0.759	1544
cellular process	GO:0009987	7.33E–14	0.202	0.667	1355
protein binding	GO:0005515	1.01E–11	0.208	0.494	1005
intracellular	GO:0005622	2.83E–09	0.198	0.628	1276
intracellular part	GO:0044424	7.78E–09	0.198	0.612	1245
regulation of biological process	GO:0050789	9.75E–09	0.209	0.387	787
biological regulation	GO:0065007	1.48E–08	0.207	0.412	838
cellular metabolic process	GO:0044237	2.57E–08	0.202	0.496	1008
metabolic process	GO:0008152	6.45E–08	0.200	0.542	1101
primary metabolic process	GO:0044238	6.54E–08	0.201	0.503	1022
signal transduction	GO:0007165	1.50E–07	0.223	0.202	410
membrane	GO:0016020	1.68E–07	0.207	0.367	746
regulation of cellular process	GO:0050794	2.65E–07	0.207	0.365	743
cell communication	GO:0007154	2.75E–07	0.219	0.228	463
estrogen biosynthetic process	GO:0006703	3.22E–07	0.909	0.005	10
testosterone 17-beta-dehydrogenase activity	GO:0050327	3.22E–07	0.909	0.005	10
estrogen metabolic process	GO:0008210	3.42E–07	0.846	0.005	11
organelle	GO:0043226	1.08E–06	0.198	0.533	1084
cytoplasm	GO:0005737	1.76E–06	0.199	0.476	967
intracellular organelle	GO:0043229	2.12E–06	0.197	0.531	1079
anatomical structure development	GO:0048856	2.61E–06	0.217	0.206	418
macromolecule metabolic process	GO:0043170	3.65E–06	0.201	0.416	845
multicellular organismal development	GO:0007275	3.67E–06	0.214	0.225	458
macromolecule metabolism	GO:0043283	4.19E–06	0.201	0.410	833
cellular macromolecule metabolism	GO:0034960	4.37E–06	0.203	0.380	773
cellular macromolecule metabolic process	GO:0044260	4.49E–06	0.203	0.383	779
multicellular organismal process	GO:0032501	4.86E–06	0.210	0.267	543
membrane-bounded organelle	GO:0043227	5.34E–06	0.198	0.493	1002
retinoic acid receptor activity	GO:0003708	5.88E–06	0.769	0.005	10
retinoid-X receptor activity	GO:0004886	5.88E–06	0.769	0.005	10
thyroid hormone receptor activator activity	GO:0010861	5.88E–06	0.769	0.005	10
thyroid hormone receptor coactivator activity	GO:0030375	5.88E–06	0.769	0.005	10
protein complex	GO:0043234	6.47E–06	0.216	0.200	406
intracellular membrane-bounded organelle	GO:0043231	7.12E–06	0.198	0.491	998
macromolecular complex	GO:0032991	7.75E–06	0.211	0.243	494
system development	GO:0048731	7.81E–06	0.217	0.189	384
cellular biosynthetic process	GO:0044249	9.90E–06	0.207	0.295	599

developmental process	GO:0032502	1.03E–05	0.210	0.255	519
biosynthetic process	GO:0009058	1.26E–05	0.206	0.301	611
molecular transducer activity	GO:0060089	1.43E–05	0.235	0.100	203
signal transducer activity	GO:0004871	1.43E–05	0.235	0.100	203
estradiol 17-beta-dehydrogenase activity	GO:0004303	1.72E–05	0.714	0.005	10
receptor activator activity	GO:0030546	1.72E–05	0.714	0.005	10
steroid dehydrogenase activity, acting on the CH-OH group of donors, NAD or NADP as acceptor	GO:0033764	1.72E–05	0.714	0.005	10
nitrogen compound metabolic process	GO:0006807	1.75E–05	0.205	0.310	631
cell differentiation	GO:0030154	2.69E–05	0.223	0.137	278
cellular component organization	GO:0016043	3.03E–05	0.211	0.221	450
organ development	GO:0048513	4.20E–05	0.219	0.152	310
cellular developmental process	GO:0048869	4.22E–05	0.221	0.142	288
transferase activity	GO:0016740	4.56E–05	0.219	0.151	306

Supplemental Table 23. GO analysis of 292 genes exhibiting concentrated regulatory rewiring of multiple TFs.

Name	GOID	P	Q(GW)	Q(FG)	Count
estrogen biosynthetic process	GO:0006703	1.21E–11	0.500	0.032	10
testosterone 17-beta-dehydrogenase activity	GO:0050327	1.21E–11	0.500	0.032	10
estrogen metabolic process	GO:0008210	2.25E–11	0.476	0.032	10
vitamin D receptor binding	GO:0042809	3.47E–11	0.333	0.039	12
retinoic acid receptor activity	GO:0003708	4.04E–11	0.455	0.032	10
retinoid-X receptor activity	GO:0004886	4.04E–11	0.455	0.032	10
thyroid hormone receptor activator activity	GO:0010861	4.04E–11	0.455	0.032	10
thyroid hormone receptor coactivator activity	GO:0030375	4.04E–11	0.455	0.032	10
estradiol 17-beta-dehydrogenase activity	GO:0004303	6.98E–11	0.435	0.032	10
receptor activator activity	GO:0030546	6.98E–11	0.435	0.032	10
steroid dehydrogenase activity, acting on the CH-OH group of donors	GO:0033764	6.98E–11	0.435	0.032	10
thyroid hormone receptor binding	GO:0046966	2.68E–10	0.286	0.039	12
retinoic acid receptor binding	GO:0042974	4.71E–10	0.370	0.032	10
steroid dehydrogenase activity	GO:0016229	4.71E–10	0.370	0.032	10
androgen metabolic process	GO:0008209	2.27E–09	0.323	0.032	10
ligand-dependent nuclear receptor transcription coactivator activity	GO:0030374	5.55E–09	0.256	0.035	11
nuclear hormone receptor binding	GO:0035257	2.15E–08	0.181	0.042	13
receptor regulator activity	GO:0030545	2.72E–08	0.256	0.032	10
hormone receptor binding	GO:0051427	4.98E–08	0.169	0.042	13
ligand-dependent nuclear receptor activity	GO:0004879	5.89E–08	0.208	0.035	11
cellular_component	GO:0005575	1.16E–07	0.030	0.771	239
hormone biosynthetic process	GO:0042446	1.20E–07	0.222	0.032	10
molecular_function	GO:0003674	2.18E–07	0.030	0.774	240
transcription coactivator activity	GO:0003713	5.99E–07	0.105	0.055	17
steroid biosynthetic process	GO:0006694	3.23E–06	0.129	0.039	12
cellular hormone metabolic process	GO:0034754	5.72E–06	0.149	0.032	10
binding	GO:0005488	9.49E–06	0.030	0.668	207
protein heterodimerization activity	GO:0046982	1.08E–05	0.085	0.055	17
cell	GO:0005623	1.14E–05	0.030	0.710	220
cell part	GO:0044464	1.14E–05	0.030	0.710	220
receptor signaling protein activity	GO:0005057	1.16E–05	0.114	0.039	12
oxidoreductase activity, acting on the CH-OH group of donors	GO:0016616	2.68E–05	0.092	0.045	14
hormone metabolic process	GO:0042445	3.51E–05	0.111	0.035	11
protein binding	GO:0005515	3.77E–05	0.032	0.477	148
transcription cofactor activity	GO:0003712	3.87E–05	0.074	0.058	18
transcription activator activity	GO:0016563	5.63E–05	0.067	0.065	20
succinate-CoA ligase activity	GO:0004774	7.10E–05	0.400	0.013	4
regulation of hormone levels	GO:0010817	7.36E–05	0.089	0.042	13
biological_process	GO:0008150	1.19E–04	0.029	0.713	221
ammonia ligase activity	GO:0016211	1.61E–04	0.333	0.013	4
oxidoreductase activity, acting on CH-OH group of donors	GO:0016614	1.68E–04	0.078	0.045	14

Supplemental References

E. W. Abrams, M. S. Vining, D. J. Andrew. Trends Cell Biol. 13, 247-254 (2003).

M. Adams et al., Science 287, 2185 (2000).

H. Akashi, Genetics 136, 927 (1994).

A. Alexa, A. Rahnenfhrer, T. Lengauer, Bioinformatics 22, 1600 (2006).

J. B. Amaral, G. M Machado-Santelli. Micron 39, 1222-1227 (2008). M. Anisimova, Z. Yang, Mol. Biol. Evol. 24, 1219 (2007).

M. Ashburner et al., Nat. Genet. 25, 25 (2000).

Y. Benjamini, Y. Hochberg, J. R. Stat. Soc. Ser. B Stat. Methodol. 57, 289 (1995).

G. Bernardi, Gene 241, 3 (2000).

L. Bromham, R. Leys, Mol. Biol. Evol. 22, 1393 (2005).

Bovine Genome Sequencing and Analysis Consortium. Science 324, 522 (2009).

N. Bray, L. Pachter, Genome Res. 14, 693 (2004).

M. Bulmer, Genetics 129, 897 (1991).

J. Castresana, Mol. Biol. Evol. 17, 540 (2000).

F. Chen, A. J. Mackey, C. J. Stoeckert, Jr., D. S. Roos, Nucleic Acids Res. D363 (2006).

A. Conesa et al., Bioinformatics 21, 3674 (2005).

T. De Bie, J. P. Demuth, N. Cristianini, M. W. Hahn, Bioinformatics 22, 1269 (2006).

D. A. Drummond, C. O. Wilke, Cell 134, 341 (2008).

R. Durbin, S. Eddy, A. Krogh, G. Mitchison, Biological sequence analysis. Probabilistic Models of Proteins and Nucleic Acids (Cambridge University Press, 1998).

L. Duret, Curr. Opin. Genet. Dev. 12, 640 (2002).

S. R. Eddy, Bioinformatics 14, 755 (1998).

E. Elhaik, D. Graur, K. Josic, G. Landan. Nucleic Acids Res. 38, e158 (2010).

W. Fletcher, Z. Yang, Mol. Biol. Evol. 27, 2257 (2010).

H. Gingold, Y. Pilpel, Mol. Syst. Biol. 7, 481 (2011).

R. Gouveia-Oliveira, P. Sackett, A. Pedersen, BMC Bioinformatics 8, 312 (2007).

M. Kaneshina, S. Goto, Y. Sato, M. Furumichi, M. Tanabe, Nucleic Acids Res. 40, D109 (2012).

E. F. Kirkness et al., Proc. Natl. Acad. Sci. U.S.A. 107, 12168 (2010).

C. Kosiol, M. Anisimova, Methods Mol. Biol. 856, 113 (2012).

T. M. Hambuch, J. Parsch, Genetics 170, 1691 (2005).

S. B. Hedges, J. Dudley, S. Kumar, Bioinformatics 22, 2971 (2006).

A. Heger, C. P. Ponting, Genetics 177, 1337 (2007).

R. Hershberg, D. A. Petrov, Annu. Rev. Genet. 42, 287 (2008).

D. W. Huang, B. T. Sherman, R. A. Lempicki, Nat. Protocols 4, 44 (2008).

S. Jia., A. Meng, Developmental Dynamics 236, 913 (2007).

G. Jordan, N. Goldman, Mol. Biol. Evol. 29, 1125 (2012).

F. G. Jorgensen, M. H. Schierup, A. G. Clark, Mol. Biol. Evol. 24, 611 (2007).

K. Katoh, K. Misawa, K. Kuma, T. Miyata, Nucleic Acids Res. 30, 3059 (2002).

W. J. Kent, Genome Res. 12, 656 (2002).

F. Krueger, S. R. Andrews, Bioinformatics 27, 1571 (2011).

S. Lall et al., Curr. Biol. 16, 460–471 (2006).

H. Li et al., Bioinformatics 25, 2078 (2009).

S. Q. Le, O. Gascuel, Mol. Biol. Evol. 25, 1307 (2008).

A. Löytynoja, N. Goldman, Science 320, 1632 (2008).

A. Löytynoja, N. Goldman, Proc. Natl. Acad. Sci. U.S.A. 102, 10557 (2005).

P. Markova-Raina, D. Petrov, Genome Res. 21, 863 (2011).

V. Matys et al., Nucleic Acids Res. 31, 374 (2003).

B. Misof, K. Misof, Syst. Biol. 58, 21 (2009).

Y. Moriya, M. Itoh, S. Okuda, A. Yoshizawa, M. Kanehisa, Nucleic Acids Res. 35, W182 (2007).

H. Niculita, J. Billen, J, L. Keller. Arthropod Structure & Development 36, 135– 141 (2007).

C. Notredame, D. G. Higgins, J. Heringa, J. Mol. Biol. 302, 205 (2000).

L. F. Pavon, M. I. Camargo-Mathias. Micron 36, 449–460 (2005).

J. S. Pedersen, G. Bejerano, A.Siepel, K. Rosenbloom, K. Lindblad-Toh et al., PLoS Comput. Biol. 2, e33 (2006).

O. Penn, E. Privman, G. Landan, D. Graur, T. Pupko, Mol. Biol. Evol. 27, 1759 (2010).

D. A. Petrov, D. L. Hartl, Proc. Natl. Acad. Sci. U.S.A. 96, 1475 (1999).

J. B. Plotkin, G. Kudla, Nat. Rev. Genet. 12, 32 (2011).

E. Privman, O. Penn, T. Pupko, Mol. Biol. Evol. 29, 1 (2012).

E. Proux, R. A. Studer, S. Moretti, M. Robinson-Rechavi, Nucleic Acids Res., Database Issue 37, D404 (2008).

J. R. Powell, E. N. Moriyama, Proc. Natl. Acad. Sci. U.S.A. 94, 7784 (1997).

M. Punta et al., Nucleic Acids Res. Database Issue 40, D290 (2002).

S. Richards et al., Nature 452, 949 (2008).

T. B. Sackton, A. G. Clark, BMC Genomics 10, 259 (2009).

T. B. Sackton et al., Nat. Genet. 39, 1461 (2007).

A. Schneider et al., Gen. Biol. Evol. 1, 114 (2009).

Sea Urchin Genome Sequencing Consortium. Science 314, 941 (2006).

A. Stamatakis, Bioinformatics 22, 2688 (2006). D. C. Shields, P. M. Sharp, D. G. Higgins, F. Wright, Mol. Biol. Evol. 5, 704 (1988).

R. R. Sokal, F. J. Rohlf. Biometry, 3rd ed. W. H. Freeman and Company, G12 (1995).

A. Stark et al., Nature 450, 219–232 (2007).

W. J. Swanson, R. Nielsen, Q. Yang, Mol. Biol. Evol. 20, 18 (2003).

H. Tanaka et al., Insect Biochem. Mol. Biol. 38, 1087 (2008).

The Gene Ontology Consortium, Nat. Genet. 25, 25 (2000).

The UniProt Consortium, Nucleic Acids Res. 40, D71 (2012).

N. Tintle, B. Borchers, M. Brown, A. Bekmetjev, BMC Proceedings 3, S96 (2009).

S. Vicario, E. N. Moriyama, J. R. Powell, BMC Evol. Biol. 7, 226 (2007).

I. M. Wallace, O. O'Sullivan, D. G. Higgins, C. Notredame, Nucleic Acids Res. 34, 1692 (2006).

J. H. Werren et al., Science 327, 343 (2010).

W. S. Wong, Z. Yang, N. Goldman, R. Nielsen, Genetics 168, 1041 (2004).

F. Wright, Gene 87, 23 (1990).

Z. Yang, R. Nielsen, N. Goldman, A.-M. K. Pedersen, Genetics 155, 431 (2000).

Z. Yang, Mol. Biol. Evol. 24, 1586 (2007).

Z. Yang, M. dos Reis, Mol. Biol. Evol. 28, 1217 (2011).

J. Zhang, R. Nielsen, Z. Yang, Mol. Biol. Evol. 22, 2472 (2005).

Z. Zou et al., Genome Biol. 8, R177 (2007).